Asphalt concrete stiffness prediction based on composition and binder properties

MSc Thesis

Road and Railway Engineering

TU Delft

J. Droogers

Nieuw-Vennep, 2018

Boskalis Nederland

Boskalis

TUDelft

TU Delft student number:

4318080

Under supervision of:

Prof.dr.ir. S.M.J.G. Erkens (chair)   TU Delft

Prof.dr.ir. E.H.E.J.G. Schlangen   TU Delft

Ir. L.J.M. Houben   TU Delft

Ir. B.W. Sluer   Boskalis

Ir. N.R.Z. Poeran   Boskalis

Preface

This thesis report is the result of my graduation project at Boskalis Nederland. Through the university I got in contact with Boskalis, which provided me the possibility of performing research using their laboratory, knowledge and expertise. From several topics I chose the possibility to do research on the prediction of functional properties of asphalt concrete. During the process I decided to focus on the prediction of asphalt concrete stiffness. This topic is in line with my specialization road and railway engineering at TU Delft. Besides, it is a relevant topic for Boskalis since the development of these prediction models is crucial for the introduction of functional verification.

In this report some useful conclusions are drawn for the prediction of asphalt concrete stiffness and a proposal is made for a new model. Also recommendations are given for further research on this topic. The report can serve other purposes as well. For future independent research on asphalt stiffness, chapter 2 gives an overview of the existing models and the underlying tests and mixes. Conclusions in the other chapters are based on a database that has been composed specially for this research. For further research with this database, all corresponding tests have been described in detail in chapter 3. Chapter 4 can be used to gain insight in the dependence of asphalt concrete stiffness on certain asphalt characteristics. Some steps have been taken in the problem of the determination of the binder glassy modulus in section 4.3.7.

I would like to thank the thesis committee for their contribution to the realization of this project. Special thanks goes to Berwich Sluer and Natascha Poeran from Boskalis for keeping me in the right direction during the process. I would also like to thank Boskalis' asphalt laboratory team which helped me during the two months of performing tests.

I wish you a pleasant read,

Joost Droogers

Nieuw-Vennep, 2018

Summary

Boskalis Nederland is currently taking the first steps in the introduction of functional verification of asphalt works in The Netherlands. At this moment the verification of delivered works is based on non-functional properties, like binder properties, void content and level of compaction. However, functional properties are used in design and they determine the lifespan of the pavement. Functional tests are more time-consuming and due to the fact that characteristics develop over time, the tests can only be performed after eight weeks. A model for estimating the functional properties of the delivered works is required, so that functional lab tests become unnecessary. Functional tests will only be performed if the model rejects the work. In this research only the prediction (+/- 10%) of the functional property *stiffness* of asphalt concrete mixes is considered.

As a starting point in the research eight existing asphalt concrete stiffness prediction models are investigating. They are used to gain insight in candidate predictive parameters and a possible structure for a new model. Most models originate from Belgium or the United States. A comparison between the databases used by the authors is included. These databases determine the applicability of the model. Test conditions and mixes differ from Dutch standards. For this reason, a new database was set up at Boskalis. This database consists of data of seven asphalt concrete mixes (base, bind) including mixes with RAP and polymer modified binders. In total 46 candidate predictive parameters are determined, including all predictive parameters of the existing models. The candidate predictive parameters are addressed in three different groups: binder properties, volumetric properties and gradation properties. They are assessed on precision, theoretical preference, and the correlation with the asphalt concrete stiffness. It can be concluded that the binder stiffness, the penetration value, the volume fractions, coefficient of uniformity and the maximum aggregate size are preferred in a new model. The binder glassy modulus can best be obtained by determining the asymptote of the master curve, but cannot be precisely determined. Models like the Van der Poel nomograph used for the determination of predictive parameters should be avoided due to inaccuracy and inapplicability.

Subsequently, the existing models are all applied on the Boskalis database. In order to correct for the differences in mixes and test conditions, the coefficients of the existing models have been fitted. The unfitted models show low accuracy in general while some fitted models show higher accuracy. Outstanding is the accuracy of the Jacobs model, both fitted and unfitted. This model is based on a linear regression analysis, which has been used for building a complete new model in the end. In total eight regression models have been obtained, with different starting points. The last model is preferred for its accuracy, simplicity and the significance and theoretical value of the predictive parameters. The used predictive parameters are the binder stiffness, and the air and aggregates fractions. 90% of the predictions deviate less than 10% from the measurements.

The conclusion can be drawn that a multiple linear regression model is simple and accurate compared to existing (un)fitted models. Further accuracy can possibly be achieved by performing separate analyses for mixes with polymer modified binders. The Boskalis database needs to be extended for this reason. Another recommendation is to extend the variation in binder content and include different kind of surface layer mixes as well. More research should be done on the spread of data of both predictive parameters and the asphalt concrete stiffness.

Table of contents

1   Introduction

1.1   Problem definition

The Netherlands is a country with a high quality road infrastructure (Waze 2017). Due to years of research, new developments like the introduction of porous asphalt, good quality control and an extensive maintenance program, Dutch roads belong to the best of the world. Nevertheless, in this field still many developments are taking place. Over the years, the government in the Netherlands has shifted many responsibilities, like maintenance, from the road authority to the contractor. Instead of prescribing a particular asphalt concrete mix, functional requirements are given. The road should fulfil its function for a certain number of years and the asphalt concrete should have certain properties, while the design of the pavement is the responsibility of the contractor. Contracts can include maintenance of a particular road section for a certain number of years, as well. Since the shift of responsibilities from the government to the contractors, large companies started their own research departments.

Because this shift of responsibilities, contractors need to be able to prove that the properties of the asphalt concrete works are similar to those obtained in type tests. This verification exists since in the construction phase many steps are taken which can influence the final quality of a pavement negatively. For example, poorly compacted asphalt at a lower temperature will result in a much lower asphalt concrete quality. At this moment this verification is based on the composition and binder properties of asphalt concrete like the density, the grading of the mix, and the penetration of the reclaimed bitumen. These parameters can be determined by measurements on the road, and by testing cores taken from the road (field cores) in the lab. The obtained values are compared to certain limits, which can be found in the 'standaard RAW bepalingen' (CROW, 2014), which is a Dutch contract specification in the geotechnical, pavement and hydraulic engineering business. These limits have been determined empirically.

Due to the development of new asphalt mixes with higher RAP percentages, modified binders and composite fillers it is questionable if these checks do still guarantee the actual quality of the delivered work sufficiently. According to Boskalis, this way of verification is not in line with high quality asphalt pavements in the Netherlands. A good indication of the delivered quality is desired for a fair assessment of the contractors. The functional properties fatigue and stiffness are directly used in the design of new asphalt concrete pavements. Boskalis is defender of the introduction of functional verification, where the verification of new asphalt pavements is based on functional properties. This offers the possibility to directly compare the assumed functional properties in the design and the actual functional properties of asphalt in the road. Boskalis is currently taking the first steps in introducing this new way of verification.

Functional properties include stiffness, fatigue resistance, permanent deformation resistance and indirect tensile strength (before and after submersion in water) (RAW, 2015). Some of these properties are determined in the lab for the specification of new asphalt concrete mixes by tests. The Dutch standards prescribe the four point bending test on prismatic specimens to determine stiffness and fatigue resistance, the triaxial test to determine the resistance to permanent deformation and the indirect tensile test to determine the tensile strength. For these tests cylindrical and prismatic specimens are produced in the lab. In order to determine these properties from field cores for verification purposes, test specimens must be drilled from the road. This is a time consuming and laborious process. Test specimens are only allowed to be tested after eight weeks according to the standard, since the properties are believed to be relatively constant in time by then. For functional tests multiple specimens are tested in order to increase the reliability of the data. Moreover, the capacity of laboratories of contractors is

limited. The aforementioned points make the introduction of functional verification a difficult process. Some steps are currently taken to overcome these problems. Instead of using prismatic test specimens, research has been done on determining the stiffness and fatigue resistance on cylindrical specimens (CIT-CY), which are easier to obtain from the road. However, the stiffness and fatigue resistance determined in a four-point bending test differs from that in the CIT-CY.

1.2   Objectives

Functional verification will be easier, quicker and cheaper if the determination of the functional properties did not purely depend on tests. Another way of determining functional properties is the use of prognosis models. These models use non-functional properties as predictive parameters like composition and binder properties, which are easier to determine than the functional properties themselves. Currently the following tests are done for the (composition-based) verification process of new asphalt concrete in the Netherlands:

-   Thickness of the layers (RAW 2015 test 63)
-   Grading (NEN-EN 12697-2) (NEN, 2015)
-   Binder content (RAW 2015 test 65.0)
-   Void content (RAW 2015 test 69.0)
-   Degree of compaction (RAW 2015 test 66)
-   Penetration of reclaimed bitumen (NEN-1426) (NEN, 2015)

The output of these tests can be used as input for prediction models for functional properties. If most of the work can be verified using a model, less of the time-consuming functional lab tests are necessary. Besides, the functional properties can be determined shortly after the construction phase, so correcting measures can be taken earlier. Functional tests are only allowed at specimens at an age of at least eight weeks as mentioned before . A model for prediction of functional properties for the Dutch practice does not exist at this moment and must be developed. Currently existing models are developed outside the Netherlands and are based on data obtained with other tests on different mixes. The goal of this study is to develop a prediction model for the functional properties based on the Dutch data and standards.

The motivation for research on this topic is the introduction of functional verification. However, a high quality prediction model can serve many other purposes as well. It can help to speed up the iterative design of new mixes. Besides, it can provide insight in the influence of the included parameters on the functional properties. This can be a reason for further research.

Four functional properties have been mentioned before. From a design point of view stiffness and fatigue resistance have the highest priority since they are directly used in the design of asphalt pavements. According to Shen & Carpender (2007) fatigue has a dependence on the stiffness. Moreover, more research has been done abroad on the prediction of the stiffness, which gives a starting point in the process. Therefore, in this thesis, stiffness prediction has been chosen as the main topic. Since the asphalt stiffness is particularly important for base and subbase layers, the research will focus on asphalt concrete mixtures (NEN-EN 13108-1) only. For developing a new model a database is composed, which includes asphalt concrete mixes with RAP and polymer modified binders. Currently existing models are verified using this database and used as a starting point for building a new model. The following questions will be answered:

Main question:

Can a model be developed that accurately (+/- 10%) predicts the stiffness modulus of asphalt concrete for functional verification to be introduced in the future?

Sub questions:

a. Which parameters are relevant for the prediction of the stiffness of asphalt concrete?
b. To which extend do currently existing models predict the stiffness of asphalt concrete accurately?
c. Which relations can be found between predictive parameters and the asphalt concrete stiffness?
d. Which structure for the development of a new model can best be chosen?
e. Does the proposed model satisfy the requirements and accuracy for functional verification?

1.3   Report structure

For answering these questions, a stepwise research has been done. First of all, the existing literature will be reviewed in chapter 2. Earlier models are presented with their background and limits. The corresponding tests will be described briefly. These models will be used to gain insight in the possible relevant parameters for predicting stiffness in chapter 4 by using lab results from Boskalis. These lab results, as described in chapter 3, will be used in a statistical analysis as well. This analysis results in insight in the relations between the parameters and the asphalt concrete stiffness. Also the spread of the data and the mutual relations will be reviewed. In chapter 5, the currently existing models are verified using the Boskalis database and the pros and cons per model are discussed. In chapter 6, proposals are made for new models. These models will be assessed on their accuracy and suitability for functional verification. Finally, conclusions are drawn and recommendations are made in chapter 7.

2   Existing asphalt concrete stiffness prediction models

2.1   Introduction

Stiffness is an important functional design parameter for road construction. Together with the thickness of the layers, it determines the stiffness of the construction as a whole. Together with the load and the total height of the structure, the strain at the bottom of an asphalt pavement can be calculated. In a given material, the higher the strain, the higher the fatigue damage. A completely stiff structure is undesirable since the pavement should be able to deform as a result of thermal stresses and subsoil settlements. Each case has its own optimal combination of layers, thicknesses and asphalt properties, among which the stiffness modulus. Therefore, stiffness of the asphalt concrete is an indispensable input parameter for pavement design.

As a start in the analysis, a literature study has been carried out. This study includes the tests as used in The Netherlands and all over the world as well as some important currently existing models. A research on existing models has been carried out for the following three reasons:

- To gain insight in possible valuable existing models.
- To gain insight in relevant parameters for implementation in a new model.
- To gain insight in the possible approaches for developing a new stiffness model and to decide if one of those models can be used as a starting point.

The existing models will be evaluated both quantitatively and qualitatively. Data from several Dutch asphalt concrete mixes is used as input for the models (chapter 3). Attention should be paid to the input used for the development of the existing models. This data determines the validity range of the models. Another important aspect is the background of each model. Different researchers use different approaches for developing their stiffness prediction model.

Serious research on stiffness prediction of asphalt concrete mixes has been performed since the 50's. The most famous model is probably the Shell model, which was published in 1977. An even earlier version of this model was developed in 1954 by Van Der Poel. A lot of research has also been carried out in Belgium by Louis Francken, and in the United States by Witczak. An extended review and comparison of these models is given in paragraph 2.3.

2.2   Stiffness tests

Different stiffness test standards are used all over the world. Since January 2005 the NEN-EN 12697-26 (NEN, 2018) is the standard for EU countries. In this standard nine different tests for determining the stiffness modulus are described:

- Two point bending test on trapezoidal specimens (2PB-TR)
- Two point bending test on prismatic specimens (2PB-PR)
- Three point bending test on prismatic specimens (3PB-PR)
- Four point bending test on prismatic specimens (4PB-PR)
- Test applying indirect tension to cylindrical specimens (IT-CY)
- Direct tension-compression test on cylindrical specimens (DTC-CY)
- Test applying direct tension to cylindrical specimens (DT-CY)
- Test applying direct tension to prismatic specimens (DT-PR)
- Test applying cyclic indirect tension to cylindrical specimens (CIT-CY)

These tests are described in Annex A-F. The reason for the description of more than one test is the history of different stiffness tests used all over Europe. The advantage of the European norm is the increase in uniformity in conducting tests. However, there are still multiple tests allowed, where different tests can give different outcomes by testing the same material. For this reason, in the Netherlands the four point bending test on prismatic specimens (4PB-PR) is prescribed in the standard 'Standaard RAW bepalingen' (RAW, 2015). This prescription is more detailed than the general NEN-EN.

The four point bending test is carried out on prismatic specimens with dimensions 450x50x50mm (4PB-PR). These specimens are supported near the ends with a spacing L of 420 mm. The bar is loaded at two points in between the supports with a spacing l of 140 mm in such a way that the setup is symmetrical. An example of the setup is shown in Figure 1 (NEN, 2018). The specimen is than loaded by a force equivalent to a strain of 50 µm/m. This is done at a range of loading frequencies and at a temperature of 20˚C. The final stiffness is defined at a temperature of 20˚C and 8 Hz.
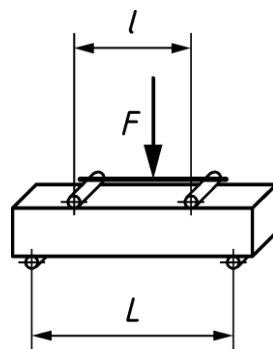
Figure 1 – Concept of the 4PB-PR. Reprinted from NEN-EN 12697-26, 2018, p. 14

The two point bending test on trapezoidal specimens (2PB-TR) is also briefly presented, since the models developed by Francken in Belgium (section 2.3.3) are based on results from this test. In this test, trapezoidal specimens with a height of 250 mm are glued to a metal stand and loaded by a single point load at the top of the sample. A force will be applied at the head corresponding to a maximum strain of 50 µm/m. The concept of this test is shown in Figure 2 (NEN, 2018).
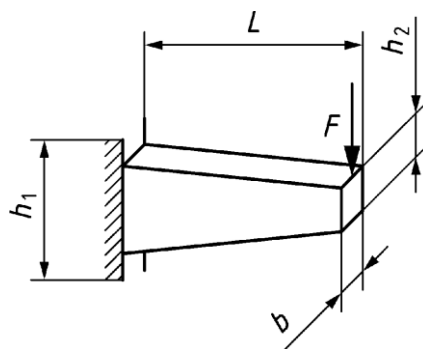
Figure 2 – Concept of the 2PB-TR. Reprinted from NEN-EN 12697-26, 2018, p. 14

The stiffnesses as a result of both tests are not interchangeable. There are too many differences in the descriptions of the tests and the test specimens. For example, in the 2PB-TR, a frequency range is described (NEN, 2018), while this is not the case for the 4PB-PR. The 4PB-PR procedure prescribes an acclimatization time, while the 2PB-TR does not. Both tests can be carried out with specimens aged between 2 weeks and 2 months. The age can

have a significant influence on the stiffness while the timeframe is large (Marsac, 1999). This example illustrates the importance of recording all test conditions in detail. For a valid research, test results from only one test under exactly the same conditions should be used. Extra care should be given to the input used for developing the existing models.

Another standardized European test is the Indirect Test applying Cyclic Indirect Tension to Cylindrical specimens (CIT-CY). This test is interesting as cylindrical test specimens can be easily obtained from the road compared to the prismatic specimens for the 4PB-PR test. Use of cylindrical specimens for the verification of new asphalt structures is desirable and therefor the stiffnesses obtained in these tests will be.used for the database for the new model At Boskalis, it was concluded that the stiffnesses obtained in the CIT-CY and 4PB-PR are comparable. The stiffness determined in the CIT-CY is on average 10% higher in value than the 4PB-PR stiffness (Poeran, Sluer, & Telman, 2018). The CIT-CY test is performed at a cylindrical specimen which is vertically loaded by a pulse load corresponding to a deformation between 0.005% and 0.01% of the specimens diameter in the horizontal direction. The temperatures and dimensions are specified in NEN-EN 12697 (NEN, 2018). The norm also specifies a formula for calculating the asphalt concrete stiffness using the dimensions, deformation and applied force.

1 loading piston
2 test specimen
3 extensometer
4 deflection strip
5 loading strips
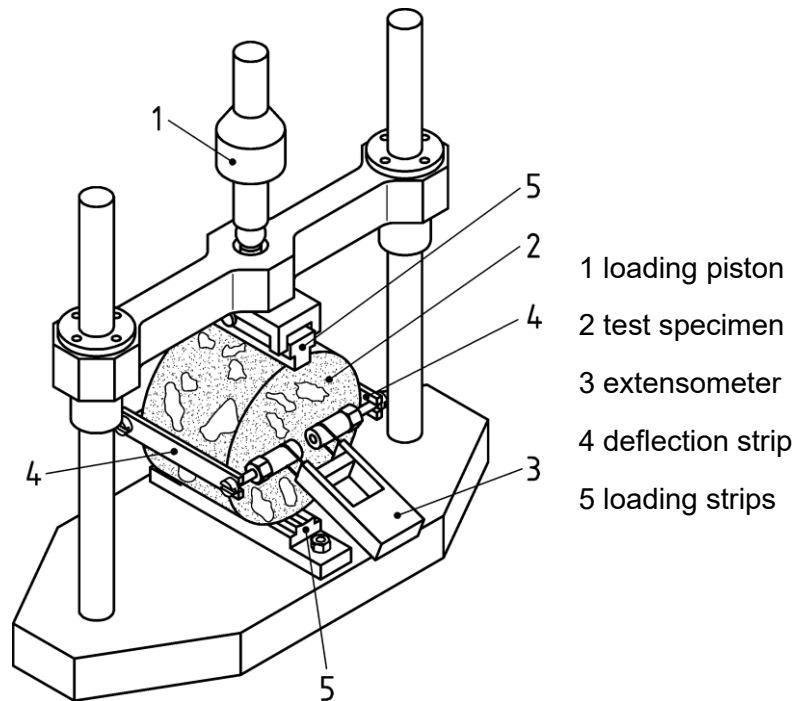
Figure 3 – Example of a setup of the CIT-CY. Reprinted from NEN-EN 12697-26, 2018, p. 41

For other models considered in this study, tests from the United States are used. D3497-79 (ASTM International, 2003) is a test on cylindrical test specimens. These specimens are loaded by a stress controlled load at three loading frequencies and three temperatures.

Another American test is specified in the TP62-03 norm (AASHTO, 2007). The superpave shear tester is a machine that can perform multiple tests. The *Frequency Sweep test at Constant Height* (FSCH) (AASHTO, 2007) is performed for determination of the shear dynamic modulus. A sample is typically 150 mm in diameter and 50 mm in height. The specimen is glued in between two platens which are moved side-to-side. The force is increased till a maximum strain of 0.01% is reached. The force is sinusoidal and the test is conducted at

several frequencies. A formula is used for calculating the stiffness. By estimating the Poison ratio, this dynamic shear modulus can be converted to the dynamic stiffness modulus.

The simple performance test is an unconfined test conducted at cylindrical specimens as well. These specimens, with a diameter of 150 mm and a height of 170 mm, are loaded by a controlled sinusoidal compressive stress at various frequencies. The chamber in which the specimen is placed is temperature controlled. The resulting displacement is then measured by sensors. These test results are included in Al-Khateeb's database (Table 1, page 24).

2.3 Existing asphalt concrete stiffness prediction models

2.3.1 Shell Nomograph

The first model to mention is the famous Shell nomograph (Bonnaure, Gest, Gravois, Ugé, 1977) as shown in Figure 4, which is developed in 1977. The model uses as input the three different volume fractions and the binder stiffness. For the determination of this stiffness, reference is made to the Van Der Poel nomograph (Appendix A) (1954). The graph can be used without any numerical calculations. As long as the input parameters are known, the asphalt concrete stiffness can be simply determined using a ruler.
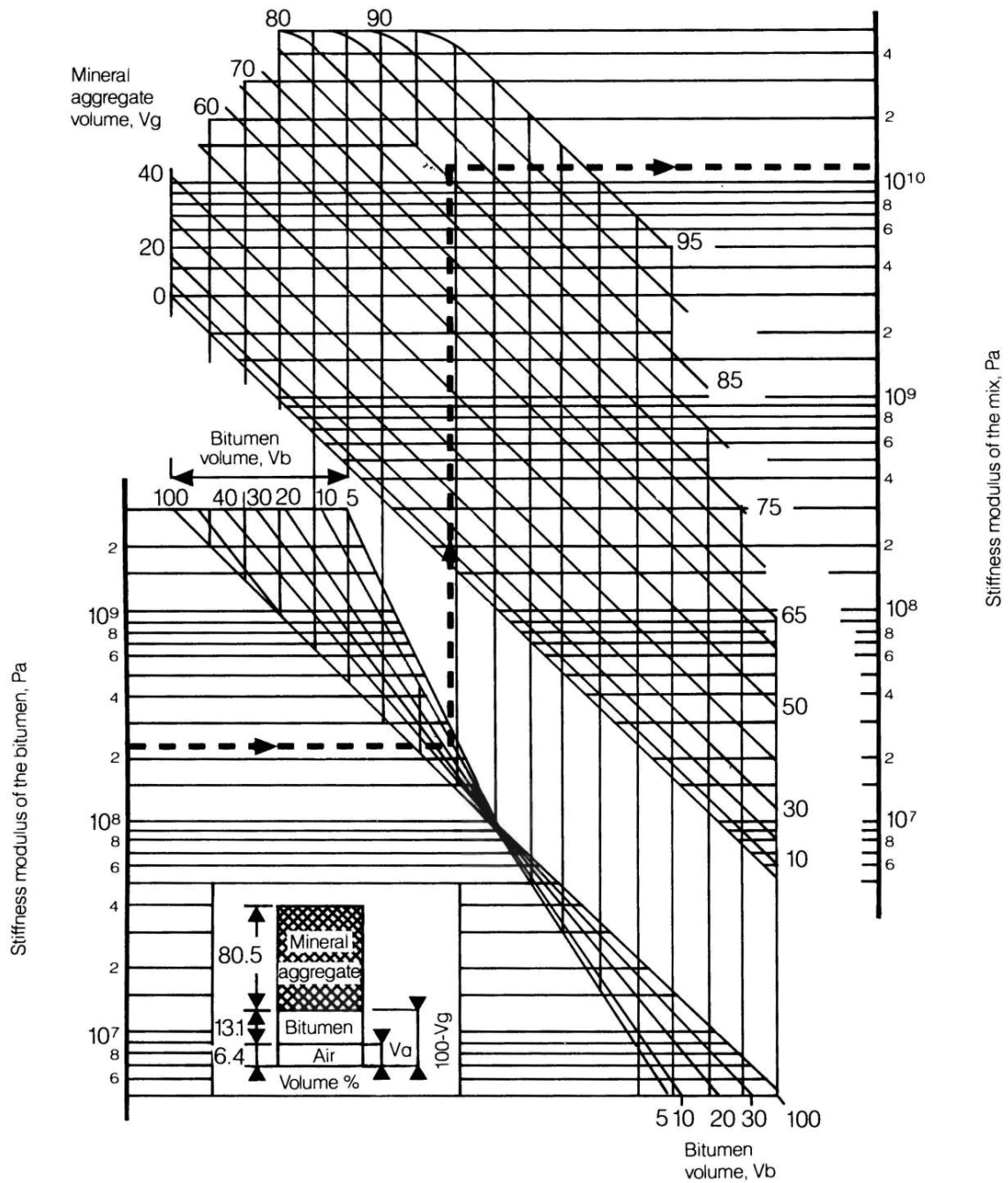
Figure 4 – Shell nomograph, reprinted from A new method of predicting the stiffness of asphalt paving mixtures, Bonnaure et al, 1977

The nomograph is derived from the following formulas:

$$\beta_1 = 10.82 - \frac{1.342(100 - V_g)}{V_g + V_b} \tag{1}$$

$$\beta_2 = 8.0 + 0.00568V_g + 0.0002135V_g^2 \tag{2}$$

$$\beta_3 = 0.6\log(\frac{1.37V_b^2 - 1}{1.33V_b - 1}) \tag{3}$$

$$\beta_4 = 0.7582 * (\beta_1 - \beta_2) \tag{4}$$

For $5*10^6$ N/m^2 < S_b < 10^9 N/m^2:

$$\log S_m = \frac{\beta_4 + \beta_3}{2}(\log(S_b) - 8) + \frac{\beta_4 - \beta_3}{2}|\log S_b - 8| + \beta_2 \tag{5}$$

For 10^9 N/m^2 < S_b < $3 * 10^9$ N/m^2:

$$\log S_m = \beta_2 + \beta_4 + 2.0959(\beta_1 - \beta_2 - \beta_4)(\log S_b - 9) \tag{6}$$

Where:

V_g = volume aggregates (%)

V_b = volume bitumen (%)

S_{bit} = bitumen stiffness (Pa)

S_m = asphalt concrete stiffness (Pa)

Bonnaure et al (1977) developed the model based on 2PB-TR test results from 12 different mixes. Their approach was to determine the stiffness of both the mix and the binder at various temperatures by tests and the Van der Poel nomograph respectively. By plotting both stiffnesses in one graph, a function can be found to describe their relation. A statistical analysis showed that this relation can best be presented as a function of the aggregate fraction V_g. In the statistical analysis some basic boundary conditions have been used. The stiffness of the mix should be equal to the stiffness of the binder when the aggregate fraction (V_g) is zero, and the stiffness of the mix should be equal to the elastic modulus of the aggregate when the asphalt contains no air and binder (V_g = 100%). It appeared that the relation between mix and binder stiffness can best be described using different relations for two binder stiffness intervals. The results of the statistical analysis where finally rationally and numerically verified.

The Shell model is not build for the stiffness prediction of new Dutch mixes, and its applicability on these mixes is not guaranteed. First of all, the model is outdated. The tested mixes used in this analysis contain no reclaimed asphalt or modified binders. Moreover, the model is not made for predicting stiffness moduli of newer asphalt mix designs, like porous asphalt. The test conditions are not verified, and the 2PB-TR test is used for determination of the stiffness, which is not the Dutch standard. Also, the number of parameters included is limited. According to the Shell pavement design manual (Shell, 1978) this method can predict the stiffness with an accuracy of a factor 1.5 to 2, which is not in line with the desired accuracy for functional verification (+/- 10%). However, the approach used for building the formulas can be a starting

point for a new model since it is simple and analytical. The model can also give insight in the importance of the included parameters.

2.3.2 Asphalt Institute

An early method developed in the United States is the Asphalt Institute Model (Hwang and Witczak, 1979). The following relations were found using a regression analysis:

$$E^* = 100,000 * 10^{\beta_1} \tag{7}$$

$$\beta_1 = \beta_3 + 0.000005\beta_2 - 0.00189\beta_2 f^{-1.1} \tag{8}$$

$$\beta_2 = \beta_4^{0.5} T^{\beta_5} \tag{9}$$

$$\beta_3 = 0.553833 + 0.028829(P_{200}f^{-0.1703}) - 0.03476V_A + 0.07037\lambda + 0.931757f^{-0.02774} \tag{10}$$

$$\beta_4 = 0.483V_b \tag{11}$$

$$\beta_5 = 1.3 + 0.49825\log f \tag{12}$$

Where:

f = loading frequency (Hz)

T = temperature (°F)

V_a = volume air voids (%)

λ = bitumen viscosity at a temperature of 77°F (10^6 poises)

P_{200} = percentage by weight of aggregate passing through a No. 200 sieve (US system) (%); No. 200 sieve = 0.075 mm

V_b = volume bitumen (%)

E* = asphalt concrete stiffness (psi)

This model was developed for the computer program DAMA (an elastic multi-layer program) and uses more predictive parameters than the Shell model, including the filler fraction (P_{200}) and the viscosity. The viscosity may be estimated from the following relationship:

$$\lambda = 29508.2(P_{77°F})^{-2.1939} \tag{13}$$

Where:

$P_{77°F}$ = bitumen penetration at 77°F or 25°C (= pen) (dmm)

Since the derivation of the model is missing, the approach of Hwang and Witczak is unclear. It is assumed that the model is based on a regression analysis on stiffness data as a result of former tests and standards from the US. Moreover, Witczak published newer versions of his own stiffness prediction model in 1999 and 2006, which are assumed to be more accurate. The Asphalt Institute model is included in the comparison though, since the way the model is build, with the use of multiple dependent variables ($\beta_1 - \beta_5$), is completely different from other models. A study of this model can be interesting.

2.3.3 Francken

Another interesting model is the Belgium model of Francken (1977). Earlier versions are presented in papers of Francken, Vanaelstraeten and Clauwaert going back to 1975. This model includes the often-used volumetric parameters V_a, V_b and V_g, and two binder properties: the stiffness and glassy modulus of the bitumen. The model has been used in the prediction program PRADO.

The approach of this model is that the stiffness modulus is a multiplication of the purely elastic modulus E_∞ and the reduced modulus R^* as a function of the temperature and the frequency.

$$|E*|(T,Fr) = E_\propto * R^*(T,Fr) \; (MPa) \tag{14}$$

$$E_\propto = 14360 \left(\frac{V_g}{V_b}\right)^{0.55} \exp(-0.0584 V_a) \tag{15}$$

$$\log(R^*) = \log(B*)(1 - 1.35(1 - \exp(-0.13\left(\frac{V_g}{V_b}\right))(1 + 0.11\log(B*)) \tag{16}$$

$$B* = \frac{S_{bit}(T,F_R)}{S_{bit,inf}} \tag{17}$$

Where:

V_a = volume air voids (%)

V_g = volume aggregates (%)

V_b = volume bitumen (%)

S_{bit} = bitumen stiffness (MPa)

$S_{bit,\infty}$ = bitumen glassy modulus (MPa)

E^* = asphalt concrete stiffness (MPa)

The relation for the reduced modulus as presented is used in most papers of Francken and Vanelstraeten concerning this model and implemented in the PRADO program. In Francken and Clauwaert (1987) another version of this relation is presented in the form of an integral. The approach of Francken is that the stiffness of the mix has a certain maximum value, which is expressed as the purely elastic modulus. The value of this purely elastic modulus is determined by the fractions only. The reduced modulus R^* is a value between 0 and 1 and determines the part of the purely elastic modulus that represents the actual stiffness based on the volumetric parameters and binder stiffness. Again, on binder level, a distinction is made between the maximum binder stiffness (the glassy modulus) and the actual stiffness. The ratio between these two determines the actual predictive parameter B^*. The stiffness of the binder can also be expressed in the shear modulus using the following relation:

$$S_{bit} = G^* * 2(1 + v) \tag{18}$$

Where:

S_{bit} = bitumen stiffness (MPa)

G^* = bitumen shear modulus (MPa)

v = Poisson ratio

Since only a ratio of the actual binder stiffness and the glassy modulus determines the predictive parameter B*, S_{bit} and $S_{bit,\infty}$ can be replaced by G* and G^{*}_{∞} which is done in the implementation in the prediction software PRADO (Francken, 2003). It should be noted that Christensen (paragraph 2.6) did research on the conversion by equation 18 by comparing measured binder shear moduli and measured binder stiffness moduli and claimed that this conversion is inaccurate. He assumed a Poisson ratio of 0.4. Telman & Van den Berg (Appendix H) tried to obtain a value for the Poisson ratio by fitting the Hirsch model (section 2.3.5). This procedure did not lead to increased accuracy and the Poisson ratio tended to the lower constrain.

The Francken model is developed using a combination of an empirical and a rational approach. Parts of the formulas are fits on the data of 60 mixes. The data of these mixes is obtained from 2PB-TR tests on cores from the road and cores from the lab. Interesting is the parameter $S_{bit,\infty}$. This glassy modulus has different definitions in the literature and can best be described as the stiffness of the bitumen when it behaves like glass. This value can be approximated by determining the stiffness at very low temperatures and high frequencies. In the literature, it is assumed that the glassy stiffness modulus can be approximated by a conservative value of 3000 MPa (Francken, 1977). Mohan (2010) did research on this assumption and concluded that the glassy modulus is a sensitive parameter in the model and this value cannot just be estimated. In section 4.3.7 further research on the determination of this parameter will be performed.

For Dutch practice, the model has potential to serve as a starting point for a new model. The number of parameters is limited, and the model is based on both empirical and analytical relations. However, the model is even older than the Shell model, and is based on 2PB-TR tests. Not all test conditions can be verified, and the influence of reclaimed asphalt concrete is not included. The validity of the model using modified binders, which were not included as input for the development of the model, has been verified by Francken (1996). The approach used for the development of the model, the fact that the model is implemented in modern computer programs and the fact that it has been presented in many papers and is based on some European tests makes it an interesting model for further research.

2.3.4 Witczak

Witczak, professor of Civil Engineering at the Arizona State University, published his first stiffness prediction model in 1972 and presented his most recent model in 2006. An earlier version was published in 1999, which is governed by equation 19 (Witczak, 1999).

$$
\begin{aligned}
Log&|E^*| \\
&= -1.249937 + 0.029232 P_{200} - 0.001767(P_{200})^2 - 0.002841 P_4 - 0.058097 V_A \\
&\quad - 0.82208 * \frac{V_{beff}}{(V_{beff} + V_A)} \\
&\quad + \frac{(3.871977 - 0.0021 * P_4 + 0.003958 P_{38} - 0.000017(P_{38})^2 + 0.005470 P_{34}}{1 + e^{(-0.603313 - 0.313351 log f - 0.393532 log \eta)}}
\end{aligned}
\tag{19}
$$

The most recent version of his model is given by equation 20 (Witczak 2006).

$$
\begin{aligned}
log|E^*| \\
= -0.349 + 0.754(|G_b{}^*|^{-0.0052}) \\
* \left(6.65 - 0.032p_{200} + 0.0027p_{200}{}^2 + 0.011p_4 - 0.0001p_4{}^2 + 0.006p_{38} - 0.00014p_{38}{}^2 \right. \\
\left. - 0.08V_A - 1.06 \left(\frac{V_{beff}}{V_A + V_{beff}} \right) \right) \\
+ \frac{2.56 + 0.03V_a + 0.71 \left(\frac{V_{beff}}{V_a + V_{beff}} \right) + 0.012P_{38} - 0.0001p_{38}{}^2 - 0.01p_{34}}{1 + e^{(-0.7814 - 0.5785 log|G_b{}^*| + 0.8834 log\delta_b)}}
\end{aligned}
\tag{20}
$$

Where:

$G_b{}^*$ = shear modulus of the binder (psi)

δ_b = phase angle (˚)

f = loading frequency (Hz)

V_A = volume air voids (%)

V_{beff} = volume effective binder (%)

P_{200} = mass percentage aggregates passing 0.075 mm sieve (%)

P_4 = cumulative mass percentage aggregates retained at 4.75 mm sieve (%)

P_{38} = cumulative mass percentage aggregates retained at 9.5 mm sieve (%)

P_{34} = cumulative mass percentage aggregates retained at 19 mm sieve (%)

η = binder viscosity (10^6 poise)

E^* = asphalt concrete stiffness (10^5 psi)

Instead of using the binder viscosity η for defining the binder properties (Witczak 1999), the stiffness modulus of the binder is used in the 2006 model. The viscosity of the binder in the 1999 model is obtained from the ASTM A_i -VTS_i equation, and thus depends indirectly on the binder shear stiffness:

$$
\eta = \frac{G_{bit}{}^*}{10} * \left(\frac{1}{\sin\delta} \right)^{4.8628}
\tag{21}
$$

$$
log\, log\, \eta = A + VTS\, log\, T
\tag{22}
$$

Where:

η =binder viscosity (cP)

G^* = binder complex shear modulus (Pa)

δ = phase angle (˚)

A, VTS = regression parameters

T = temperature (˚F)

Using the first equation, the binder viscosity can be estimated from some fundamental binder properties. The second equation can be used to obtain a relation for the viscosity for any

temperature. When at least two sets of G*, δ and T values are known for a particular binder, a regression analysis can be conducted to determine A and VTS. In order to verify this relation, further research will be done in section 4.3.4. Witczak mentioned that using the viscosity as a predictive parameter in stiffness models is cumbersome, since the shear modulus can be measured in DSR tests and could be used as direct input in the model. For this reason, G_b^* is implemented in the 2006 model.

The approach which is used for the development of the models is based on statistical fits. The choice for the predictive parameters is based on previous publications and a sensitivity analysis. Each candidate parameter was plotted versus the stiffness and the variance was determined. The parameters with the largest variance were considered the most important for the determination of the stiffness. It should be noted that it is not always possible to look at just one parameter by keeping other parameters constant since the research is always limited to available test results, which are mostly obtained with tests on existing mixes used in practice.

Witczak used a standard sigmoidal function for developing his formula's:

$$y = \delta + \frac{\alpha}{1 + e^{\beta - \gamma x}} \tag{23}$$

Using this equation, Witczak made a similar assumption as the Belgian model (Francken). The stiffness has a certain maximum value, which is equal to δ + α. The minimum value is equal to δ. All values in between this maximum and minimum value are defined by the factors β and γ. Witczak claims that this is the best function to define the master curve and to eliminate unrealistic values at the extremes. By determining the dependency (tangent) of a certain parameter at high and low values of the stiffness, a choice was made for including that parameter in the δ, α, β and/or γ part of the equation.

The final equations of the prediction models are fits on the available data. Some candidate models were considered, and with the help of Microsoft Excel's solver, the best possible fit was found using a least squares solution. The way the equations for δ, α, β and γ are build have no rational background. The database used for the 2006 model is an extended version of the 1999 database. This is another reason the model has a different shape. Finally, Witczak did an extensive verification of his models.

The applicability of the Witczak models on Dutch mixes is not guaranteed. The mixes and tests used by Witczak for developing his models don't agree to Dutch practice and standards. The database used by Witczak is impressive. The 2006 model is based on 346 mixes with different compositions and binders, including aging. This improves the fit. However, no differentiation is made for different kind of mixes (i.e. surface layer mixtures vs. base layer mixes). Developing different models for different kind of mixes could have made the models more accurate for particular situations. Another disadvantage of the models is the quality of the input data. The database in the 2006 model is a combination of the 1999 database and the test results of 6 different projects. The stiffness modulus determination is based on different tests. Besides, it is unlikely that the test conditions in these tests were equal. The parameters included are based only on earlier American models, mostly Witczak's. For this reason, other candidate parameters, like the glassy modulus in the model of Francken, are not considered. The models of Witczak are the only models in this report taking into account the gradation of the asphalt concrete. Besides, the models are based on a large database and include many parameters. Especially for research on potentially interesting predictive parameters in a new model, the choice is made for further evaluation of these two models.

2.3.5 Hirsch

The Hirsch model (Christensen, Pellinen and Bonaquist, 2003) was presented in 2003:

$$|E^*|_{mix} = P_C * \left(4200000 \left(1 - \frac{VMA}{100} \right) + 3|G^*|_{binder} \left(\frac{VFB * VMA}{10000} \right) \right)$$
$$+ \frac{(1 - P_C)}{\left(\dfrac{1 - \dfrac{VMA}{100}}{4200000} + \dfrac{VMA}{3VFB|G^*|_{binder}} \right)} \tag{24}$$

$$P_C = \frac{\left(20 + \dfrac{VFB * 3|G^*|_{binder}}{VMA} \right)^{0.58}}{650 + \left(\dfrac{VFB * 3|G^*|_{binder}}{VMA} \right)^{0.58}} \tag{25}$$

Where;

G_b^* = binder shear modulus (psi)

VMA = voids in the mineral aggregate (%)

VFB = voids filled with bitumen (%)

E^*_{mix} = asphalt concrete stiffness (psi)

A complete different approach is chosen for the development of this model. The main assumption of the Hirsch model is that asphalt concrete consists of three fractions (air, binder and aggregate) with their own stiffnesses. Together, these fractions can behave like a series system, a parallel system, or a combination. At high temperatures, the binder stiffness decreases, becomes more viscous and the asphalt concrete behaves more like a series system, since there is less interaction between the aggregates and the binder. At low temperatures, the asphalt concrete behaves more like a parallel system since the stiffer binder puts the aggregates together.

During derivation of the model some combinations of parallel and series systems were considered, with the result that the combination in Figure 5 resulted in the most accurate predictions. This model was mathematically written and forms the basis of the Hirsch model. The proportion of the parallel phase is expressed by the factor Pc (equation 25), while the series phase is expressed by the factor (1-P_c). Three models where finally compared: one using the mastic stiffness, one including factors for the film thickness, and one simple version. By using experimental data the models were verified, and the conclusion was drawn that the accuracy of the models is similar, thus the simple model is the best to choose. In the equation of P_c, three regression constants are included that are used to fit the model to a database. This makes the model a combination of an empirical and rational model. The model was verified by multiple datasets and compared to Witczak's model. It is claimed that the accuracy is at least as high as the Witczak model (2006).

Va'p = volume aggregates in parallel part
Vmp = volume mastic in parallel part
Va's = aggregate contact volume in parallel part
Va's = volume air in series part
Vms = volume mastic in series part
Vvs = volume air in series part
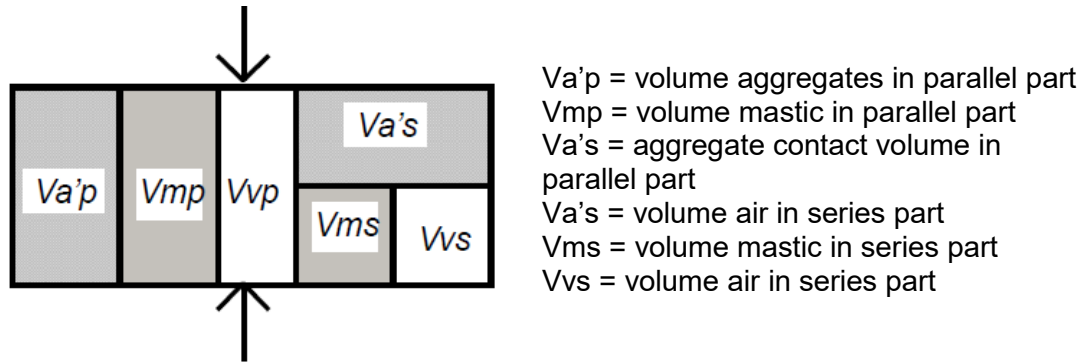
Figure 5 – The arrangement of the phases used in the final Hirsch version, reprinted from Hirsch Model for Estimating the Modulus of Asphalt Concrete, W. Christensen, 2003, p. 126

Hirsch' model can be interesting for predicting the stiffness of Dutch mixes since the approach is more fundamental and step-wise. The main assumption is the law of mixtures. The dependence of the model on regression analysis is kept to a minimum compared to Witczak's model, which makes it more widely applicable. Other parameters can be added by changing corresponding parts of the formula's. For example, if a second binder property should be built into the model as a predictive parameter, the corresponding parts of the formula to the binder phases can be reformulated. The amount of data (18 mixes) and parameters (3) used in the model is limited compared to Witczak's database. The stiffness data is obtained from the superpave shear tester. Mixes were used with 8 different binders and 5 different gradations. The model can give insight in possible relevant parameters, but the model is particularly interesting for its approach. Therefore the model is included in the analysis.

2.3.6   Al-Khateeb

The Al-Khateeb model was published in 2006 (Al-Khateeb, 2006) :

$$|E^*| = 3\left(\frac{100 - VMA}{100}\right)\left(\frac{\left(90 + 1.45\frac{|G^*|_b}{VMA}\right)^{0.66}}{1100 + \left(0.13\frac{|G^*|_b}{VMA}\right)^{0.66}}\right)|G^*|_g \tag{26}$$

Where:

$G_b{}^*$ = binder shear modulus (Pa)

$G^*{}_G$ = glassy shear modulus of the binder (10^9 Pa)

VMA = voids in the mineral aggregate (%)

E^* = asphalt concrete stiffness (Pa)

The Al-Khateeb model is based on the law of mixtures like the Hirsch model, and was developed with the intension to do better predictions at high temperatures and low frequencies. Al-Khateeb started with a parallel system, and finally used a modified version of the contact volume P_c as presented in the Hirsch model in his derivation. At the end two models are presented with five and four regression constants respectively. These constants were determined with a least squares error solution using a database with 6 mixes. For this database 'simple performance tests' (paragraph 2.2) were conducted. Finally the model as presented above was chosen to be the most promising. At the end, the model was verified and it was shown that the prediction is more accurate at high temperatures and low frequencies compared to the Hirsch model.

Al-Khateeb claims that his model is more accurate at predicting the stiffness at higher temperatures and low frequencies compared to the Hirsch model. He verified both models using his own database, which could give a distorted picture. A model is most accurate for its original database. It should be noted that Al-Khateeb used a relatively small database with only 6 mixes. Besides, his model includes 2 extra regression constants, and uses one less predictive parameter, making the asphalt concrete stiffness dependent on two predictive parameters only. The contact volume P_c was obtained from the derivation of the Hirsch model. The glassy shear modulus is also included in the model under the assumption that its value can be estimated at 1 GPa. For these reasons, the more fundamental Hirsch model is considered a better starting point for developing a new model based on the law of mixtures for the Dutch practice. However, the model of Al-Khateeb will be part of the analysis to draw final conclusions about the prediction.

2.3.7   Jacobs

The last model considered is a recent simple model developed by Jacobs at BAM (Jacobs, Qiu, Frunt, & Rering):

$$S_{mix\_4PB} = -52.3Pen + 1219.9\frac{V_g}{V_b} - 698.1V_a + 4344.3 \qquad (27)$$

Where:

Pen = penetration bitumen (dmm)

V_a = volume air voids (%)

V_g = volume aggregates (%)

V_b = volume bitumen (%)

S_{mix_4PB} = asphalt concrete stiffness (MPa)

Jacobs didn't use a fundamental approach but chose a linear multivariable regression analysis as a base for his model. By using the statistical software SPSS, the dependence of each parameter to the asphalt concrete stiffness has been determined. Only the relevant parameters are included in the final model, in which only linear terms are used. For the development of the model a database is used which includes surface, binder and base layer mixes.

The model is simple compared to other prediction models. The assumption is made that each parameter has a linear relationship with the stiffness, which can be point of discussion. Furthermore, the model has no fundamental basis and is obtained using a statistical software. Still this model can be interesting for the development of a new model for the Dutch practice since it is based on an extensive Dutch database. It is the only model that uses 4PB-PR test results as input. The simplicity of the model can be an advantage if the model appears to be accurate. Besides, the model is unique in using the ratio between the aggregate and binder fractions as a direct predictive parameter. Implicitly, the variables N_{gyr} (number of gyrations needed to achieve the aimed air voids content) and D_{max} (maximum aggregate size in the mix) are part of the model as well. They appeared to have no significant relation with the stiffness, whereby the regression parameter has been put to 0.

2.4   Relevance

The models presented above differ in their approach and underlying database. This thesis is focused on the development of a new model based on the Dutch standards and CY-IT tests.

However, none of the above mentioned models are based on these standards and tests. The Jacobs model is based on Dutch mixes and data, which makes the underlying database more relevant. The Hirsch model is based on tests abroad, but a more fundamental approach has been used. A summary of the input for the databases used for the development of each model is given in Table 1. The Boskalis database (chapter 3) is included in this database as well. Since this background does not say anything about the predictive capacity, all models will be further analysed in chapter 5.

Parameter	Unit	Francken	Jacobs	Shell	Witczak 1999	Witczak 2006	Hirsch	Al-Khateeb	Asphalt Institute	Boskalis
Year of development	Year	1987	?	1977	1999	2006	2003	2006	1979	2018
Range V_a	%	1 - 33	1.5 - 6	0 - 31	?	?	5.6 - 11.2	7 (target value)	?	3.5 - 6.3
Range V_g	%	65 - 84	81.4 - 87.0	60 - 87	?	?	?	?	?	81.8 - 86.6
Range V_b	%	5 - 30	8.8 - 15.9	6 - 40	?	?	?	?	?	9.6 - 13.4
Range VMA	%	?	?	13 - 40	?	?	13.7 - 21.6	?	?	13.4 - 18.2
Range $S_{bit,inf}$	MPa	8340 - 31000	?	?	?	?	?	?	?	1351-3970
Range Pen (25°C)	0,1*mm	17 - 99	18 - 90	41 (40 - 50), 18 - 44 after extraction	?	?	?	?	?	31 - 61
Range δ_b	°	?	?	?	?		?	?	?	36 - 46
Range D_{max}	mm	12 - 32	6 - 22	25	?	?	37.5	37.5	?	22
Range E_{mix} (8 Hz, 20°C)	MPa	?	3797 - 12892	?	?	?	183-20900	?	?	6234 - 10787
Range RAP rate	%	? (assumption 0)	30% - 60%	? (assumption 0)	?	?	?	?	? (assumption 0)	0% - 65%
Bitumen types	-	?	?	Conventional	Conventional, polymer modified	Conventional, polymer modified, rubber modified	Conventional, air-blown, polymer modified	Conventional, air-blown, polymer modified	?	Conventional, polymer modified
Bitumen aging	-	?	?	Yes	No	Yes	?	?	?	No
Binder stiffness test	-	direct measurements or vd Poel	Test not performed	vd Poel	Test not performed	DSR	DSR or mathematical model	DSR	?	DSR
Asphalt concrete stiffness test	-	2PB-TR	4PB-PR	2PB-PR	D3497 (tests on cylindrical specimens)	D3497, AASHTO TP62-03 (cylindrical tests)	SST FSCH (tests on cylindrical specimens)	SPT (simple performance test) (tests on cylindrical specimens)	?	CIT-CY
Temperatures asphalt concrete stiffness tests	°C	-20, -5, +15, +30	20?	-15, +9, +30	5, 25, 40 (D3497)	5, 25, 40 (D3497), -10, 4, 21, 38, 54 (TP62-03)	4, 21, 38	4, 19, 31, 46, 58	?	20
Frequencies asphalt concrete stiffness tests	Hz	3, 10, 30, 54, 97	0,1 - 30	4, 40, 50	1, 4, 16 (D3497)	1, 4, 16 (D3497), 25, 10, 5, 1, 0.5, 0.1 (TP62-03)	0.1, 5	0.1, 0.5, 1, 5, 10	?	30, 10, 8, 5, 2, 1, 0.5, 0.2, 0.1, 30
Kind of mixes (according to paper)	-	lab compacted, sawed from the road	Surface, binder and base layer	road, airfield and hydraulic applications	lab compacted	Conventional, unmodified, lime- or rubber modified, plant and field cores	?	lab produced, lab compacted and field cores	?	Asphalt concrete. Base, bind- and top layer, lab compacted
number of mixes	-	60	162	12	149	346	18	6	?	7

Table 1 – Overview of input used for developing the models

3   Database

3.1   Introduction

For the verification of the models as presented in chapter 2, the determination of relevant parameters and the possible development of a new model, a database has been built by performing tests on several different asphalt concrete mixes and their binders. This database includes all the predictive parameters used in the models in chapter 2 and the asphalt concrete stiffness. Beforehand it cannot be said which parameters are relevant for the prediction of the asphalt concrete stiffness. This is why other parameters are included in the database as well, like the age of the asphalt concrete during testing and the percentage of RAP. These parameters are not included in the models in chapter 2. It is expected that special surface layer mixes like porous asphalt (ZOAB) and stone mastic asphalt (SMA) behave differently due to their high void content and mastic content respectively. For this reason the choice is made to focus on asphalt concrete mixes only. Asphalt concrete is mostly used in base layers, where the stiffness determines the deformation at the bottom of the structure. This deformation has an impact on the fatigue life thereafter, which makes the prediction of the stiffness of asphalt concrete mixes the project with the highest priority.

For building a new model, the predictive parameters determined in the tests will be ranked based on their relevance in chapter 4. This ranking is based on the relation with the asphalt concrete stiffness and on the precision of that parameter. A parameter that is determined in an inaccurate test should not be used as a predictive parameter in the new model since it makes the final predictions less reliable. For this reason, if possible, the data has been obtained twice by performing two identical tests. Two results are the minimum for gaining insight in the spread in data. A full overview of the included parameters of the database can be found in Appendix B.

3.2   Mixes

The database used for the project was built specially for this research. The database includes functional properties of 7 asphalt concrete mixes (base, bind and / or surface layer) used by Boskalis these days or in the recent past. The mixes differ in binder type, gradation, use and amount of RAP and aggregate type. An overview of the mixes is given in Table 2.

Mix number	Max aggregate size (mm)	RAP (%)	Binder	Aggregate type	Target density (kg/m³)	Target binder content (%) (m/m)	Application
252	22	65	70/100 + RAP binder	Scottish granite	2386	4.3	Base
248	22	60	70/100 + RAP binder	Scottish granite + ECO granulate	2368	4.3	Base
938	22	50	Sealoflex 5-50HT + RAP binder	Scottish granite + bestone	2390	4.3	Base / bind
210	16	0	40/60	Scottish granite + bestone	2351	4.3	Base / bind
212	16	65	70/100 + RAP binder	Scottish granite + bestone	2360	4.3	Base
218	16	60	70/100 + RAP binder	ECO granulate	2350	4.3	Base / bind
451	11	0	40/60	Bestone	2369	5.8	Top

Table 2 – Overview mixes in the Boskalis database

3.2.1 RAP

Five of the mixes contain RAP (reclaimed asphalt pavement). For environmental and economic reasons high amounts of this reclaimed asphalt content are used in mixes in The Netherlands. Only Jacobs (section 2.3.7) stated that he used data of mixes containing RAP for developing his model. Mixes with RAP should be included in the analysis since the goal is to support the functional verification process, which includes the verification of mixes with RAP. To keep the database as diverse as possible, mixes were chosen with different RAP contents.

The use of RAP in asphalt concrete mixes has the disadvantage that the properties of the RAP and the interaction with the new materials is unknown. Besides, the properties of the RAP (i.e. gradation, binder properties and density) can highly differ per batch of RAP. For this reason, only one batch of RAP is used for all the mixes. This makes a comparison between the different mixes more fair and limits the variation between specimens of the same mix, making the correlations with the asphalt concrete stiffness stronger (chapter 4). This RAP batch is obtained from the APA (Asfalt Productie Amsterdam). Multiple tests have been performed for characterizing the RAP for the calculation in the mix designs. A representative sample has been extracted. A machine washes the binder off the aggregates using Methylene. The clean aggregates are then sieved to obtain the sieve curve. By weighing the sample before and after the washing process, the binder content can be obtained (NEN-EN 12697-1). Finally, the mix of binder and methylene has been heated for the methylene to evaporate. The resulting bitumen has been used for binder research (paragraph 4.3).

3.2.2 Binder variation

The mixes contain different binders. The majority contain conventional binders, while the 938 mix contains a polymer modified binder. For the mixes containing RAP, the binder is a combination of the RAP binder and new 70/100 bitumen. The target binder content is 4.3% for all mixes except mix 451, which has a target binder content of 5.8% (m/m). This mix is the only surface layer mix in the database.

3.2.3 Gradation variation

The database also has variation in gradation. Different maximum aggregate sizes and different sieve curves have been used in the several mix designs.

3.3 Sample production

The asphalt concrete test specimens have been manufactured using the type test. In this type test, the gradation, aggregate type, and binder content are written. For the mixes with RAP, the gradation is a combination of the newly added aggregates and the aggregates in the RAP. First, the sieve curve of this RAP was obtained by sieving representative samples. Representative samples have been made according to NEN-EN 932-2 (NEN, 1999). It should be noted that it is difficult to obtain a representative sample, and that this can have a negative influence on the accuracy of the sieve curve of the RAP. Since the sieve curve of the RAP is fixed, the gradation of the mix can be adjusted by the added new aggregates. A calculation has been done to approximate the desired sieve curve. The amount of new binder has been chosen in such a way that the total binder content approximates the target binder content.

Since RAP batches differ in gradation and binder content, it is difficult to exactly reproduce the mix as used in type tests of RAP mixes. This makes the results of different researches on the same mix less comparable. However, the mixes within this database are built from the same batch of RAP. The differences in RAP should be taken into account when extending the database or by applying the models in chapter 2 and 6 on mixes build from different RAP batches. This can have an impact on the accuracy of the models.

The resulting mix design has been used to produce a plate with dimensions of 500*500*100 mm. The aggregates and binder have first been weighted and warmed, than mixed and finally poured into a mold. Using the dimensions of the mall, and the target density as specified in the type test, the amount of asphalt concrete needed is calculated. A roller is used to compact (static) the asphalt and to flatten the top of the plate. At the laboratory of Boskalis, a special ramp is used to compact the plate by the roller from different directions to simulate the field conditions. A ruler has been used to check the smoothness of the surface of the plate.

The plate was left for cooling for at least one day. Than the specimens are obtained from the plate using a pillar drill. For the CIT-CY, cylindrical specimens are used with a height of 40 mm and a diameter of 100 mm. A polishing machine was used to reduce the height to 40 mm by polishing both the top and bottom of the sample. In total 12 samples were produced per mix from which at least 8 were used to obtain the stiffness. The specimens were measured and weighted for determination of the density (both hydrostatic and volumetric). Finally the specimens were put in a climate chamber at 15°C. Marsac (1999) concluded that the asphalt concrete stiffness increases in time up to 5.4 MPa per day. For this reason, the samples were tested at the same age (+/- 6 weeks), with a maximum deviation of 1 week. In this way, it is ensured that the resting time of the specimens is not a highly influencing factor in the model.

3.4 Asphalt stiffness tests

The asphalt concrete stiffness data has been obtained by the CIT-CY test as described in paragraph 2.2. The new model will be used to predict the stiffness at a temperature of 20°C and a frequency of 8 Hz. For this test a Boskalis protocol is used. In this protocol the specimen is tested at one temperature and at frequencies of 30, 10, 8, 5, 2, 1, 0.5, 0.2, 0.1, and 30.0 Hz. The first specimen is used for finding the load corresponding to an approximate strain of 60 µm/m. It is assumed that this strain is high enough to measure the stiffness accurately without

damaging the specimen (viscous behaviour). The stiffness is determined at 30 Hz twice. If the outcomes differ highly (> 15%), the specimen is assumed to be damaged during the testing. As an extra check, the specimen is turned 90˚ and tested a second time. These results can be compared to get a feeling for the influence of the direction of testing.

3.5   Binder tests

All the existing models from chapter 2 use a predictive parameter that characterizes the binder. The model of Jacobs uses the traditional penetration as a predictive parameter, while most models use the binder stiffness. In older models, like the model of Francken, the binder is characterized indirectly by the penetration. The Van de Poel nomograph is used to convert this penetration index into the binder stiffness. The Witczak (1999) and Asphalt Institute model use the viscosity as predictive parameter for characterizing the binder.

All the binders used in the mixes have been tested separately. RAP is used in 5 mixes. These mixes contain both virgin bitumen and bitumen from the RAP. Since the latter is expected to have a large influence on the properties of the asphalt concrete, bitumen has been blended according to the mass ratios of the bitumen in the mix design. All binder tests have been performed on this blended bitumen as well. The following protocol has been used for this blending:

1. Obtain the recovered bitumen according to NEN-EN 12697-4 (NEN, 2015) and prepare the virgin and recovered bitumen according to NEN-EN 12594 (NEN, 2014). Pour the bitumen separately in clean moulds.
2. Cut or break the cold bitumen from the moulds in small pieces and add them together according to the mass ratio obtained from the mix design in a clean bucket.
3. Heat the bucket for 30 minutes at 180 ˚C (penetration bitumen) or 190 ˚C (polymer modified bitumen).
4. Stir the melted bitumen by hand 100 times clockwise and 100 times anti clockwise with an approximate frequency of 2 Hz.
5. Repeat step 3, step 4 and finally step 3.
6. Pour the warm bitumen.

The following binders were tested for the database:

a) RAP bitumen
b) Bitumen 40/60 (BituNed)
c) Bitumen 70/100 (BituNed)
d) Multiflex bitumen 100S
e) Sealoflex bitumen 5-50PA
f) Sealoflex bitumen 5-50HS
g) Sealoflex bitumen 5-50HT
h) Blended bitumen according to design mix 252
i) Blended bitumen according to design mix 248
j) Blended bitumen according to design mix 938
k) Blended bitumen according to design mix 218
l) Blended bitumen according to design mix 212

Bitumen d-g are polymer modified bitumen. k is a mix of RAP bitumen and polymer modified bitumen Sealoflex 5-50HT.

3.5.1 Traditional tests

Two penetration and Ring and Ball tests have been carried out for each of the virgin and blended bitumen according to NEN-EN1426:2015 and NEN-EN1427:2015 respectively (NEN, 2015). All tests have been carried out twice for research on the spread.

3.5.2 DSR tests

The Dynamic Shear Rheometer (DSR) has been used to obtain the binder shear stiffness and the viscosity of each binder. First three amplitude sweeps at -10°C, 20°C and 40°C were performed on each binder. In these dynamic tests an increasing strain was applied while the stiffness was continuously calculated. At a certain strain level (LVE), the stiffness will drop. This is an indication that the specimen has been damaged. The used software RheoCompass proposes a safe strain level at which the specimen will remain intact. This strain level was used in the frequency sweep tests. In the frequency sweep test, the specimen is loaded by a sinusoidal load at different frequencies (0.1-15 Hz) and temperatures (-10, 0, 10, 20, 30, 40, 50°C). The polymer modified binders have also been tested at 60°C and 70°C. A sample with a height of 2 mm and a diameter of 8 mm has been used for testing at temperatures of 20°C and lower, while a sample with a height of 1 mm and a diameter of 25 mm has been used at temperatures of 20°C and higher. Both samples were tested at 20°C. This division is made to satisfy the maximum capacity of the machine at lower temperatures and to ensure the accuracy at higher temperatures (a larger sample results in more accurate measurements). A master curve was constructed at a reference temperature of 20°C. Viscosity tests are carried out at high temperatures of 135°C and 150°C. In this test the DSR measures the viscosity (unit: MPa*s) at several combinations of shear strains and shear rates. It is chosen to define the viscosity as the average value at a shear rate of 500 [1/s] over the several shear strains. All the DSR tests are performed in duplicate for research on the spread of the data.

The models of chapter 2 use binder stiffness instead of shear stiffness as predictive parameter. The DSR uses the shear stiffness as output parameter. The linear elastic theory (equation 18) is used to convert this value to binder stiffness, assuming a Poisson ratio of 0.3. Pouget et al. (2012) determined the poisons ratio from experimental data of a 50/70 bitumen at 10°C as a function of the loading frequency and found values around this 0.3 for a frequency of 8 Hz. Even dough a Poisson's ratio of 0.3 is used throughout this report, it should be noted that this ratio can change for different temperatures, loading times and bitumen types. Additional binder properties, like the glassy modulus are also included in the database. This parameter can be obtained from the master curve. More detailed information is given in section 4.3.7.

3.6 Gradation parameters

The Witczak models use gradation parameters as predictive parameters. The sieve curve is directly obtained from the mix design. The weighing of the aggregates for building the asphalt concrete plate was done carefully at a scale. To check to gradation afterwards, a small amount of asphalt was crushed and washed. The clean aggregates were then sieved again. No significant differences (> 5%) were found.

Standard European sieve sizes C22.4, C16, C11,2, C8, C5.6, 2 mm, 0.5 mm, 180 μm and 500 μm were included in the database, as well as the American sieve sizes P200, P4, P38 and P34 for the Witczak and Asphalt Institute models, see chapter 2. The American sieve values are obtained using linear interpolation. The maximum aggregate size and the coefficients of uniformity and curvature are included in the database as well. More detailed information is given in paragraph 4.5.

3.7 Volumetric parameters

Returning predictive parameters in the existing models of chapter 2 are the volumetric parameters V_a, V_b, V_g, VMA (voids in mineral aggregates), and VFB (voids filled with binder). These values were all obtained using the volumetric density of the asphalt concrete, the bitumen density (as indicated by the producer) and the density of the aggregates. The latter has been calculated by the mix design and the individual densities of the new aggregates and the RAP aggregates which have been determined using a pycnometer, which is specified in test 79 (RAW, 2015).

The following relations were used to obtain the volumetric parameters:

$$V_b = \frac{M\%b * \rho_{asphalt}}{\rho_{bitumen}} \tag{28}$$

$$V_g = \frac{M\%g * \rho_{asphalt}}{\rho_{aggregates}} \tag{29}$$

$$V_g + V_b + V_a = 1 \tag{30}$$

$$VMA = V_a + V_b \tag{31}$$

$$VFB = \frac{V_b * 100}{VMA} \tag{32}$$

Where:

V_a = volume air voids (%)

V_g = volume aggregates (%)

V_b = volume bitumen (%)

M%b = mass percentage bitumen (%)

M%g = mass percentage aggregates (%)

$\rho_{asphalt}$ = density asphalt concrete (kg/m^3)

$\rho_{bitumen}$ = representative density bitumen (kg/m^3)

$\rho_{aggregates}$ = representative density aggregates (kg/m^3)

VMA = voids in the mineral aggregate (%)

VFB = voids filled with bitumen (%)

3.8 Comparison databases

The variation in predictive parameters in the database defines the applicability of a model based on this database. In Table 1, the Boskalis database can be compared to the databases used for the existing models presented in chapter 2. The Boskalis database has the advantages of uniformity in tests and test conditions and equally aged specimens during testing. These influence factors will not be a cause of spread during the development of a new model. The disadvantage is that those influencing factors cannot be examined. The database includes RAP and modified binders, which are commonly used nowadays, but which are missing in the databases of some older models. However, since only asphalt concrete mixes are included, the model's applicability on porous asphalt and stone mastic asphalt (SMA) cannot be guaranteed. Variation in volumetric parameters V_a, V_b, and V_g is limited compared

to the database used for the Shell model. The same holds for the penetration. Therefore, a model based on the Boskalis database will presumably have a smaller range of validity for these predictive parameters compared to a model based on the Shell database.

4   Predictive parameters

4.1   Introduction

The existing models presented in chapter 2 use different predictive parameters in different combinations and with different units. A new model should include predictive parameters that fulfil the following conditions:

1. The predictive parameter has a strong correlation with the asphalt concrete stiffness. This relation should be a causal relationship.
2. The predictive parameter can be obtained as easily and precisely as possible (see also section 4.3.1).

All possible predictive parameters included in the database are reviewed separately in the following chapters. First the asphalt stiffness itself is reviewed in paragraph 4.2. The predictive parameters are reviewed in the paragraphs 4.3 – 4.5.

4.2   Asphalt concrete stiffness S_{mix}

The stiffness is defined as the relation between the applied stress and the resulting strain. Asphalt concrete is a viscoelastic material and behaves differently at different temperatures and loading frequencies/times. Multiple quantities have been introduced for describing the stiffness of asphalt concrete. The resilient modulus is the stiffness obtained by a load without a specified waveform and rest period. The complex or dynamic modulus is the stiffness obtained by a sinusoidal or haversine load with no rest period. This complex modulus can be divided in the storage and loss moduli, which represent the part of the energy that is stored in the material and the part that is dissipated (''lost'') during loading. The complex modulus is often referred to as the dynamic modulus, as used in the majority of the presented models in chapter 2 (Huang, 2004). The older models of Francken and Shell use the term stiffness modulus for describing the dynamic modulus. In this report, we refer to this dynamic modulus by the term asphalt concrete stiffness.

The results of the asphalt stiffness tests as described in paragraph 2.2 were checked for large deviations. First, the stiffness measured at the beginning of the test is compared to the stiffness measured at the end of the test. The test starts and ends with a loading frequency of 30 Hz. The average difference between both 30 Hz stiffnesses of all mixes was 2.75%. No tests exceeded the 15% difference, where the specimen is assumed to be damaged. Most of the specimens were tested a second time, for which the specimen was turned approximately 90°. Subsequently, the difference was calculated between the 8 Hz stiffness values. The average difference for all mixes was 5.0%. 3 stiffness values were not included in the database since their difference was larger than 15% after turning them 90°. In this case the specimen was assumed to be damaged. The range of stiffnesses is 6234 MPa to 10787 MPa. The number of valid stiffness values per mix varies from 8 to 12. An overview of the average stiffness values per mix is given in Figure 6.
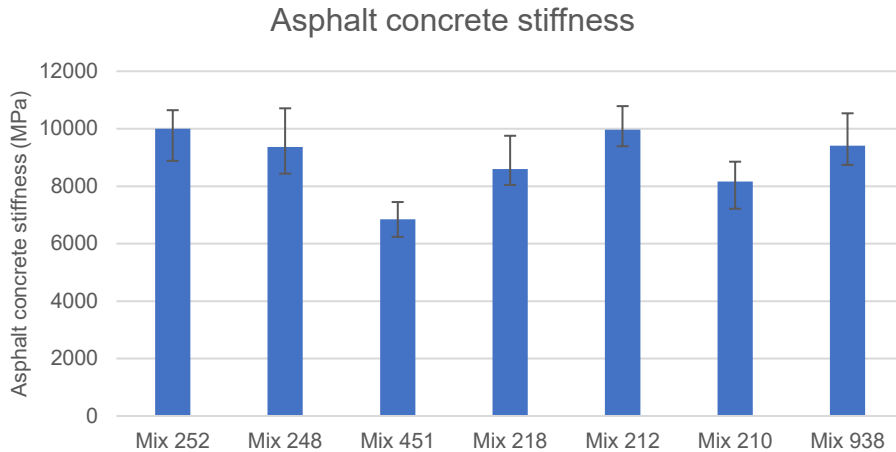
Figure 6 - Asphalt concrete stiffness

It can be seen from the figure that the measured stiffness value ranges of the mixes overlap. Most of these mixes can be seen as similar when it comes to their stiffness. This implies that the possibilities of distinctively measuring the stiffness are limited, despite the facts that there is quite some variation in stiffness values and the assumed damaged specimens are left out. The stiffness range within each mix is large compared to the total range of stiffnesses. It should be noted that only one type of asphalt (asphalt concrete) with similar stiffnesses is included in the database, which keeps the variation limited. The variation within one mix can be caused by measurement errors, unexpected permanent deformation during testing and differences in the individual specimens of each mix. These can differ in compaction and composition. More large aggregates can be present in a specimen by chance. The unpredictability of the composition of the RAP can also increase the data spread (Figure 7).

Figure 7 – A piece of metal was found in the specimen during polishing

4.3   Binder characterization parameters

4.3.1   Precision

Binder properties are obtained using the DSR and traditional tests as described in paragraph 3.5. All tests were performed in duplicate. As stated before, a predictive parameter should be precisely determinable. A test result is called precise in this report if the measurement error is small compared to the range of test results. This ratio is called the precision of parameter X,

which is mathematically described by equation 33 for the Boskalis dataset. n Different types of bitumen are included, with two measurements ($X_{n,1}$ and $X_{n,2}$) for each bitumen.

$$precision(X) = \frac{average\ measurement\ error(X)}{range(X)} * 100\%$$

$$= \frac{\sqrt{\frac{\sum_{i=0}^{n} Var(X_{n,1}, X_{n,2})}{n}}}{\max(X) - \min(X)} * 100\% \tag{33}$$

The equation has been used to obtain the precision of all the binder characterization parameters. It can be seen from Figure 8 that the viscosity and softening point can be obtained precisely while the glassy modulus cannot be obtained precisely. All binder properties satisfy an assumed maximum precision of 5%, except the phase angle and glassy modulus.
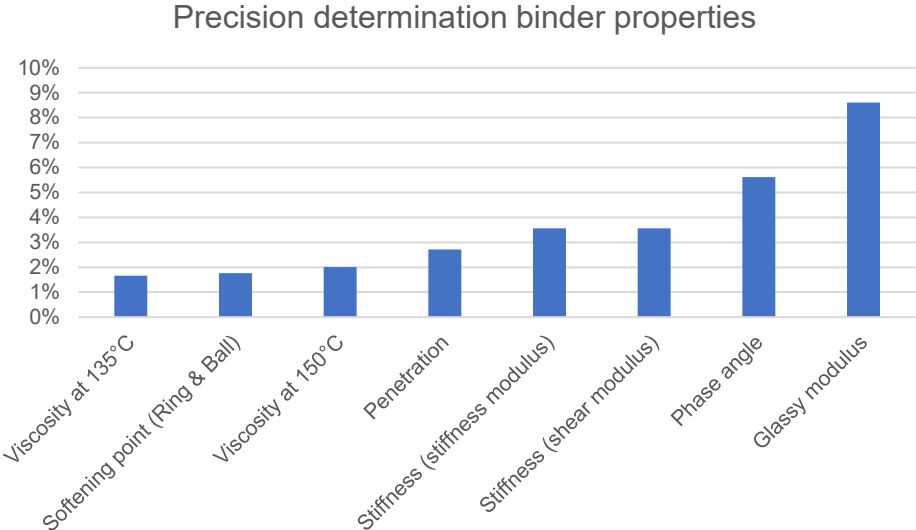
Figure 8 - Precision determination binder properties

It should be noted that these values can change by extending the database. By plotting the residues as a function of the actual value of the parameter, the precision can further be investigated. An example of such a residue plot is given in Figure 9. From the funnel-shaped point cloud it can be concluded that the larger the Pen value, the larger the deviation, and the smaller the precision. If a model uses the penetration as a predictive parameter, the accuracy will decrease at increasing pen values. Similar plots have been made for the other binder characterization parameters and are included in Appendix D. A funnel-shaped point cloud can be found in the Ring and Ball residue plot as well. The other parameters show no clear relation between the measured value and the residue. It can be concluded that the precision is independent on the measured value for those cases.

Figure 9 - Residue plot penetration

4.3.2   Binder stiffness

The binder stiffness is included as a predictive parameter in five of the models presented in chapter 2. The value is obtained from the master curve which is computed by the program RheoCompass. This program combines the stiffness results at different loading frequencies and temperatures into one master curve at a reference temperature of 20°C. Since the CIT-CY tests are conducted at a temperature of 20°C and 8 Hz, the binder stiffness values are obtained for the same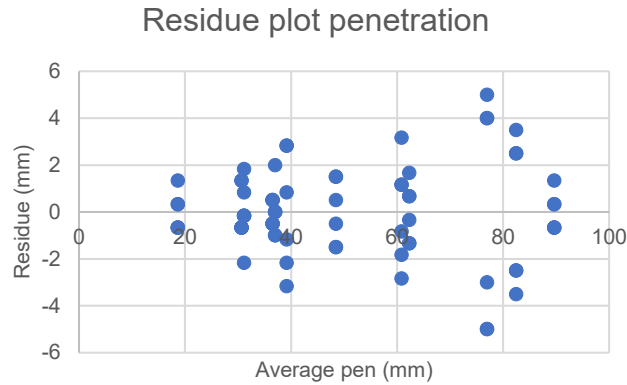 conditions. When a data point was not available at a frequency of 8 Hz, linear interpolation was used. The linear elastic theory (equation 18) is used to convert this value to binder stiffness, assuming a Poisson ratio of 0.3. Pouget et al. (2012) determined the poisons ratio from experimental data of a 50/70 bitumen at 10°C as a function of the loading frequency and found values around this 0.3 for a frequency of 8 Hz. Even dough a Poisson's ratio of 0.3 is used throughout this report, it should be noted that this ratio can change for different temperatures, loading times and bitumen types.

From theory, the binder stiffness is the most preferred binder characterization parameter to be included as a predictive parameter in a new asphalt concrete stiffness prediction model, since both parameters describe the same characteristic and bitumen is a component of asphalt concrete.

Three types of binders were tested: Virgin bitumen from the oil refinery, reclaimed RAP bitumen and blended bitumen according to the mass ratios in the different mix designs (paragraph 3.5). Most existing models presented in chapter 2 are based on databases without mixes with RAP. Using the blended binder properties as input for those models is an option for taking the influence of the RAP binder into account. The RAP binder can have a significant influence on the properties of the blended binder. For example, the 212 mix has a RAP content of 65%. The virgin 70/100 binder has a stiffness of 9.31 MPa (8 Hz, 20°C), while the RAP binder has a stiffness of 48.19 MPa. The blended bitumen of this mix has a stiffness of 31.86 MPa. For this reason, in a new prediction model, the influence of the RAP binder should be taken into account. A plot of the *virgin* bitumen as a function of the asphalt concrete stiffness is given in Figure 10. RAP bitumen is not taken into account here.
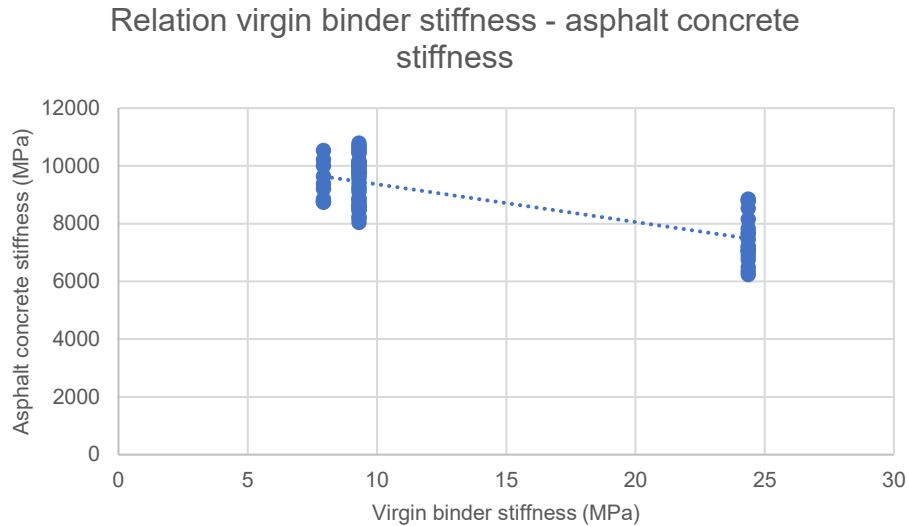
Figure 10 - Relation virgin binder stiffness - asphalt concrete stiffness, leaving out the effect of the RAP binder

This graph shows a negative relation between asphalt concrete stiffness and binder stiffness, which is highly illogical. It implies that using a stiffer binder results in a less stiff asphalt concrete pavement. This confirms the proposition that the influence of the RAP binder cannot be neglected. It should be noted that there is not only variation in binder stiffness in the specimens, but also in gradation and volumetric parameters. No correction for these variations was made for the binders in Figure 10.

In Figure 11, the blended binder stiffnesses are plotted versus the asphalt concrete stiffness. For the mixes without RAP, the binder stiffness of the virgin bitumen has been used on the horizontal axis. The brown line represents the linear trend line (least squares solution) for the stiffnesses of all the mixes with conventional penetration bitumen. In the graph, a distinction is made between the mixes.
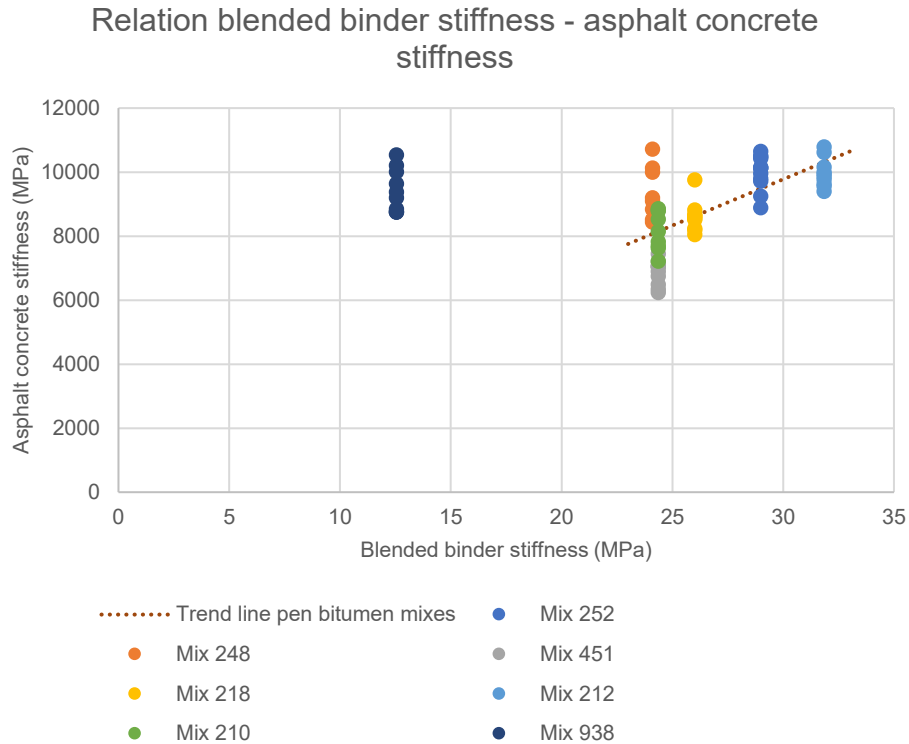
Figure 11 - Relation blended binder stiffness - asphalt concrete stiffness

From the graph it can be seen that there is a clear positive relationship between the stiffness of the blended bitumen and the asphalt concrete stiffness. An outlier is mix 938, which has not been used in computing the trend line. This asphalt concrete mix has a relatively high stiffness compared to the very low blended binder stiffness. It should be noted that mix 938 is the only mix with a polymer modified binder, which can be the cause. In the new model, extra care should be taken in the prediction accuracy of mixes with polymer modified binders. From Figures 10 and 11 it can also be concluded that there is no perfect relation between S_{mix} and S_{bit}, since there is significant spread in the S_{mix} measurements. This spread is visible as large 'columns' of data points for each mix. It confirms the assumption that there are more relevant parameters to be included for developing a new accurate model.

4.3.3 Van der Poel nomograph

It can be seen from Table 1 that the Shell and Francken models use the Van der Poel nomograph (Appendix A) to determine the binder stiffness. These models were developed in times where no Rheometers were available, and only conventional bitumen were used in asphalt concrete mixes. The Van der Poel nomograph is based on simple creep and dynamic tests (Van der Poel, 1954). Shahin and McCullough (1972) tried to find an equation that fits the Van der Poel nomograph and found the following relations:

For $10^{-8} < S_{bit} < 1$ MPa;

$$
\begin{aligned}
log_{10}S_{bit} = {} & -1.90072 - 0.11485T - 0.38423PI - 0.94259\log t - 0.00879T * \log(t) \\
& - 0.05643PI * \log(t) - 0.02915(\log(t))^2 - 0.51837 * 10^{-3}(T^2) \\
& + 0.00113 * (PI^3 * T) - 0.01403 * (PI * T^3) * 10^{-5}
\end{aligned} \tag{34}
$$

For 1 < S_{bit} < 2000 MPa;

$$log_{10}S_{bit} = -1.35927 - 0.06743T - 0.90251\log(t) + 0.00038T^2 - 0.00138 \\ * (T * \log(t)) + 0.00661 * (PI * T)$$ (35)

Where:

t = loading time (1/f) (s)

T = test temperature minus softening point (°C)

PI = penetration index (equation 36) (-)

Shahin found for the two relations a determination coefficient (R^2) of 0.99 and 0.98.

Using these formulas, the applicability of the Van der Poel has been examined using the Boskalis dataset as presented in Figure 12. The loading time and temperature were chosen equal to the test conditions (1/8 s and 25 °C). The PI values follow from equation 36 and take values between 0.05 and 8.60. The measured shear stiffness values have been converted to stiffness values by equation 18 and assuming a Poisson constant of 0.3.
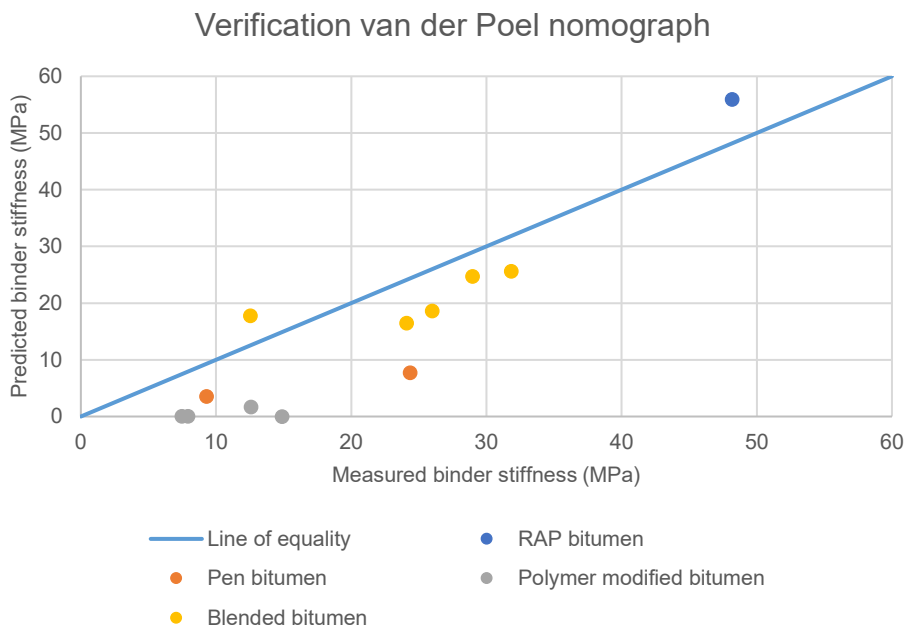
Figure 12 - Verification van der Poel nomograph

From the graph it can be concluded that the relation is inaccurate for these bitumens. In general, the Van der Poel nomograph underestimates the binder stiffness for these bitumens, but a positive relation can be observed. The best prediction is made for the RAP bitumen. The relation works surprisingly well for blended bitumen but the model is incapable of predicting the stiffness of polymer modified bitumen as expected. The model was not developed for the stiffness prediction of these polymer modified bitumen. The left outlier from the blended bitumen is mix 938, which contains a polymer modified binder as well. It should be noted that the softening and penetration measurements themselves can be inaccurate as well, but from Figure 8 it can be concluded that this inaccuracy is limited. A Poisson ratio of 0.3 is used to convert the binder shear stiffness into stiffness values by equation 18, which is an assumption.

Since polymer modified bitumen are used on a wide scale these days, and their stiffness predictions by Van der Poel are inaccurate, the use of the nomograph has no preference. Stiffnesses obtained by the Van Der Poel nomograph can differ significantly from measured stiffnesses. Using measured and predicted bitumen stiffness values as input for a model at the same time decreases the precision of this parameter. It will result in a lower accuracy of an asphalt concrete stiffness prediction model in the end.

4.3.4   Binder viscosity

Viscosity is a parameter that is included in the Witczak (1999) and Asphalt Institute models. The parameter requires extra research since it is difficult to measure the viscosity at room (20°C) temperature. At this temperature the binder is too stiff to easily measure the resistance to flow. A distinction is made between dynamic viscosity η (the ratio between shear stress τ and shear rate γ') and the kinematic viscosity ν (dynamic viscosity η divided by the density). It is unclear which kind of viscosity should be used as input for the models. Witczak used equation 21 for the determination of the viscosity. The viscosity is related to binder stiffness here. Since no density is included in this relation, it is assumed the dynamic viscosity is used by Witczak. The same holds for equation 13 with only the penetration as predictive parameter, which is used in the Asphalt Institute model. Both equations estimate the viscosity at a temperatures of 20°C. In the DSR, viscosity tests have been performed for the determination of the viscosity at temperatures of 135°C and 150°C.

The viscosities obtained by Witczak (equation 21), by Asphalt Institute (equation 13) and by measurements (section 3.5.2) show few similarities. The Witczak and Asphalt Institute show a quite linear mutual relation (trend line with $R^2 \approx 0.8$), but their viscosity results differ about a factor 100. There is no clear relation between the Witczak or Asphalt Institute viscosities and the measured viscosity data at high temperatures. The difference in temperature can be a cause of this missing relation, since the viscous behaviour of bitumen strongly depends on the temperature. The state of the bitumen changes from approximately solid to liquid in the temperature range 20°C - 150°C. At low temperatures, the flow of the material, which is closely related to the viscosity, will be much lower than at high temperatures. The measured viscosity at the two temperatures are quite similar and show an accurate linear correlation ($R^2 = 0.97$).
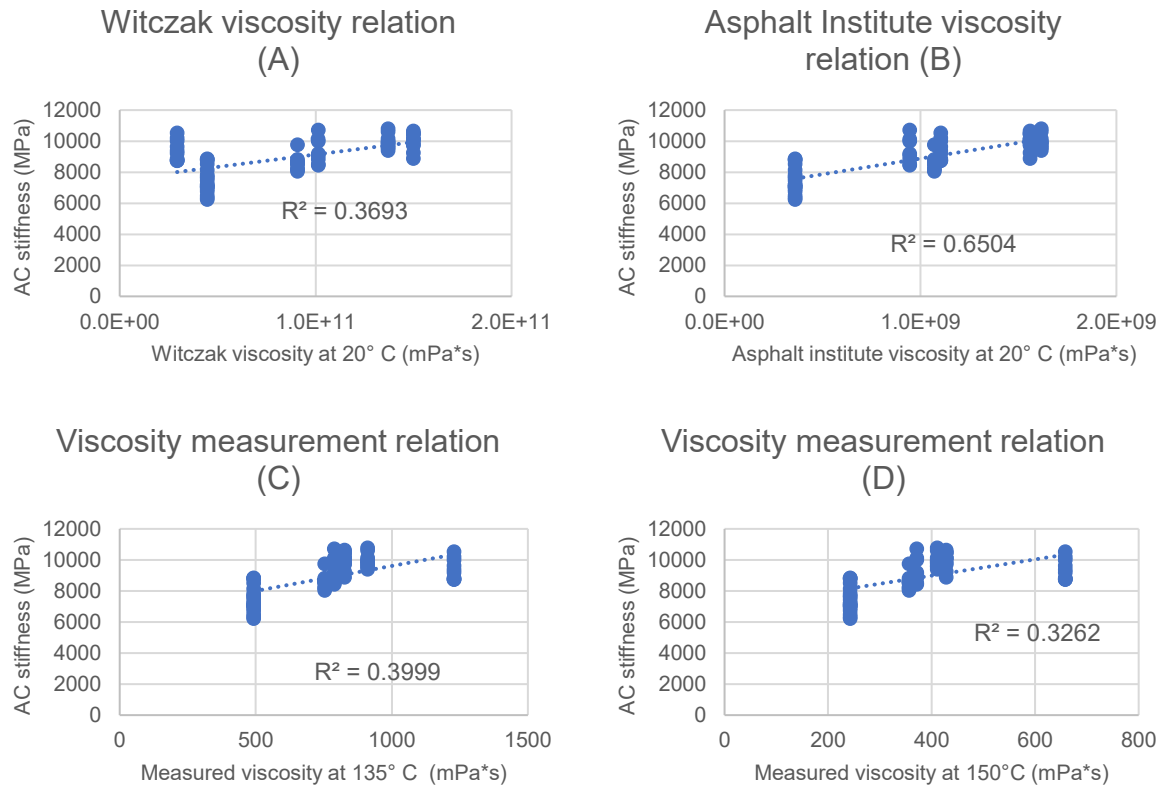
Figure 13 – Overview mutual stiffness relations

In Figure 13, the relation between the viscosity (both measurements and models) and the asphalt concrete (AC) stiffness is visualized. All relations are positive, but not accurate. The relation used in the Asphalt Institute model has the highest determination coefficient (R^2 = 0.65), while the measured viscosity shows even lower values ($R^2 \approx 0.35$). Like the binder stiffness, the large spread in asphalt concrete data is visible as large 'columns' of data points. It implies that viscosity cannot be the only predictive parameter in a highly accurate model.

It is questionable if the binder viscosity is theoretically a good predictive parameter for asphalt concrete stiffness. Asphalt concrete is a viscoelastic material, which means it has both viscous and elastic properties. In a short time frame and at low temperatures during loading, no creep or relaxation will be visible and the material will behave like a purely elastic material. In a large timeframe and at high temperatures, the material will start to flow in the form of creep or relaxation. Depending on the circumstances, the behaviour of the asphalt concrete is somewhere in between. Stiffness tests, including the CIT-CY, are aimed at measuring elastic responses. The material is loaded by high frequencies (short time frame) and at room temperatures, where the material approximates a purely elastic material. The tests which are used to characterize the binder should also be intended to measure elastic response. However, viscosity tests are aimed at measuring viscous response. Viscosity is defined as the resistance against a shear deformation gradient. In other words, viscosity is the force or stress that is needed to apply a shear deformation gradient (shear rate) of 1 / s (Mezger, 2014). This characterizes the flowing behaviour of the material, which is a form of viscous behaviour. For this reason, the binder stiffness, which is a test on elastic responses of the binder, is preferred over the viscosity as a binder characterization predictive parameter from a theoretical point of view.

The positive relations found in Figures 13C and 13D is not necessarily a causal one, since binder viscosity and asphalt concrete stiffness are describing different properties of different materials. More doubts about this relation arise by looking at the relation measured binder viscosity (135°C) – binder stiffness, which is a step in between. No clear relation can be found here ($R^2 \approx 0.03$). The same holds for Witczak and Asphalt Institutes viscosities and the measured viscosity at 150°C.

In conclusion, preference is given to other predictive parameters for the characterization of the binder in an asphalt concrete stiffness prediction model, like the binder stiffness. The accuracy of the relations asphalt concrete stiffness – binder viscosity is comparable to the relation asphalt concrete stiffness – binder stiffness. The best correlations can be found using the Witczak and Asphalt Institute models. However, using a model as input for another model is undesirable, since it entails extra assumptions and is at the expense of the accuracy. Besides, extra care should be given to the predictive parameters of those 'input models'. Also theoretically preference is given to the binder stiffness. From Figure 8 it can be seen that both the viscosity and the binder stiffness can be determined precisely (< 5%).

4.3.5 Traditional binder characterization parameters

For all binders used in chapter 3, the traditional binder characterization parameters penetration (in dmm) and softening point (in °C) have been determined. All tests have been performed in duplicate, which resulted in 6 (2*3) penetration results per binder and 4 (2*2) ring and ball softening point values. The average value of all results have been used in the analysis. Interesting is the precision. According to Figure 8, the parameters penetration and softening point can be determined with high precision (< 5%).

The two tests describe another parameter. The penetration is a measure for the consistency of the binder at a temperature of 25°C. At this temperature, the material is close to a solid condition. For this reason, the penetration parameter is comparable to the binder stiffness (defined at 20°C in the Boskalis database), even though the specimen endures plastic deformation in the penetration test. This assumption is supported by the high Pearson correlation coefficient of -0.81. The minus sign confirms the reasoning that a higher penetration will be found by testing a binder with a lower stiffness. They are to a certain extend interchangeable. It is not recommended to use both parameters in one model in order to avoid collinearity.

The softening point is a parameter that has a more close relation to the viscous behaviour of the binder. The specimen is loaded for a longer period and the temperature is higher in general. At the softening point, the material has flowed over a distance of 25.4 mm or 1 inch between the ring and the plate. This reasoning is confirmed by the high Pearson correlation coefficient between the softening point and the viscosity at 135°C of 0.89, which means they are interchangeable to a certain extend. The correlation with the binder stiffness is much lower (-0.36).

By combining the penetration and softening point, the penetration index was calculated by the following formula (Scarpas et al, 2015):

$$PI = \frac{20 * T_{R\&B} + 500 * \log(Pen) - 1952}{T_{R\&B} - 50 * \log(Pen) + 120} \tag{36}$$

This relation is a measure for the temperature dependency of the viscosity of the binder (Scarpas et al, 2015). In theory, this property has no clear relation with the asphalt concrete

stiffness. Viscosity and stiffness are describing different material characteristics as described in section 4.3.4. Besides, all stiffness values in the Boskalis database are determined at a temperature of 20°C. The temperature dependency is not part of the problem definition.

The relations of these traditional parameters with the asphalt concrete stiffness have been plotted in Figure 14. For the mixes with RAP, the test results from the blended bitumen have been used.
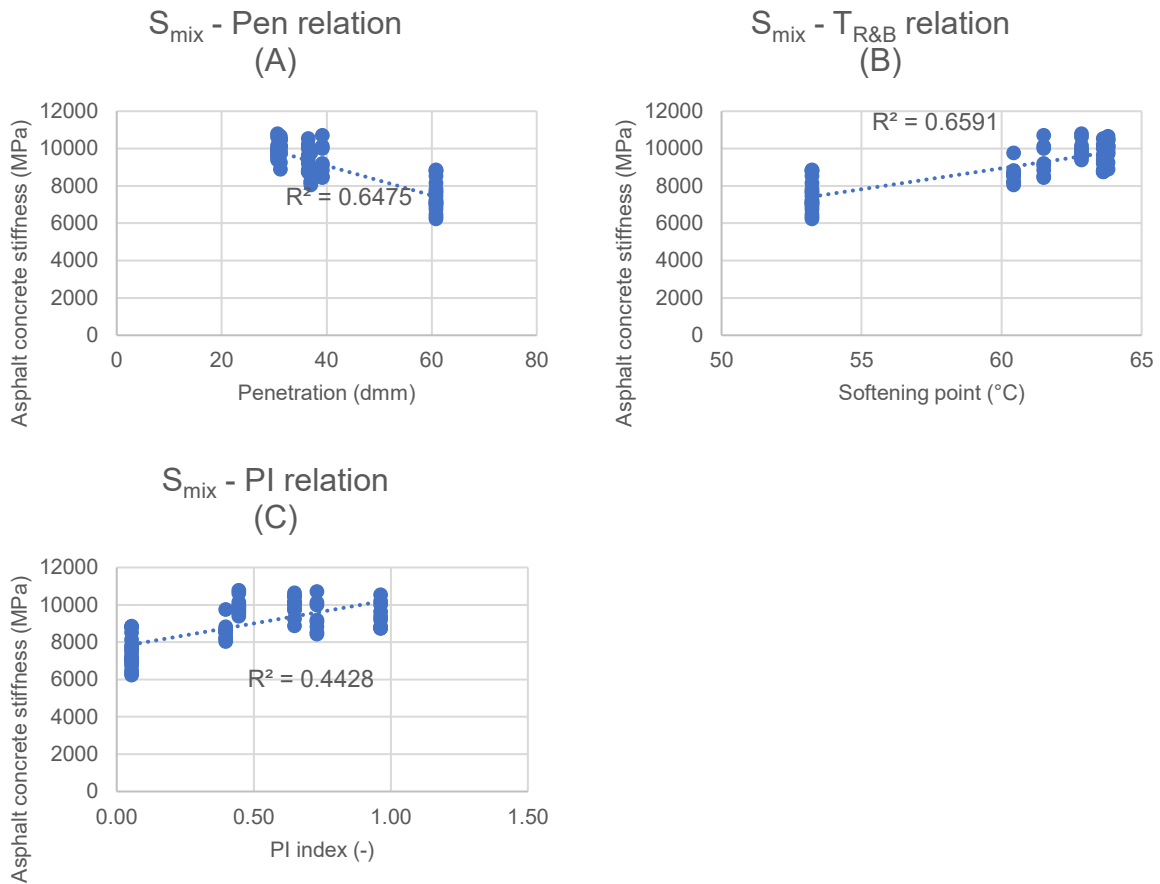
Figure 14 – Relations asphalt concrete stiffness – traditional parameters

From the graphs it can be concluded that the penetration index has no clear relation with the asphalt concrete stiffness, which confirms the theory. The relations of the penetration and softening point with the asphalt concrete stiffness are similarly accurate and the sign of the relations is in line with the expectation. From a theoretical point of view, the penetration is a preferred prediction parameter over the softening point, since the first is more closely related to the binder stiffness, and thus to the asphalt concrete stiffness. From Figure 8 it can be concluded that both parameters can be determined accurately.

4.3.6   Combined penetration relation

For estimating the penetration of a mix of bitumen, the following well known relation can be used for estimating the penetration of a mix of bitumen.

$$A * \log(Pen_A) + B * \log(Pen_B) = (A + B) * \log(Pen_{mix}) \qquad (37)$$

In this relation, A and B represent the masses of bitumen which have been mixed. The rule can be of great use in an asphalt concrete stiffness prediction model, since it could make the blending process from paragraph 3.5 unnecessary. However, from Figure 15, it can be seen that the range of predicted penetration values is smaller than the range of measured penetration values. It can be concluded that the relation is not accurate enough to be used for an asphalt concrete stiffness prediction model. As stated in section 3.1.3, it is undesirable to use a model for the determination of a predictive parameter for another model, since this is at the expense of the accuracy of the prediction.
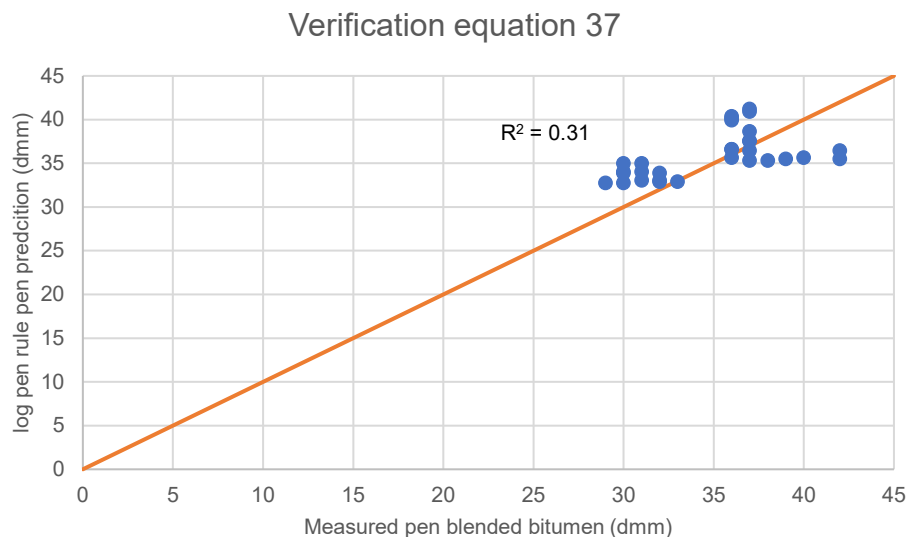
Figure 15 - Verification equation 37

4.3.7   Binder glassy modulus

Francken (section 2.3.3) and Al-Khateeb (section 2.3.6) both use a form of the glassy modulus of the binder as predictive parameter in their model. This modulus can be interpreted as the stiffness value where the material behaves like glass. As mentioned before it follows from earlier research that small changes in this parameter results in large deviations in the asphalt concrete stiffness using the Francken model (Mohan, 2010). However, a constant glassy modulus value of 3000 MPa may be assumed according to Francken, and a constant glassy shear modulus value of 1000 MPa may be assumed according to Al-Khateeb . Four options were proposed for the determination of this glassy modulus:

I.   By determination of the upper asymptote of the master curve. This is the maximum 'glassy' stiffness value the material can have.
II.   From the relation phase angle – binder stiffness. The glassy modulus can be determined by finding the stiffness at which the phase angle is equal to 0 (Anderson, 1994).
III.   By determination of the Fraass breaking point, which is the temperature at which the bitumen first becomes brittle determined in the Fraass breaking point test (NEN, 2015). By finding the stiffness at this temperature, a measure for the glassy modulus can be found.
IV.   Using the Bending Beam Rheometer, which measures the stiffness at low temperatures (NEN, 2012), which can be an indication of the glassy modulus.

The tests considered in III and IV have not been performed for the database as presented in chapter 3, so the glassy modulus was obtained directly from the stiffness data by method I and II.

I. Asymptote method

A master curve can mathematically be described as a sigmoid, which is an S shaped function with two asymptotes, which are fixed values at the y-axis. Since the binder stiffness can never be negative, the lower asymptote will be close to 0. The upper asymptote will give an indication of the glassy modulus. This asymptote is invisible for the master curves of the dataset since the used rheometer is incapable of conducting tests at extremely high frequencies and low temperatures. For this reason, the graph was extrapolated by fitting a sigmoid function using a least squares solution. The master curve is usually plotted at a logarithmic scale on both axes. The used function for fitting the master curve contains a logarithm at both sides of the equal sign for this reason:

$$log|G*| = \delta + \frac{\alpha}{1 + e^{\beta + \gamma(\log(\frac{1}{f}))}}$$

(38)

At very high frequencies, the y value of the upper asymptote of this graph, which is assumed to approximate the glassy modulus, can be mathematically described as:

$$G_{bit,inf} = 10^{\delta + \alpha}$$

(39)

Note that the master curve obtained from the DSR software gives the shear stiffness as output. By assuming a Poisson ratio of 0.3, this value can be converted to S_{bit} by equation 18.

In Figure 16, the master curves (shear moduli) of modified bitumen Sealoflex 5-50PA have been plotted with their corresponding fit.

Figure 16 - Mastercurve fitting Sealoflex 5-50PA

From this graph it can be concluded that the sigmoidal fit is not accurate at low frequencies when presented in log log scale. To achieve this fit, a standard least squares solution has been used. A better fit in log log scale could possibly be achieved by introducing a logarithm in the least squares equation (equation 40). In this way, the fit is less dominated by large errors at high frequencies.

$$\sum \left(\log \frac{measured\ data}{predicted\ data} \right)^2 \rightarrow min \tag{40}$$

This approach led indeed to better fits at low frequencies, but this was at the expense of the accuracy at high frequencies. The high frequencies lie closer to the upper asymptote, which is the point of interest. For this reason, the inaccuracy of the fit at low frequencies in a logarithmic scale is ignored, and a normal least squares error solution has been used. This resulted in accurate fits at high frequencies (+/- 1 MPa for the last 5 data points). In Figure 16 the two independent master curves have been plotted. At the frequency range of the measured data, the two curves lie close to each other. It can be seen from the graph that despite the high accuracy of the fit, the error between both master curves grows due to extrapolation by the sigmoidal fits. The dashed lines represents the asymptotes of both fits. Due to the logarithmic scale, the picture is distorted, and the shear moduli corresponding to the asymptotes differ significantly. A glassy shear modulus of 652 MPa ($S_{bit,inf}$ = 1695 MPa) was found for the first dataset, while for the second dataset a value of 915 MPa ($S_{bit,inf}$ = 2379 MPa) was found.

II.   Phase angle = 0 method

Anderson (1994) suggested that the glassy modulus can be estimated by finding the stiffness at which the phase angle is 0. At this phase angle, the material behaves completely elastic. An applied stress results directly in a strain without any phase lag. This phase angle is an output parameter of the DSR master curve analysis as well. The phase angle is given in relation with the frequency. If the frequency corresponding to a phase angle of 0 is known, the corresponding binder stiffness modulus can be found using the master curve. This method requires fits for both the phase angle and the stiffness modulus. A sigmoidal function has been used to fit the phase angle curve as well. Since the phase angle is usually plotted at a logarithmic frequency axis and a linear phase angle axis, the following curve was used for fitting:

$$\phi = \delta + \frac{\alpha}{1 + e^{\beta + \gamma(\log(\frac{1}{f}))}} \tag{41}$$

A normal least squares error was used for fitting the relation. The fitted line, and the process of finding the glassy modulus by this method is graphically presented in Figure 17.
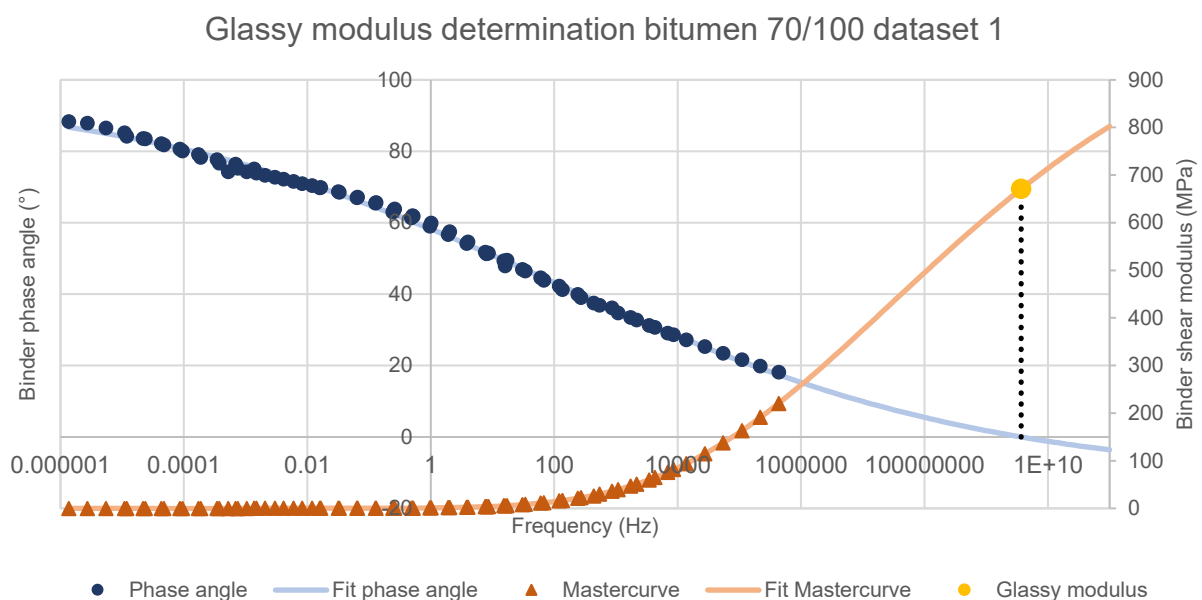
Figure 17 - Glassy modulus determination bitumen 70/100 dataset 1

A first look onto this graph suggests that this approach is a solid method for the determination of the glassy modulus. However, the method has some large drawbacks which are listed below:

- The method is based on two fitted sigmoid functions instead of one, which makes the prediction at least twice as unreliable as the asymptote method (I).
- It is unclear which curve form can best be used for fitting the phase angle data. The S-shape is not clearly visible for the phase angle data of some binders. Using equation 41 for fitting give highly inaccurate results for some binders.
- For many binders no intersection between the fitted phase angle relation and the x-axis was found since the lower asymptote of the sigmoid has a positive phase angle value.

According to this analysis, there is no stiffness were the phase angle is equal to 0, and no corresponding glassy modulus can be found.

- The phase angle is 0 at high frequencies. At those frequencies, the phase angle relation approaches its asymptote, which means the slope of the curve becomes gentle. A small change in the fitted formula will shift the intersection with X axis significantly. This makes the prediction even more relying on a good fit with the data, which is a difficult task as mentioned before.
- If the lower asymptote of the phase angle sigmoid fit was negative, glassy modulus values were found that highly differ from the values found using the first (I) method.

For these reasons the asymptote method (I) was used for determination of the glassy modulus. For all binders in the Boskalis database, two independent master curves were obtained. For each master curve, a glassy modulus was found. The average of these two values was used in the continuation of this research. The two values and their average can be read from Figure 18. Note that the shear moduli have been converted to stiffness moduli here using equation 18 and assuming a Poisson ratio of 0.3.
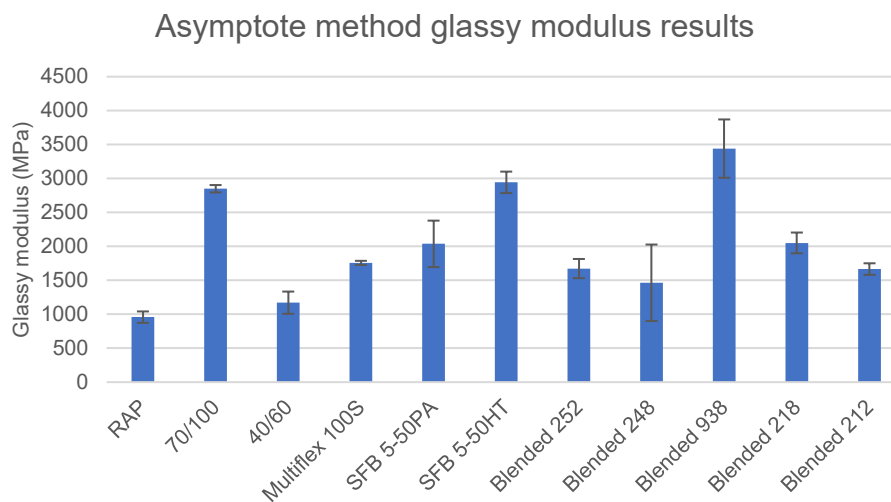
Figure 18 - Asymptote method glassy modulus results

It can be seen from the figure that glassy modulus values of the same binder can differ significantly. The precision of the parameter is low, which is confirmed by Figure 8. For some binders, like the 70/100 bitumen, the glassy modulus results were quite similar. The blended bitumen glassy moduli vary widely. Francken (1987) used a glassy modulus of 3000 MPa in his model which was assumed to be a safe upper limit for all bitumen. It can be concluded from the above results that the actual glassy moduli can come close to this value. The glassy modulus of mix 938 even exceeds this value. It should be noted that Pouget et al (2012) showed that at high loading frequencies the Poisson ratio decreases, which would lower the glassy modulus results in Figure 18. A significant spread can be observed in the glassy modulus results in general. Assuming a fixed glassy modulus value of 3000 MPa is inaccurate. This is in line with Mohan's conclusion (2010). The glassy moduli obtained using this asymptote method will be used in the further analysis of the Francken and Al-Khateeb models in section 5.3.2.

4.3.8 Mutual relations binder characterization parameters

An overview of the Pearson correlation coefficients between each binder characterization parameter and the asphalt concrete stiffness is given in Table 3. It should be noted that the Pearson correlation coefficient only considers linear relations. Other variations in the mixes, like the volumetric proportions and the gradation fluctuate as well.

Parameter	Pearson correlation coefficient with asphalt concrete stiffness
Ring & Ball softening point blended bitumen	0.81
Penetration blended bitumen	0.80
Glassy modulus virgin bitumen	0.76
Stiffness virgin bitumen	0.76
Penetration virgin bitumen	0.75
Phase angle blended bitumen	0.73
Phase angle virgin bitumen	0.71
Viscosity 135°C blended bitumen	0.63
Viscosity 150°C blended bitumen	0.56
Glassy modulus blended bitumen	0.32
Viscosity 150°C virgin bitumen	0.23
Stiffness blended bitumen	0.16
Ring & Ball softening point virgin bitumen	0.10
Viscosity 135°C virgin bitumen	0.09

Table 3 – Correlation between binder characteristics and asphalt concrete stiffness

Traditional binder characterization parameters penetration and softening point of the blended bitumen show a high correlation with the asphalt concrete stiffness. Viscosities of both virgin bitumen and blended bitumen show a less clear relationship. Surprising is the low correlation between the stiffness of the blended bitumen and the asphalt concrete stiffness. As mentioned before, it should be noted that this low correlation can be partly explained by the polymer modified bitumen in mix 938. By leaving this mix out of the analysis, the correlation coefficient increases significantly from 0.16 to 0.67.

To keep a new asphalt concrete model simple, it should include as few parameters as possible, with the best possible prediction results. Some predictive parameters are mutually related. This implies they are to a certain extend interchangeable in a model. This is the case for the softening point and the viscosity as described in section 4.3.5. Binder stiffness and penetration are also interchangeable as described in section 4.3.5. Adding both parameters will result in collinearity (Field, 2013), reducing the reliability of a model. Other strong correlations can be found between Ring & Ball softening point and PI, Ring & Ball softening point and viscosity, and glassy modulus and viscosity. A matrix with all mutual relations between binder characterization parameters can be found in Appendix E.

4.3.9 Conclusion binder characterization parameters

The following can be concluded for binder characterization predictive parameters for a new asphalt concrete stiffness prediction model:

- The influence of the RAP binders used in asphalt concrete cannot be neglected. A way of including this influence is by using blended bitumen properties instead of using the virgin binder characteristics only.
- Models used for the determination of predictive parameters (log pen rule, viscosity prediction models and the Van der Poel relation) should be avoided. They are

inaccurate in general and their use goes at the expense of the accuracy of the stiffness prediction. No polymer modified bitumen were implemented in these models.

- Theoretically, the binder stiffness is the best parameter to choose as predictive parameter for a model. However, this parameter shows average correlations with the asphalt concrete stiffness. A good alternative is the use of the penetration, which can be measured surprisingly accurate.
- Viscosity and Ring & Ball softening point are theoretically less interesting predictive parameters, but the latter has quite a high correlation with the asphalt concrete stiffness.
- Determination of the glassy modulus from the master curve is possible by finding its asymptote. These values are unprecise and show large deviations. Preference is given to a model without the glassy modulus as predictive parameter.
- Extra care should be given to mixes with polymer modified binders. The test results often form the outlier in a linear trend, like in the case of the binder stiffness.
- Interchangeable parameters should not be included in a stiffness prediction model in order to avoid collinearity.

4.4 Volumetric predictive parameters

All models presented in chapter 2 contain at least one volumetric predictive parameter. The traditional parameters V_a, V_b and V_g and combinations of them are further analysed in sections 4.4.1 till 4.4.3.

4.4.1 Traditional volumetric parameters V_a, V_b and V_g

Traditional parameters V_a, V_b and V_g are the air, binder and aggregate fractions respectively. The more air in a mix, the more space for particles to move during loading, and the lower the asphalt concrete stiffness. Therefore, a larger air percentage V_a will result in a lower mix stiffness S_{mix} in theory. This is in line with the negative relation found in Figure 19. The determination coefficient R^2 is equal to 0.10. From the figure it can be concluded that mix 451 is a clear outlier. This can be explained by the large binder fraction of mix 451. Without this mix, a significantly higher R^2 value of 0.57 is found. The negative relation between V_a and the asphalt concrete stiffness can also be found by considering individual mixes.

Figure 19 - Relation percentage air voids - asphalt concrete stiffness

Another simple volumetric parameter is the aggregate fraction (V_g). If the stiff aggregate fraction increases, the stiffness of the mix as a whole will increase as well. This is confirmed by an accurate positive relation between V_g and the asphalt concrete stiffness, with a determination coefficient of 0.77.

In Figure 20, the relation V_b - S_{mix} is plotted. From the figure it can be seen that the Boskalis database has limited variation in V_b values. Only two 'columns' of data points are visible. All mixes have a target binder content of 4.3% (m/m), except for mix 451, which has a target binder content of 5.8% (m/m). From the figure a clear negative relation can be observed as expected. The larger the soft binder fraction, the lower the overall stiffness of the mix. Due to the limited variation in data, no assertion can be made about the kind of relationship (linear, quadratic etc).
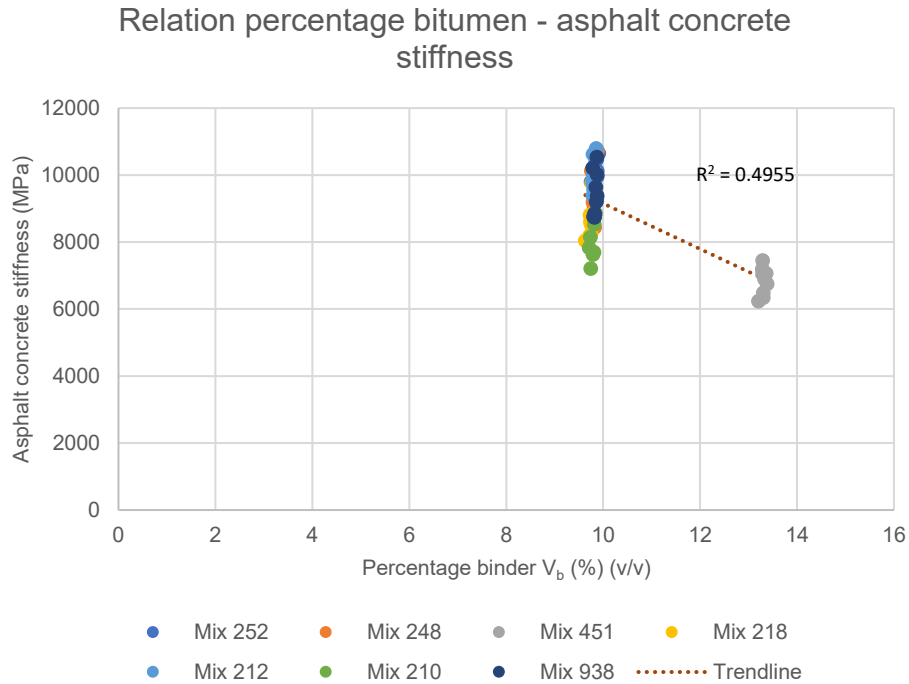
Figure 20 - Relation percentage bitumen - asphalt concrete stiffness

4.4.2   Combinations of V_a, V_b and V_g

In the Hirsch and Al-Khateeb models, the voids in the mineral aggregate (VMA) is used as a predictive parameter. This parameter is officially defined as the volume of space between the aggregate particles of a compacted mixture that includes air voids and the effective binder (Liu, 2016). The effective binder is the binder not absorbed by the aggregates. The part that is absorbed by the aggregates is assumed to be negligible. Therefore, the VMA is obtained by equation 31. A linear trend line was fitted over the VMA - S_{mix} data with a determination coefficient of 0.77. The relation is similar to the $V_g – S_{mix}$ relation, but mirrored. VMA is interchangeable with the parameter V_g since their sum is always 1. Including both VMA and V_g in a new asphalt concrete stiffness prediction model is unnecessary and causes collinearity.

In the Witczak and Hirsch models, the voids filled with bitumen (VFB) is used as a predictive parameter. This parameter is defined as the share of the voids that is effectively filled with bitumen (Liu , 2016). This relation has been simplified and is given by equation 32. The effective binder content was replaced by the total binder content. The found relation with the asphalt concrete stiffness is negative as expected. Due to limited variation in the database, a very small determination coefficient was found ($R^2 = 0.0255$). Mix 451 is a clear outlier here as well.

Another parameter considered is the V_g/V_b ratio, as used in the Francken model. The parameter is interesting because this ratio does not depend on the level of compaction. A determination coefficient value of 0.54 was found for the relation with the asphalt concrete stiffness, which is low due to the limited variation in the database.

Other candidate predictive parameters are the density and the target density. The latter is not considered interesting since the model should be based on the actual properties. The density can be a predictive parameter, but using the volumetric fractions instead make more sense. These values indicate the volumetric structure. There is already compensated for their individual densities (equations 28, 29, and 30).

4.4.3 Relevance

It can be concluded that the volumetric parameters as described above do have a relationship with the asphalt concrete stiffness as expected. One or more volumetric parameters should be included in an asphalt concrete stiffness prediction model. A good approach is to keep the predictive parameters as simple as possible by using V_a, V_b and V_g. It should be noted that they are interrelated, since the sum of the fractions is always equal to 1, or 100% in case of percentages. Including two of these three parameters is sufficient for including the three separate influences. Collinearity will be avoided. Another logical approach is the use of V_g/V_b and V_a. V_g/V_b indicates the aggregates/binder ratio (hot mix properties) while V_a is proportional to the level of compaction (density). In this approach, these influences are considered separately. It should be noted that V_a does not perfectly reflect the level of compaction, since this parameter is also influenced by the grading. This becomes more important if the Boskalis database is extended with mixes with a truly different grading, like porous asphalt. Less preference is given to the use of VMA and VFB since they are normally not used in describing Dutch asphalt concrete mixes. Using Pearson's correlation coefficient to quantify the relation with the asphalt concrete stiffness, preference is given to the use of V_g, V_b/V_g or VMA. VFB is least correlated and is therefore again less preferred as predictive parameter.

4.5   Gradation characterization parameters

In the Boskalis database, many parameters are included describing the characteristics of grading and the aggregates. The Pearson correlation values with the asphalt concrete stiffness are presented in Table 4.

Parameter	Pearson correlation coefficient with the asphalt concrete stiffness
Coefficient of uniformity	0.80
Percentage retained at 3/8 inch sieve (US standards)	0.79
Percentage passing C11.2 sieve	-0.79
Percentage passing C8 sieve	-0.78
Percentage passing 0.5 mm sieve	0.78
Percentage passing 2 mm sieve	-0.72
Maximum aggregate size	0.70
Percentage passing 0.180 mm sieve	0.58
Percentage retained at #4 sieve (US standards)	0.56
Percentage passing C16 sieve	-0.54
Percentage retained at 3/4 inch sieve (US standards)	0.54
Percentage passing C5,6 sieve	-0.53
Percentage passing 0.063 mm sieve	-0.48
Percentage passing C22.4 sieve	-0.47
Coefficient of curvature	0.18
Percentage passing #200 sieve (US standards)	0.05

Table 4 – Correlation between gradation characteristics and asphalt concrete stiffness

In theory, the maximum aggregate size has a positive relation with the stiffness. The only place in a mix where significant deformation can occur is in between the aggregate particles. The larger the particles, the less of these transitional zones exist. The large particles form a solid backbone of the mix. This expected positive relation is in line with the positive Pearson correlation coefficient of 0.70. The correlation is high compared to some other gradation characterization parameters.

The individual sieve sizes can be ranked based on their correlation with the asphalt concrete stiffness. The upper and lower sieve sizes are least correlated, while most sieves in between (C11,2; C8) have a much higher correlation. It is known from theory that a dense graded mix has a higher stiffness. In a dense mix, the spaces in between the larger particles are filled with smaller particles. There is minimal space for the particles to move, which results in a stiffer mix. Porous asphalt is open graded and has in general a much lower stiffness, despite the large particles used. One individual sieve size parameter does not characterize the shape of the sieve curve. In a dense graded mix, the sieve curve will be close to the Fuller curve. In theory, instead of individual sieve sizes, better predictive parameters are the coefficients of uniformity and curvature. These parameters are a measure for the grading of the material as a whole. The coefficients are defined by equation 42 and 43 (Viswanadham):

$$C_u = \frac{D_{60}}{D_{10}} \tag{42}$$

$$C_c = \frac{(D_{30})^2}{D_{10} * D_{60}} \tag{43}$$

Where:

C_u = coefficient of uniformity

C_c = coefficient of curvature

D_{10} = grain diameter at 10% passing

D_{30} = grain diameter at 30% passing

D_{60} = grain diameter at 60% passing

The coefficients D_{10}, D_{30} and D_{60} are obtained by linear interpolation. The larger C_u or C_c, the better the grading. A positive relation with the asphalt concrete stiffness is expected from theory and confirmed by the positive Pearson correlation coefficients of 0.80 and 0.18 for C_u and C_c respectively. Since C_u has a relatively high correlation with the asphalt concrete stiffness, this parameter is preferred over C_c as a predictive parameter in a new model. It should be noted that the variation of C_u and C_c in the Boskalis database is limited since only asphalt concrete mixes are included. By extending the database with other surface layer mixes, like porous asphalt, the correlations with the asphalt concrete stiffness can possibly increase significantly.

5 Model verification

5.1 Introduction

Eight asphalt concrete stiffness prediction models are presented in chapter 2. In chapter 4 the Boskalis database as described in chapter 3 has been used for an extensive review on the predictive parameters for an asphalt concrete stiffness prediction model. This database will be used in this chapter for the assessment of the models based on their predictive parameters, accuracy and applicability to the Dutch tests and standards.

5.2 Assessment models based on predictive parameters

From chapter 4 it follows that certain binder, volumetric and gradation characterization parameters are less preferred as predictive parameters, since they cannot be determined precisely or they have little or no correlation with the asphalt concrete stiffness. Also from a theoretical point of view a certain parameter can have preference over others. In the sections 5.2.1 – 5.2.3 the models will be assessed on their predictive parameters. Each group of predictive parameters will be addressed separately.

5.2.1 Bitumen properties as predictive parameters

In section 4.3.9 it was concluded that the bitumen stiffness and the penetration are preferred binder characterization parameters as predictive parameters in an asphalt concrete stiffness prediction model. These parameters can be precisely determined, make from a theoretical point of view sense and have a relatively high correlation with the asphalt concrete stiffness. The Penetration is only used by Jacobs, while Francken, Shell, Witczak (2006), Hirsch and Al-Khateeb use the binder stiffness as predictive parameter. However, the Francken and Al-Khateeb models are less preferred since they use the glassy modulus as a predictive parameter as well, which cannot be precisely determined (Figure 8). The Asphalt Institute and Witczak (1999) models use the bitumen viscosity as a predictive parameter, which is theoretically a less preferred parameter (section 4.3.4).

5.2.2 Volumetric predictive parameters

According to section 4.4.3, two approaches are preferred for dealing with the volumetric parameters for a model: including two of the three volumetric fractions (1) or separating the influences of the mixing ratio's (V_g/V_b) and the compaction (V_a) (2). Both Witczak's models and the asphalt institute and Shell models are in line with the first approach, while Francken, Jacobs and Shell used the second approach. Hirsch and Al-Khateeb use VMA as predictive parameter, which is a good alternative for V_g (section 4.4.2). However, the Hirsch model also uses the VFB which has a very low correlation with the asphalt concrete stiffness according to section 4.4.2. Al-Khateeb uses only one volumetric parameter (VMA) and therefor does not account for the three fractions (V_a, V_b, V_g) separately.

5.2.3 Gradation predictive parameters

The only models using predictive parameters characterizing the gradation are the Witczak and the Asphalt Institute models. The Witczak models use four different fractions, which are not multiplied by one another. This implies that each fraction has its individual influence on the binder stiffness according to Witczak. The Asphalt Institute model only uses one fraction (P200) as gradation predictive parameter. According to paragraph 4.5, the gradation as a whole has an influence on the asphalt concrete stiffness in theory. This makes the models of Witczak and Asphalt Institute less preferred. Some coefficients corresponding to volumetric

parameters in the Witczak models are very small, and some volumetric parameters have been squared without a theoretical explanation. The model is overfilled with parameters whose contribution has not been theoretically verified.

5.3 Assessment models based on accuracy

All models were evaluated by plotting the measured values versus the predicted values of the considered model. An example of such a plot is shown in Figure 21 for the Hirsch model. The measured and predicted asphalt concrete stiffnesses are presented on the horizontal and vertical axes respectively. The line of equality represents the locations in the graph where the predicted values are equal to the measured values. The close to this line, the better the prediction. The data points corresponding to a particular mix have been grouped by a color. This gives more insight in the predictive capacity of the model for a certain mix. The model under predicts the stiffness if the data points are under the line of equality, while the model over predicts the stiffness if the data points are above the line of equality. An overview of the plots for the other models can be found in Figure 24. Larger graphs can be found in Appendix F. The overview of the coefficients of determination is graphically shown in Figure 22.
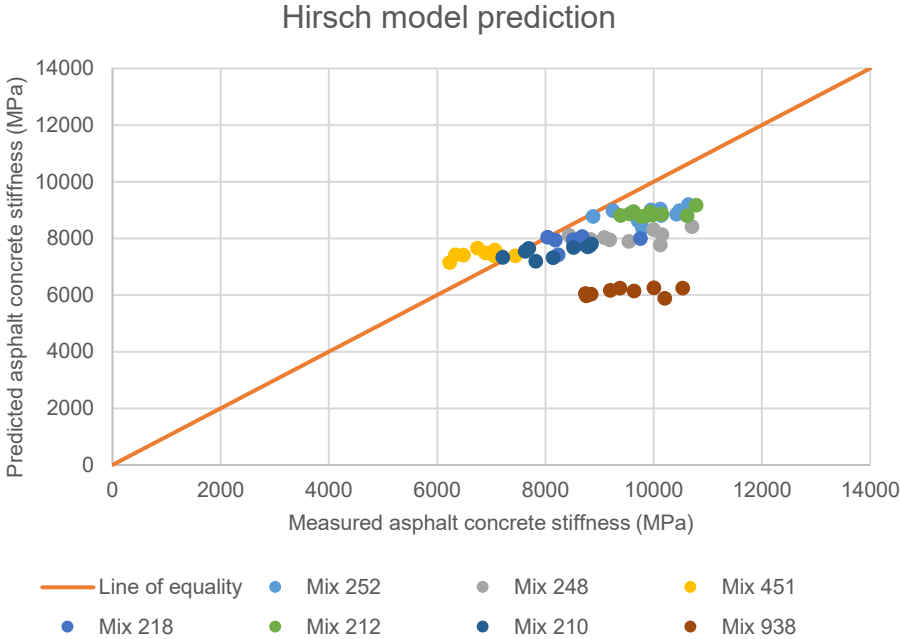
Figure 21 - Hirsch model prediction

5.3.1 Accuracy

The coefficient of determination (R^2) is a value between 0 and 1 indicating the accuracy of the model. The larger this value, the larger the part of the measured data that can be explained by the model (Field, 2013). From Figure 22 it can be concluded that the prediction of the Hirsch model is the least accurate, despite the fundamental approach that was used (see also section 2.3.5). The Shell and Witczak model predictions are better, but still a low determination coefficient can be found (0.4-0.5). The Jacobs model is at the top of the list with a relatively high determination coefficient of 0.79. A possible reason for this high accuracy is the Dutch database used for the model. Jacobs is the only one using Dutch tests and standards for the development of his model.

5.3.2 Glassy modulus

The Al-Khateeb and Francken models both use the glassy modulus as a predictive parameter. A value of 3000 MPa may be assumed according to Francken as a safe upper limit of the glassy modulus in the case this parameter is unknown. Al-Khateeb suggested a safe upper limit for the glassy shear modulus of 1000 MPa. The binder glassy modulus values obtained in section 4.3.7 by the asymptote method are used to verify the models. In a second analysis, the constant values of 3000 MPa (stiffness) and 1000 MPa (shear stiffness) were used in the models of Francken and Al-Khateeb respectively. The resulting R^2 values are both shown in Figure 22. The Al-Khateeb model's accuracy (R^2) increases from 0.18 to 0.22 by using the asymptote method. However, the model remains highly inaccurate. The Francken model's accuracy decreases significantly from 0.52 to 0.22 by using the asymptote method. The Francken model results using both glassy modulus values have been plotted in Figure 23. It can be seen that the predicted values are shifted further from the line of equality in general by using the glassy modulus values obtained by the asymptote method. It can be concluded that the glassy modulus can better be kept at a constant value.
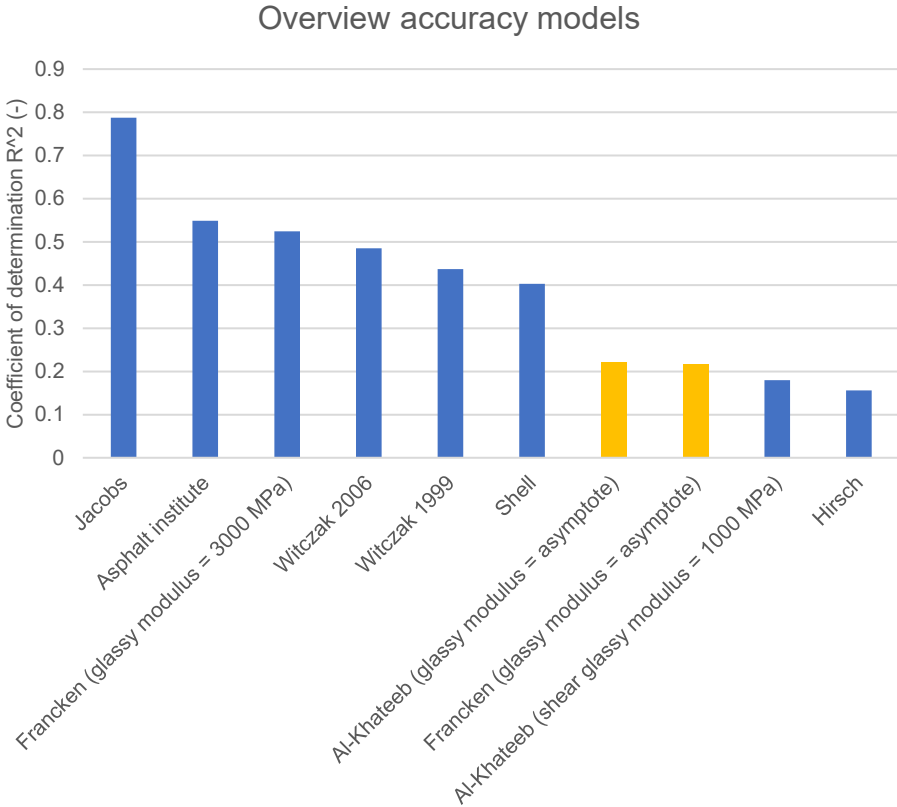

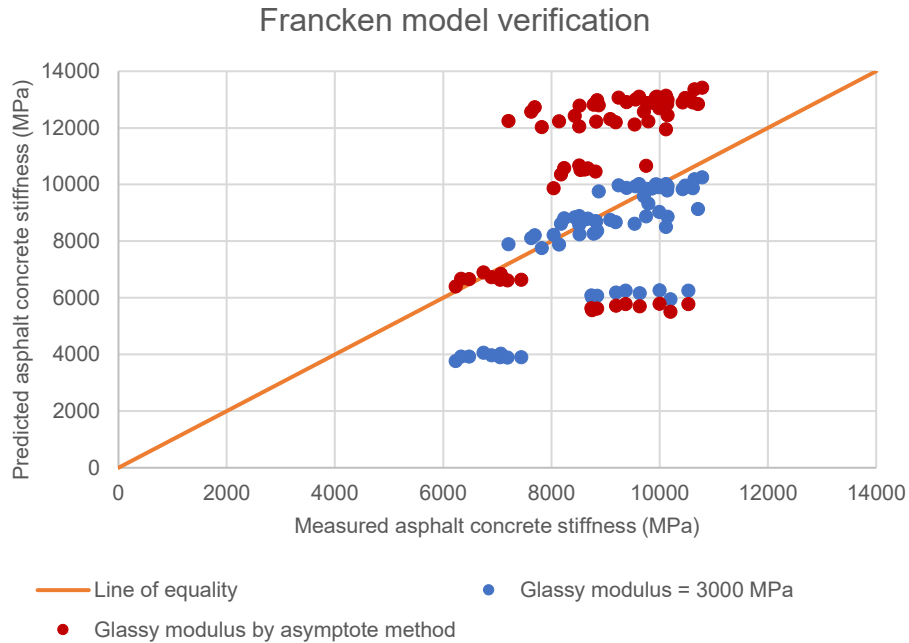
Figure 22 - Overview accuracy models

Figure 23 - Francken model verification

5.3.3   Under- and overestimation

By looking at the plots for each model in Figure 24, more statements can be made about why certain models have a lower accuracy and what are the strong and weak points of certain models. One of those weak points is over- or underestimation. Shell, Witczak (1999) and Al-Khateeb (glassy shear modulus = asymptote method) show structural underestimation, while the Witczak (2006) model shows structural overestimation. These inaccuracies do not necessarily make the model a bad model. Unit issues or different tests used for their databases can be a cause for these deviations. In paragraph 5.4, there has been corrected for these issues by fitting the relations on the Boskalis database. It should be noted that both Witczak models and the Asphalt Institute model show very large deviations from the measured stiffness values compared to the other models. The Asphalt Institute model results in predictions up to 60,000 MPa, while the Witczak model (1999) results in stiffness values lower than 2000 MPa. These results lowers the trust in these models.

5.3.4   Oversensitivity and insensitivity

More problems arise when a model partly over- or underestimates, which is the case for the Asphalt Institute model. The model is oversensitive for a certain predictive parameter. This means a certain mathematical function or transformation applied to that predictive parameter by the model is inaccurate. For the Asphalt Institute model this predictive parameter is the penetration. By changing the penetration values slightly (i.e. 5 dmm), the asphalt concrete stiffness changes in the order of thousands of MPa's. On the other hand, the Hirsch and Al-Khateeb (glassy shear modulus = 1000 MPa) models are insensitive for one predictive parameter or a combination of predictive parameters. Some data points are accurate, but the range of predicted values is smaller than the range of measured values. This is visible as a more flattened horizontal point cloud.

In the database, for each set of specimens of the same mix, one value for a binder characterization parameter is available. This value is the average of at least two tests and is assigned to the group of specimens of the corresponding mix. The latter holds for gradation

parameters as well. Meanwhile, the volumetric parameters are unique for each specimen, since each specimen was measured and weighted separately. Variation of predicted asphalt concrete values within one mix *must* be the result of variation in volumetric properties. There is little variation in predicted asphalt concrete values within one mix for the majority of the models, which means the models are insensitive for volumetric properties. This can best be seen for the Al-Khateeb model plots in Figure 24. The data points form horizontal lines per mix. On the other hand, the Shell and Jacobs models show the highest sensitivity to volumetric parameters. Positive relations can here be observed between the predicted and measured asphalt concrete stiffness within one mix.

5.3.5   Outliers

For most of the models one or more predicted values are much more inaccurate than the other predicted values. Most models have a certain insensitivity to volumetric properties and do not distinguish within a mix. This is why a group of outliers mostly belongs to one specific mix. Mix 938 is a clear outlier in the models of Shell, Francken, Witczak (2006), Hirsch and Al-Khateeb. This mix is unique in its binder, which is a combination of RAP binder and the polymer modified binder sealoflex 5-50HT. The databases of Shell and Francken did not include polymer modified binders, while Witczak and Hirsch did (Table 1). It confirms the assumption that older models are incapable of predicting the stiffness of asphalt concrete mixes with polymer modified binders. However, even some newer models have difficulties. Most models highly underestimate the stiffness of mix 938. Another outliers is mix 451 in Franckens prediction. Mix 451 is distinguishable by its high bitumen content of 5.8% (m/m).
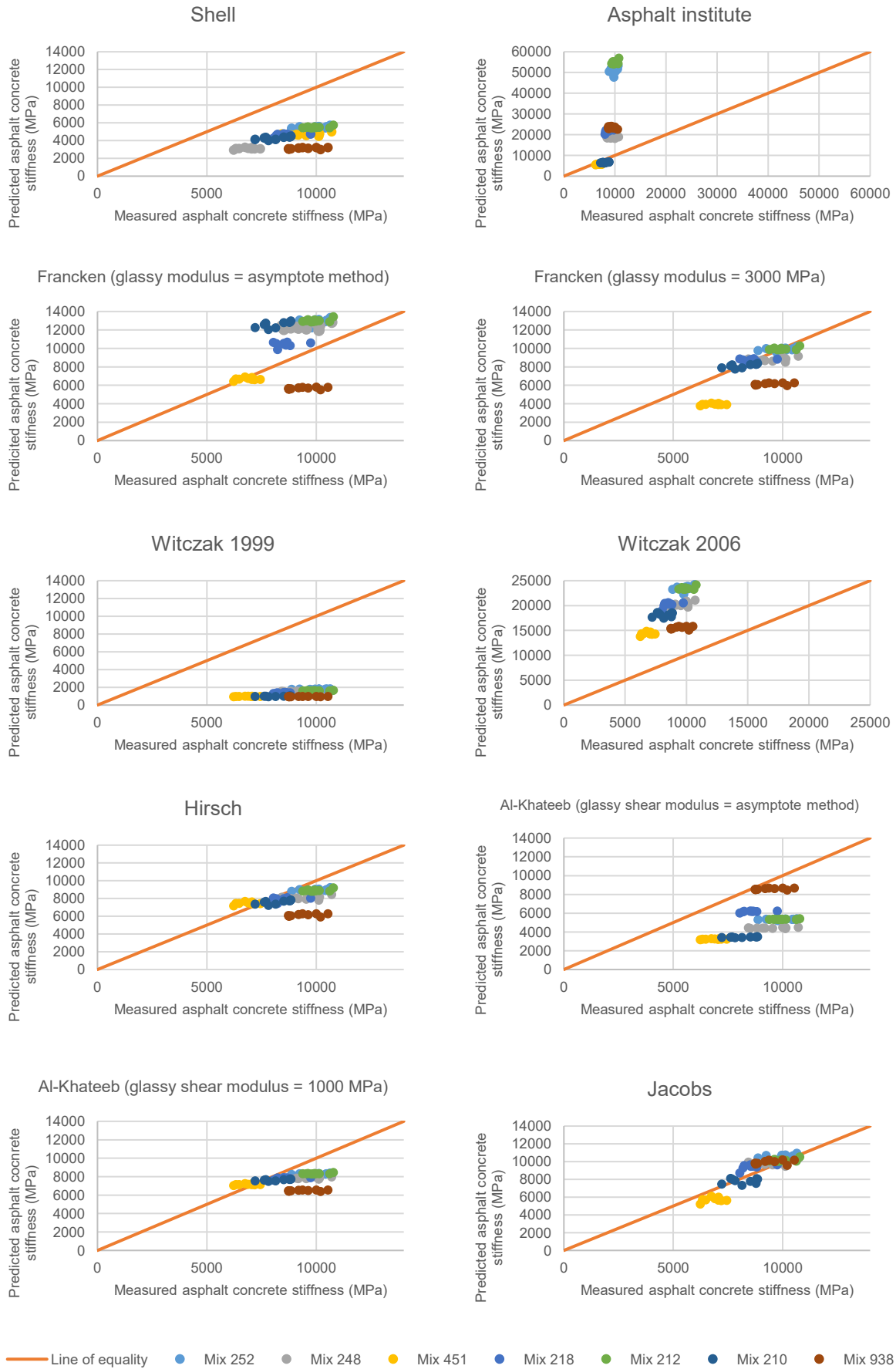
Figure 24 – Overview predictions models chapter 2

5.4   Fitted models

The asphalt concrete stiffness prediction models as presented in chapter 2 are based on other tests and standards than the data in the Boskalis database. The differences between the databases can be observed in Table 1. Using the Boskalis database for the verification of those models is not completely fair for this reason. Deviations between the measured and predicted data can be caused by these differences and do not necessarily mean the model has a low quality. A correction for these effects can be made by fitting the constants of each model to the Boskalis dataset.

5.4.1   Fitting procedure

The generalized Hirsch model as presented in equation 42 and 43 is used as an example for explaining the fitting procedure.

$$|E^*|_{mix} = P_C * \left(C7 * \left(C8 - \frac{VMA}{C9} \right) + C10 * |G^*|_{binder} \left(\frac{VFB * VMA}{C11} \right) \right)$$
$$+ \frac{(C12 - P_C)}{\left(\frac{C13 - \frac{VMA}{C14}}{C15} + \frac{VMA}{C16 * VFB * |G^*|_{binder}} \right)} \tag{44}$$

$$P_C = \frac{\left(C1 + \frac{VFB * C2 * |G^*|_{binder}}{VMA} \right)^{C3}}{C4 + \left(\frac{VFB * C5 * |G^*|_{binder}}{VMA} \right)^{C6}} \tag{45}$$

All constants in de model were changed into variables C1-CX. Some C-values were kept constant since they are based on theory or fundamental relations. C2, C5, C10, and C16 represent the conversion from shear modulus to stiffness modulus by equation 18 and are kept unchanged. A Poisson ratio of 0.5 is assumed by Christensen, which is in conflict with the findings of Pouget (2012) (section 4.3.2). C8, C9, C12, C13 and C14 represent fixed values for calculations with volumetric properties. These constants are kept unchanged as well. The left over constants are finally used as variables for fitting. For each model a careful trade-off has been made which parameters are changeable, and which should be kept constant. A least squares error has been used to fit the model. The solver function SOLVER.XLAM in Excel 2013 has been used for performing this least squares error. The original values in de model were used as start values for the analysis. A summary of the regression analysis for each model is presented in Appendix F, while the effect on the quality of the fit is shown in Figure 25.

5.4.2   Results fitted functions

The R^2 values of the fitted versions of the models are presented in Figure 25. A comparison is made with the R^2 values of the original models. From this graph it can be seen that the accuracy increases for all models. The models of Francken, Shell and Witczak (2006) show much higher accuracies after fitting ($R^2 \approx 0.8$). The models of Jacobs and Asphalt Institute show a slightly increased accuracy. The Hirsch and Al-Khateeb model accuracies do increase, but stay much lower than the other fitted models, which implies that the formula's used in their models are less applicable to the Boskalis dataset. A more extensive fitting procedure has been performed on the Hirsch model by Telman & Van den Berg (Appendix H). This resulted in similar R^2 values with a maximum of 0.31. Telman excluded mix 938 in a second analysis,

which resulted in very high R^2 values up to 0.85. In a new model extra care should be given to mixes with polymer modified binders.
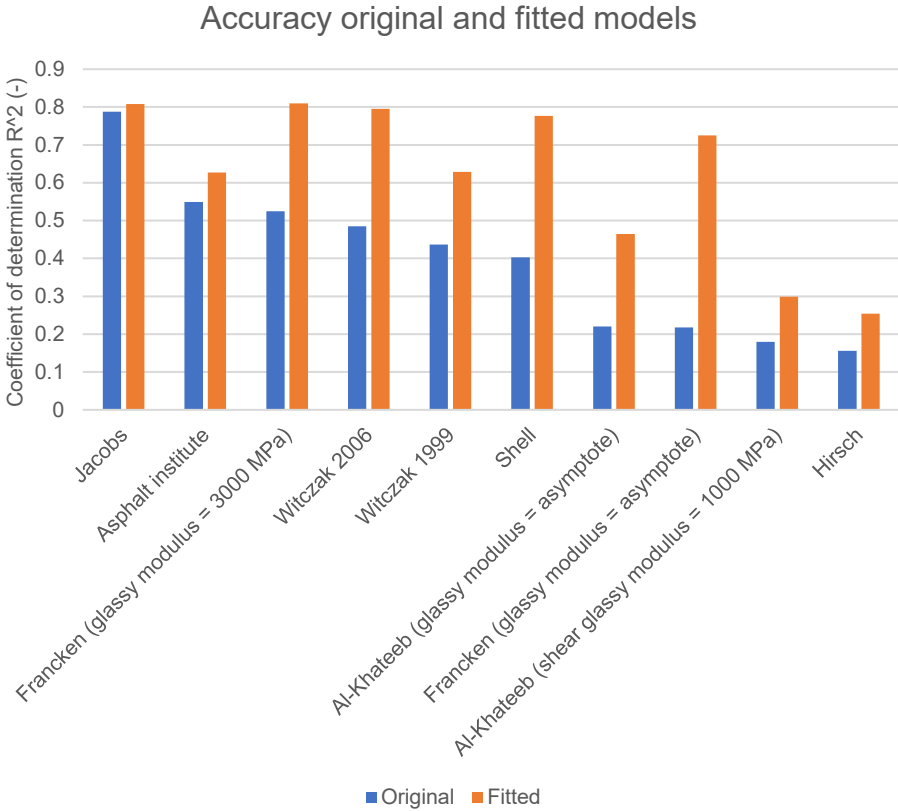
Figure 25 - Accuracy original and fitted models

5.4.3 Implications fitting process

Some points should be noted about the fitting process:

- For some models it is difficult to recall which constants follow from fundamental relations and which are the result of a regression analysis. If a mistake is made here, the model changes fundamentally.
- Valuable information from the model's original database will be lost in the case the original database is inaccessible.
- Excel's SOLVER.XLAM has its limitations. Not all possible combinations of predictive parameters are considered. The fit highly depends on the starting values.
- After fitting, some constants take values equal to 0. Depending on the corresponding part of the formula, this can result in insensitivity for certain parameters. For example, if the first constant in the Jacobs model changes from -52.3 to 0, it implies that the model becomes insensitive for the penetration. The majority of the models contain at least one constant that is set to 0 after fitting. Some constants take very large values after fitting. When this parameter is part of the denominator, this implies the model can lose the sensitivity to a certain parameter.

6 Multiple linear regression analysis

6.1 Introduction

The accuracy of the asphalt concrete stiffness prediction models as presented in chapter 2 is limited for the Boskalis database. This can be concluded from Figure 22. The process of fitting does increase the accuracy for certain models, but the determination coefficient does not exceed the value of 0.81, which can be seen in Figure 25. An interesting conclusion is that the Jacobs model's accuracy is the highest (R^2 = 0.79) out of the unfitted models. After fitting, a similarly high determination coefficient is found (R^2 = 0.81), making this model the best performing fitted model as well. Furthermore, the linear Jacobs model is a very simple model. Jacobs used a multiple linear regression analysis on his dataset. This analysis can be done easily by modern statistics software like SPSS, or be programmed in other software. However, in that case you have to add or remove variables manually. This analysis has been performed for certain combinations of predictive parameters in paragraph 6.4.

6.2 Multiple linear regression analysis in SPSS

The multiple linear regression analysis presented here is performed using SPSS. The software returns the coefficients b_X that belong to the predictive parameter X_i, which can be all the parameters that are potentially able to predict the stiffness, such as discussed in Chapter 4. and a constant C for the prediction of the dependent variable Y. The model includes n independent variables X. This linear model can mathematically be written as follows:

$$Y = b_{X1} * X_1 + b_{X2} * X_2 + \cdots + b_{Xn} * X_n + C \qquad (46)$$

The predictive parameters X used in the model can be pre-set in the software. The first is called the *enter method*. The software itself can also choose which parameters to include in a prediction model. The *forward method* starts with an empty equation, and first inserts the predictive parameter with the highest correlation. It then inserts a second predictive parameter that contributes most to the accuracy of the model. A variable is only entered into the model if the significance level of its F value is less than the preset value 0.05. The *backward method* starts with all possible predictive parameters in a model. It then takes out the predictive parameters one by one that contribute the least to the accuracy of the model. A variable is only removed if the significance level of its F value is greater than the preset value of 0.10. The *stepwise method* is a combination of both methods. After inserting a new predictive parameter, the contribution of the previously inserted parameter will be determined (Field, 2013). The methods will be applied on the Boskalis database in paragraph 6.3. It should be noted that a multiple linear regression model does not account for non-linear relations, such as S_{mix}^2. However, these usually do not have a physical meaning anyway. Also, the linear regression models described in paragraphs 6.3 and 6.5 contain no cross terms.

6.3 Regression models

Multiple starting points can be used to obtain a set of predictive parameters as input for a multiple linear regression analysis. Examples are given in the next sections.

6.3.1 Model 1: Engineering judgement ($S_{bit,blend}$, V_a, V_g/V_b)

From engineering judgement, the predictive parameter blended binder stiffness ($S_{bit,blend}$) is chosen as binder characterization parameter. Physically, the binder stiffness is the predictive parameter that is closest to the asphalt concrete stiffness. The air fraction (V_a) and the ratio

between aggregates and bitumen volumes (V_g/V_b) are chosen as in the Jacobs model. For a given grading, these parameters describe the influence of the compaction (V_a) and the ratios of the mix design (V_g/V_b) separately.

6.3.2 Model 2: Theory and precision ($S_{bit,blend}$, V_a, V_b, D_{max}, C_u)

The second model is based on theory and precision of the predictive parameters. The blended binder stiffness ($S_{bit,blend}$) is a theoretically preferred binder characterization parameter (section 4.3.9) and can be determined with average precision (Figure 8). Two simple volumetric parameters have been included (V_a and V_b) according to the first approach in section 4.4.3. V_a and V_b can be easily adjusted in the design by changing the target level of compaction or the amount of added bitumen respectively. Since also gradation characterization parameters show significant correlations with the asphalt concrete stiffness (paragraph 4.5), the predictive parameters maximum aggregate size (D_{max}) and the uniformity coefficient (C_u) are included. These parameters are preferred from a theoretical point of view as well (paragraph 4.5).

6.3.3 Model 3: Simplicity (Pen_{blend}, V_a, V_b)

Simplicity can also be chosen as a starting point for selecting predictive parameters. An easily and widely available binder characterization parameter is the penetration (Pen_{blend}). Only two simple volumetric parameters have been chosen (V_a and V_b). No gradation characterization parameters have been chosen to keep the model as simple as possible.

6.3.4 Model 4: Maximum correlation (T_{R+B}, V_g, V_b, C_u)

Predictive parameters in a linear regression model can also be chosen according to their correlation with the asphalt concrete stiffness. For each group of predictive parameters (binder characterization, volumetric properties and gradation) the predictive parameter with the highest correlation is chosen as input for the model. This results in the parameters softening point (T_{R+B}), volume aggregates (V_g), volume binder (V_b), and coefficient of uniformity (C_u). Two volumetric parameters have been included since this is sufficient for including the separate influences of all the three fractions (V_a, V_b, V_g) (section 4.4.3).

6.3.5 Model 5: SPSS – forward method

The following predictive parameters followed from SPSS by choosing the forward method:

- V_g = volume aggregates (%)
- Pen_{blend} = penetration blended bitumen (dmm)
- $S_{bit,inf,virgin}$ = glassy modulus virgin bitumen (MPa)

It should be noted that this choice of predictive parameters cannot be theoretically explained. It is not preferred to use the volume of aggregates (V_g) individually as a volumetric predictive parameter, since the influence of the other volumetric predictive parameters (V_a, V_b) is not included. Also, the glassy modulus of the virgin bitumen is not preferred as predictive parameter. This parameter is not precisely determinable and does not include the influence of the RAP in contrast to the glassy modulus of the *blended* bitumen.

6.3.6 Model 6: SPSS – backward method

The following predictive parameters followed from SPSS by choosing the backward method:

- V_g = volume aggregates (%)
- VFB = voids filled with bitumen (-)
- $\eta_{virgin,135°C}$ = viscosity virgin bitumen at 135°C (MPa*s)

- C22.4 = mass percentage of aggregates passing sieve size 22.4 mm (%)
- Age of the specimen (days)
- RAP% = percentage RAP (%)

Like in model 5, the choice of predictive parameters cannot be theoretically explained. The viscosity of the virgin bitumen is not preferred as a predictive parameter (section 4.3.4), as well as the C22.4 value (paragraph 4.5). The age of the bitumen should be unnecessary as predictive parameter, since the age at testing is kept within limits (paragraph 3.3). Besides, the number of predictive parameters is large. The model should include as few predictive parameters as possible for easy use. Striking is the difference in predictive parameters from model 5: SPSS - forward method.

6.3.7 Model 7: SPSS – stepwise method

The stepwise regression method resulted in the same predictive parameters as the forward regression method as described in section 6.3.5. For this reason, the step-wise method results have not been addressed separately.

6.4 Verification regression models

6.4.1 Accuracy regression models

In Appendix G the measured asphalt concrete stiffness is plotted versus the predicted values for each multiple linear regression model. In Figure 26 the resulting determination coefficients (R^2) have been visualized.
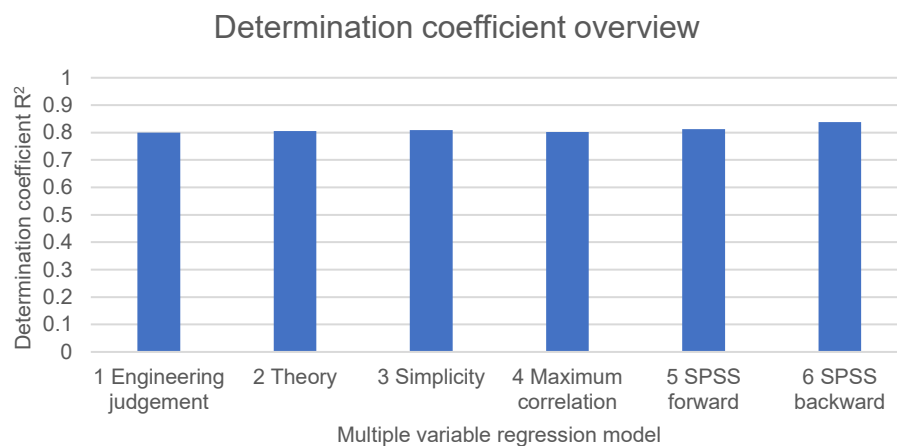
Figure 26 - Determination coefficient overview

The following can be observed:

- The forward SPSS and backward SPSS methods have the highest accuracy with a determination coefficient of 0.81 and 0.84 respectively.
- All regression models show similar accuracy (≈ 0.80).
- The accuracy of the regression models is much higher than the accuracy of the original unfitted existing models as can be seen in Figure 22. It should be noted that the regression models are based on the Boskalis dataset, while the existing models are based on their own datasets.
- The accuracy of the regression models is similar to the accuracy of the fitted existing models of Francken (glassy modulus = 3000 MPa) (R^2 = 0.81), Shell (R^2 = 0.78),

73

Witczak (2006) ($R^2 = 0.80$) and Jacobs ($R^2 = 0.81$). It should be noted that both the regression models and the fitted existing models are based on the Boskalis dataset.

From these observations the expectation arises that there is a certain maximum accuracy ($R^2 \approx 0.80$) which can be explained by the models. With the unfitted existing models as presented in chapter 2, the fitted existing models as presented in paragraph 5.4 and the regression models this 'maximum' correlation coefficient can be found. It should be noted that there is always a part of the results that cannot be explained by the model and is caused by spread in the data. Note that some asphalt concrete stiffness measurements on the same specimen exceeded the 15% difference as described in paragraph 3.4. Another interesting observation is the similarity in accuracy of the regression models. This can partly be explained by the similarity in stiffness predictions. The Pearson correlation coefficient matrix has been computed for the stiffness results of the regression models. The minimal Pearson correlation coefficient that could be found was 0.97. This confirms that the predictions of the regression models are highly equivalent. Also, by looking at the similarity of the accuracy of the various regression models in figure 26, it can be concluded that the high number of predictive parameters in model 6 has no significant added value. Model 6 is the only model with six predictive parameters.

6.4.2   Theoretical verification regression analysis

In Table 5, the regression coefficients b and the constants C of the models have been presented.

Parameter	1 Engineering judgement	2 Theory	3 Simplicity	4 Maximum correlation	5 SPSS forward	6 SPSS backward
C22.4						1028.88
Constant C	3670.02	20885.08	20572.90	-69571.47	-41557.64	-140253.95
C_u		19.81		-3.87 (b)		
D_{max}		-23.93 (a)				
Age						-167.90 (d)
Pen_{blend}			-25.64		-83.21	
RAP%						17.90
S_{bit,inf_virgin}					-0.93	
S_{bit_blend}	23.72	14.31				
$T_{R+B,blend}$				72.27		
V_a	-1019.74	-1066.11	-860.15			
V_b		-756.49	-634.79	193.19 (c)		
V_g				851.12	661.07	593.72
V_g/V_b	1130.91					
VFB						48.42 (e)
$\eta_{virgin\_135°C}$						0.44

Table 5 – Overview regression constants b and C for each model

Some coefficients b have been highlighted in red. The signs of these coefficients are *not* supported by the theory for the following reasons. The letters after the coefficients in Table 5 correspond to the letters in the following list:

a. In theory, the larger the maximum aggregate size, the higher the stiffness as explained in paragraph 4.5. This is not in line with the negative b value.

b. The better the grading, the higher the coefficient of uniformity C_u. A better graded mix results in less space for the particles to move. A lower stiffness is the result in theory as explained in paragraph 4.5. This is not in line with the negative b value.

c. The higher the share of soft binder, the lower the stiffness of the asphalt concrete stiffness. This assumed negative relation is confirmed by Figure 10. This is not in line with the positive b value.

d. According to Marsac (1999) the stiffness of asphalt concrete increases with the age. This is not in line with the negative b value.

e. The larger the VFB, the larger the share of soft bitumen in the voids. A negative relation with the asphalt concrete is expected and confirmed by a negative Pearson coefficient as described in section 4.4.2. This not in line with the positive b value.

Model 5 and 6 have no preference since the choice of predictive parameters cannot be theoretically explained. Furthermore, model 6 includes two illogical relations, and the number of predictive parameters is large. The fourth model, which is based on parameters with a high correlation with the asphalt concrete stiffness includes two illogical relations.

6.5 Model 8: Optimal model

The model as presented in equation 47 is proposed as the most optimal model for the following reasons:

- The starting point of this model is regression model 2. The included predictive parameters are theoretically preferred, have a high correlation with the asphalt concrete stiffness and can be precisely determined. The other models reach high accuracy without a theory-based choice in predictive parameters.
- D_{max} was removed from the model since the resulting regression coefficient was negative, which cannot be theoretically explained.
- C_u was removed from the model since this parameter was statistically insignificant ($p = 0.235 > 0.05$). This is possibly caused by the limited variation in this predictor parameter in the Boskalis database as described in paragraph 4.5.
- The remaining predictive parameters are statistically significant ($p < 0.05$) and the sign of their corresponding regression constant b can be theoretically explained.
- Despite the removal of two predictive parameters, the determination coefficient is still high ($R^2 = 0.80$).

$$S_{mix} = 24.131 * S_{bit,blend} - 1113.6 * V_a - 826.35 * V_b + 22062 \qquad (47)$$

Where:

$S_{bit,blend}$ = binder stiffness blended bitumen (MPa)

V_a = volume air voids (%)

V_b = volume bitumen (%)

S_{mix} = asphalt concrete stiffness (MPa)

6.5.1 Verification optimal model

In Figure 27, the predicted asphalt concrete stiffness is plotted versus the measured asphalt concrete stiffness.
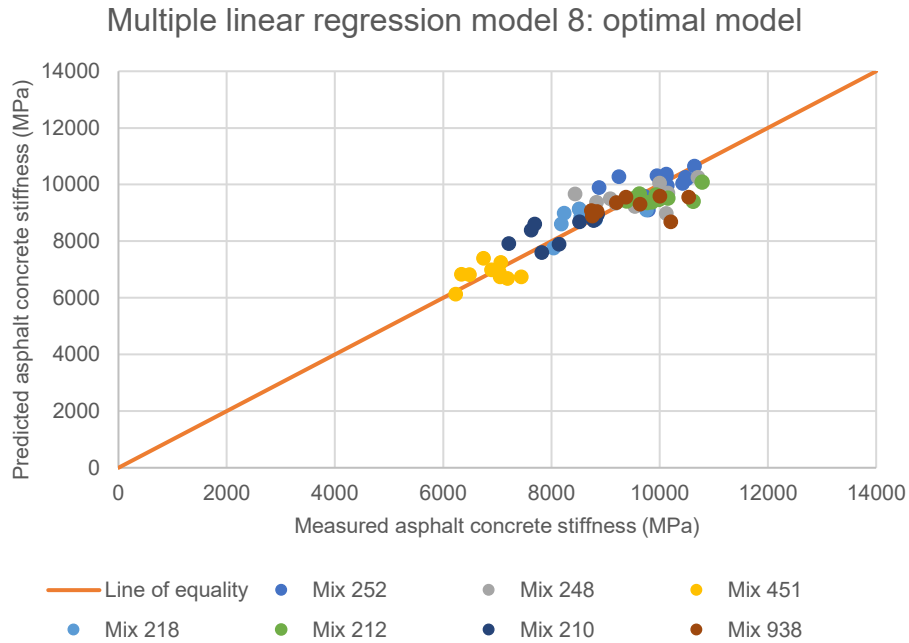
Figure 27 - Multiple linear regression model 8: optimal model

It can be seen from the figure that the prediction is accurate. The model is sensitive to volumetric parameters, since a positive relation can be observed within one mix. This can be concluded from the fact that the data points belonging to a single mix lie along the x = y line (see also section 5.3.4). No significant under- or overestimation is present. Mix 938 shows the largest deviation from the line of equality at higher stiffness values. This mix is the only mix in the Boskalis database containing a polymer modified binder.
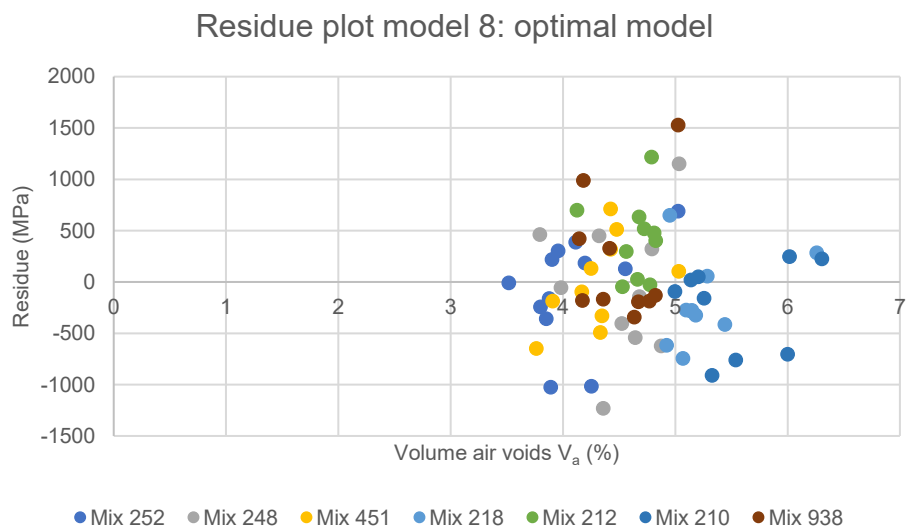
Figure 28 - Residue plot optimal model

In Figure 28, a residue plot is presented. It can be seen that there is no clear relation between the residues (measured data minus predicted data) and the air fraction (V_a), which means the

76

model is appropriate. The same holds for the other residual plots. A linear regression analysis has the disadvantage of not accounting for possible nonlinear relations. By checking the residual plots, those nonlinear relations can possibly be observed if they exist. Those non-linear relations are not observed for the predictive parameters used in equation 47. This does not necessarily mean that there is no nonlinear relation. The data should have a smaller natural spread or the database should be larger to make these relations visible. In Figure 29 a histogram of the residuals can be seen. It can be concluded that the distribution is close to a normal distribution which makes the model appropriate.

Histogram residues optimal model
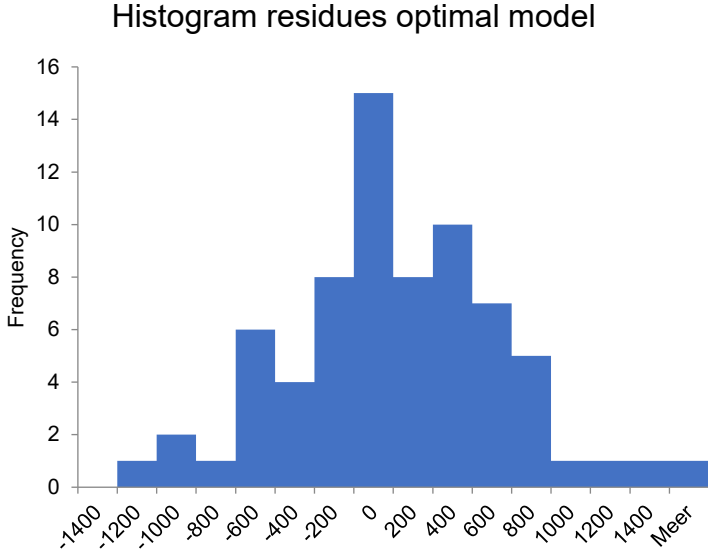
Figure 29 - Histogram residues optimal model

6.5.2 Applicability PMB mixes

As mentioned in section 4.3.2, extra care should be taken to mixes with polymer modified binders (PMB's). Mix 938 is the only mix in the Boskalis database containing a polymer modified binder. By leaving this mix out of the analysis, a significantly higher determination coefficient (R^2 = 0.85) can be found. More alarming is the change in the regression constant b corresponding to the blended binder stiffness. A regression analysis at a database without mix 938 gives a b-coefficient of 114. The original regression analysis resulted in a b-coefficient of 24. The model becomes five times more sensitive to the binder stiffness. The resulting model is presented in equation 48. In Figure 30, the predicted asphalt concrete stiffness is plotted versus the measured asphalt concrete stiffness. The Boskalis database is not sufficiently extensive to obtain a separate regression model for mixes with polymer modified binders, which could make the asphalt concrete predictions more accurate.

$$S_{mix} = 114.23 * S_{bit,blend} - 928.1 * V_a - 713.9 * V_b + 17571 \tag{48}$$

Where:

$S_{bit,blend}$ = binder stiffness blended bitumen (MPa)

V_a = volume air voids (%)

V_b = volume bitumen (%)

S_{mix} = asphalt concrete stiffness (MPa)

Multiple linear regression model 8: optimal model without mix 938

Figure 30 - Multiple linear regression model 8: optimal model without mix 938

6.5.3 Sensitivity to binder content

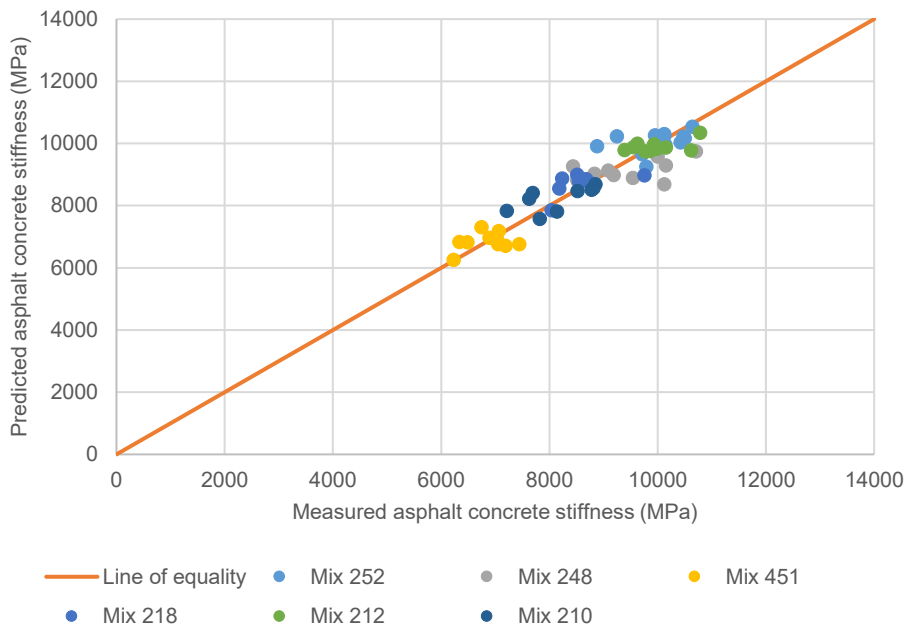Another outlier is mix 451, which has a higher bitumen content as mentioned in section 3.2.2. A regression analysis has been performed without this mix. The resulting determination coefficient drops significantly to a value of 0.61. The coefficients b corresponding to the predictive parameters $S_{bit,blend}$ and V_a stay at the same level (+/- 10%). It can therefore be concluded that V_b is a valuable parameter in a prediction model. No separate models need to be developed for mixes with high bitumen content.

6.5.4 Comparison to Jacobs model

The multiple variable regression analysis approach is also used by Jacobs, which resulted in the model as presented in equation 27. The following conclusions can be drawn by comparing the Jacobs model and the model given in equation 47.

- Jacobs uses three volumetric predictive parameters, while the model presented in equation 47 uses only two. This should be sufficient (section 4.4.3)
- Jacobs uses the penetration as predictive parameter, while the model presented in equation 47 uses the binder stiffness. Both parameters can be used since they can be determined precisely, but the binder stiffness has preference from a theoretical point of view as described in section 4.3.9.
- The penetration values of mixes with RAP in Jacobs's database are obtained by the combined penetration rule. This rule should be avoided as described in section 4.3.6. Instead, the penetration value of the blended bitumen (paragraph 3.5) should be determined by tests.
- Jacobs used a database in which the age of the specimens at testing is unknown. This can have a significant influence on the stiffness (Marsac, 1999). The influence of the age of the specimens has not been investigated in this report since the age of the specimens in the Boskalis database is kept within limits (see also paragraph 3.3).

- No mixes with polymer modified binders were included in Jacobs' database.
- Also gradation parameters have been considered in building the model as presented in equation 47.
- Jacobs's database is more extended than the Boskalis database, apart from the lack of mixes with polymer modified binders.

6.5.5   Applicability surface layer mixes

The database as described in chapter 3 contains only one asphalt concrete surface layer mix, which is mix 451. To gain more insight in the applicability of the model on surface layer mixes, the models as presented by equation 47 and 48 are verified using data of asphalt concrete mixes as presented in Table 6. These mixes contain no RAP or polymer modified binders. This data is obtained from existing available type tests and researches at Boskalis and do not belong to the database as presented in chapter 3.

Mix	Max aggregate size (mm)	Binder	Aggregate type	Target density (kg/m³)	Target binder content (%) (m/m)
A	16	70/100	Bestone	2368	5.7
B	11	40/60	Bestone + Reflexing white	2420	5.9
C	8	70/100	Bestone	2372	6.2

Table 6 – Overview surface layer mixes

The data has a lower quality. The following should be noted:

- The stiffnesses of the mixes are obtained by the 4PB-PR, while the stiffnesses of the Boskalis database (chapter 3) are obtained by the CIT-CY. The stiffness determined in the CIT-CY is on average 10% higher in value than the 4PB-PR stiffness (Poeran, Sluer, & Telman, 2018).
- No checks are done whether the specimens are damaged during testing.
- The corresponding binder data is obtained from the Boskalis database. It cannot be said if this binder data is representative (i.e. changing suppliers, different batches).
- The age of the specimens varies from 2 to 8 weeks. This time-span is much larger than in the Boskalis database (6 +/- 1 week)

In Figures 31 and 32 the measured stiffness values are plotted versus the predicted stiffness values as obtained by equations 47 and 48.

Figure 31 - Verification model equation 47
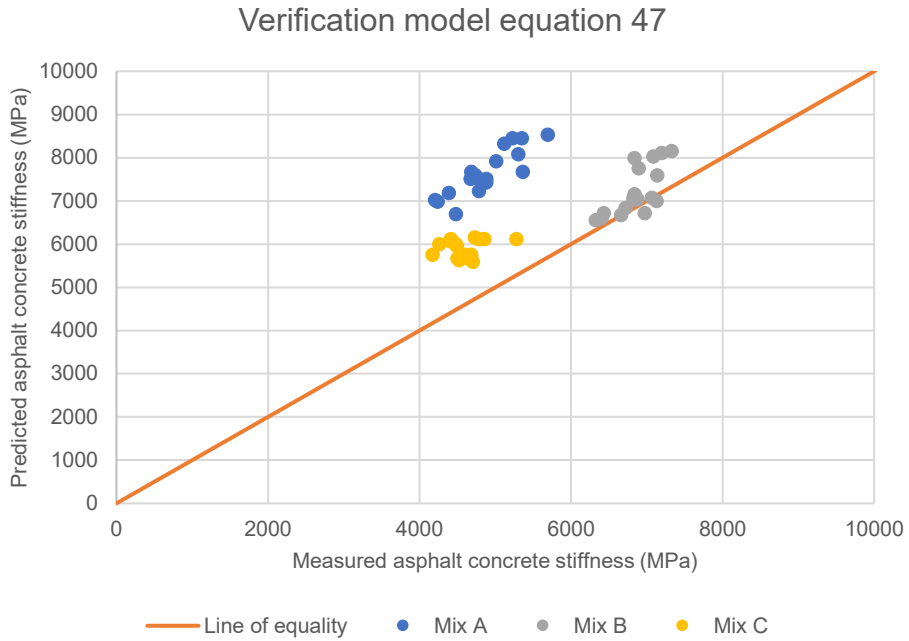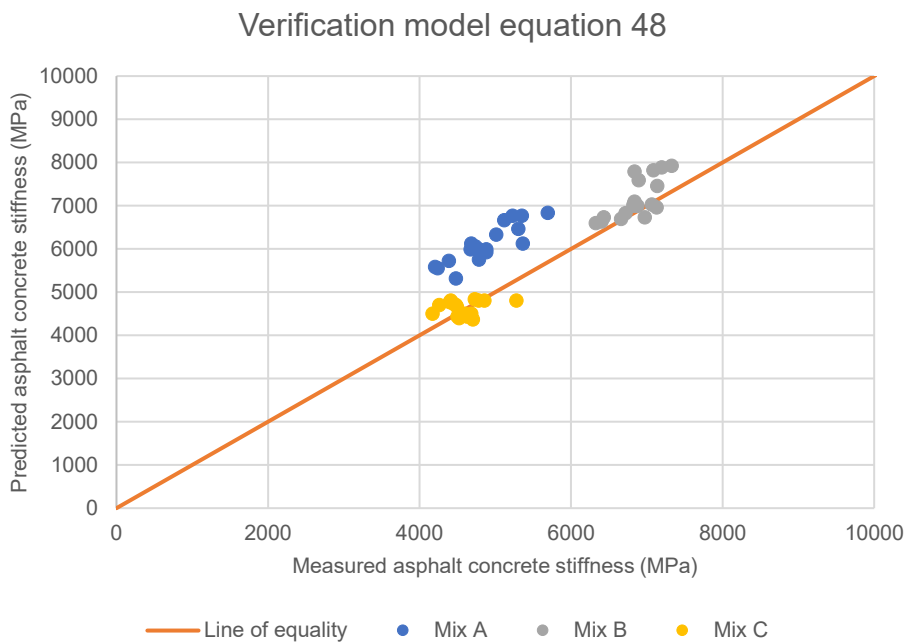

Figure 32 - Verification model equation 48

The following can be concluded from Figures 31 and 32 with in mind the aforementioned points.

- The model as presented by equation 47 is only accurate (average error < 10%) for mix B.
- The model as presented by equation 48 is only accurate (average error < 10%) for mixes B and C
- The stiffnesses of mix A are overestimated by both models.

- Both models are sensitive to volumetric parameters, since a positive relation can be observed within one mix (section 5.3.4).
- The model as presented by equation 48 is more accurate than the model presented by equation 47 when considering asphalt concrete surface layer mixes with conventional binders.

6.5.6   Applicability functional verification

The primary goal of the model given by equation 47 is to predict the stiffness for verification purposes (chapter 1). Ideally, this model will be used for the verification of the majority of the delivered works. This implies that all predictive parameters must be obtained for all new delivered asphalt works. The volumetric parameters V_a and V_b can be obtained by RAW test 65.0 (RAW, 2015), RAW test 66 (RAW, 2015) and equations 28, 29 and 30. For using this model, the binder stiffness must be known for each work to be delivered. This implies the obligation for each contractor to use a rheometer, since in section 4.3.3 it was concluded that the use of the van der Poel nomograph should be avoided. Besides, for mixes with RAP, each binder must be blended according to the protocol in paragraph 3.5, since the combined penetration rule is not preferred. Determination of the binder stiffness by a Rheometer is time-consuming. On the other hand, using a rheometer to characterize the binder is an accurate and modern approach.

On average, the error of the model as presented by equation 47 is 4.69%. 9.9% of the predicted values differ more than 10% from the measured data. This value is rather high. It roughly implies that 5% of the delivered work needs additional verification without the actual quality being insufficient. Another 5% of the work will be unjustly approved. By excluding mix 938 and analysing the resulting model as presented in equation 48, an average error of 4.32% was found. Only 4.9% of the predicted values differ more than 10% from the measured data. The model becomes twice as reliable.

7 Conclusions and recommendations

7.1 Conclusions

Predictive parameters that are relevant for an asphalt concrete stiffness prediction model are accurately determinable, theoretically preferred and have a high correlation with the asphalt concrete stiffness. Taking this into consideration, for binder characterization predictive parameters preference goes to the use of binder stiffness or penetration value. There should be accounted for the influence of the RAP (reclaimed asphalt pavement) bitumen. A proposed method is the determination of properties of blended RAP and virgin bitumen and use them as predictive parameters. For volumetric parameters the air, binder and aggregates fractions are preferred as predictive parameters. The use of only two of these three predictive parameters suffices in theory, but including them all can separate the influences of composition and compaction. The coefficients of uniformity and curvature are preferred as parameters that describe the gradation of the mix. Models like the van der Poel nomograph used for the determination of predictive parameters should be avoided since this goes at the expense of the accuracy of the asphalt concrete stiffness prediction model. Closely related properties, like binder softening point and binder viscosity, should not be used both to avoid collinearity.

The binder glassy modulus should be avoided as predictive parameter. This parameter can best be obtained by determining the asymptote of the master curve. The parameter cannot be precisely determined. The use of this glassy modulus instead of assuming a fixed value in the Francken model decreases its accuracy.

Most existing asphalt concrete stiffness prediction models are not accurate when applied at the Dutch CIT-CY Boskalis database, which includes base and bind layer mixes with and without polymer modified binders. The Jacobs model shows the highest accuracy with a resulting determination coefficient (R^2) of 0.79, while seven other models do not exceed the 0.55 value. The lowest R^2 value of 0.15 can be found by applying the Hirsch model. By fitting the coefficients on the Boskalis database, the accuracy of most models increases significantly. The R^2 of the majority of the models increase to a value larger than 0.60. The Jacobs models accuracy remains the highest ($R^2 = 0.81$), while the Hirsch models accuracy remains the lowest ($R^2 = 0.25$). The models are inaccurate since the underlying databases differ in mixes and test standards from the Boskalis database. Fitting does not fully compensate for these differences.

The asphalt concrete stiffness of Dutch mixes can be accurately predicted by the use of a multiple linear regression model. This is the same approach as used by Jacobs. A model including the binder stiffness and the air and binder fractions as predictive parameters is preferred and results in a R^2 value of 0.80. 90% of the predictions of such a model are within the 10% deviation limit, which is the desirable accuracy for functional verification. Including many more predictive parameters should be avoided. This does not significantly contribute to the accuracy of the model, and there is a large chance for relations that are not supported by the theory. No gradation characterization parameters have been included in the model for this reason. Including the binder stiffness as a predictive parameter implies the obligation of using a rheometer. Verification of the model using additional data shows varying applicability to surface layer mixes.

Advantages of the Boskalis database are the equal Dutch test conditions on samples with similar age. A large number of candidate predictive parameters has been included. A disadvantage is the limited variation in certain parameters, so that observing non-linear relations becomes difficult. The applicability of a regression model based on this database is

limited. Besides, the number of mixes with a polymer modified binder is too small to perform a well-founded separate regression analysis for this type of mixes.

The unfitted, fitted and preferred regression models show R^2 values up to 0.81. It is questionable if a higher accuracy can be achieved without more accurate asphalt concrete stiffness measurements, or without further differentiation in mixes. When plotting a random binder characterization parameter versus the asphalt concrete stiffness in the Boskalis database, mix 938 with polymer modified binder is mostly an outlier in a linear trend. The combined penetration rule and the Van Der Poel monographs are inaccurate when applying on a polymer modified binder. By performing a multiple linear regression analysis by excluding mix 938 in the database, an R^2 of 0.85 is found. 95% of the predictions of such a model are within the 10% deviation limit. The inclusion of the polymer modified binder mix in the Boskalis database reduces the accuracy of the regression model.

7.2   Recommendations

The following recommendations followed from the research:

- Extend the Boskalis database with more mixes with polymer modified binders and perform separate linear regression analyses for this group of mixes. Building one model by multiple linear regression for all kind of mixes reduces its accuracy. Presumably a more accurate model can be built by obtaining separate equations for mixes with traditional pen bitumen (1) and mixes with polymer modified binders (2). At this moment the database does not suffices for this purpose.
- Extend the Boskalis database with more variation in predictive parameters. In particular, mixes with different binder contents should be included. Subsequently, a nonlinear regression analysis can be performed for increasing the accuracy. Due to the limited size of the Boskalis database at this moment, only a *linear* regression analysis makes sense. Using a larger database for building the model will increase its applicability.
- Extend the Boskalis database with porous asphalt and stone mastic asphalt mixes and verify the applicability of the proposed models to these mixes. A more widely applicable model has more value. Alternatively, additional linear regression analyses can be performed for these groups of mixes. Since these mixes differ significantly in gradation compared to asphalt concrete mixes, inclusion of these mixes in the Boskalis database can lead to more insight in the influence of the gradation on the asphalt concrete stiffness.
- Perform a more extended research on the precision of the binder characterization parameters. Even though all binder tests have been performed twice, some circumstances were kept constant. For two parallel tests bitumen from the same can has been used. All tests have been performed using the same test device and technician. A ring trial between multiple laboratories is preferred. The results can change the preference for certain predictive parameters.
- Perform The Fraass breaking point test and determine the stiffness by using the Bending Beam Rheometer. Use the resulting estimates for the glassy modulus in the Francken and Al-Khateeb models. These glassy modulus values can possibly increase the accuracy of the model, making it an interesting model in the end. The asymptote method proved to be the best out of the two performed methods, but still resulted in an imprecisely determinable glassy modulus which decreases the accuracy of the models.
- Decrease the spread of the asphalt concrete measurements and perform a multiple linear regression analysis. This can be done by testing on larger specimens (i.e. 100 mm instead of 50 mm) or by performing the test multiple times by turning the specimen. An average value of those measurements can be determined. The spread in asphalt

concrete measurements is large, which decreases the possibilities of determining the relations with predictive parameters accurately.

- Perform research on the prediction of other functional properties, like fatigue and tensile strength using the Boskalis database. Especially fatigue is an important design parameter.
- Use the DSR to obtain the stiffnesses of mastic (binder + filler) and use these in a regression analysis. It is possible that the mastic characteristics have a much larger correlation with the functional properties of asphalt concrete than the binder characteristics only. Alternatively, Christensen, Pellinen and Bonaquist (2003) propose models containing the mastic stiffness as predictive parameter, which can be further analyzed.
- Perform research on the Poission ratio of bitumen. A fixed value of 0.3 is used for converting shear moduli into stiffness moduli. However, if the Poisson ratio varies significantly between bitumen types, it can possibly have a significant influence on the predictive parameter bitumen stiffness.
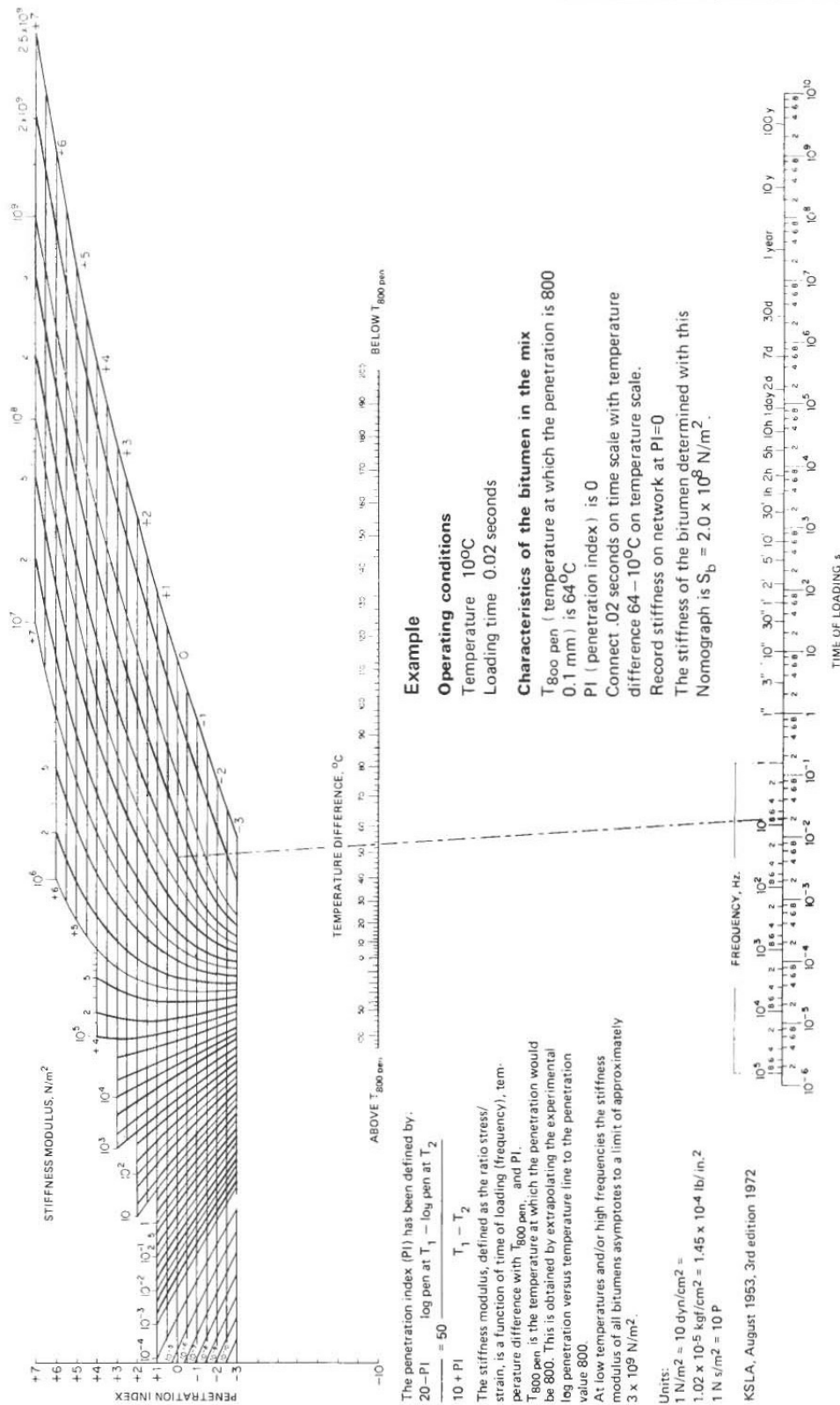
References

Shell International Petroleum Company. (1978). *Shell pavement design manual.* London: Shell International Petroleum Company.

AASHTO. (2007). T 320:2007. *Method Of Test For Determining The Permanent Shear Strain And Stiffness Of Asphalt Mixtures Using The Superpave Shear Tester (Sst)*. AASHTO.

AASHTO. (2007). TP 62-03. *Standard method for determining dynamic modulus of hot mix asphalt (HMA)*. AASHTO.

Al-Khateeb, G., Shenoy, A., Gibson, N., & Harman, T. (2006, March 27-29). A New Simplistic Model for Dynamic Modulus Predictions of Asphalt Paving Mixtures. *Asphalt Paving Technology*, *75*, pp. 1254-1293. Savannah, Georgia.

Anderson, D. (1994). *SHRP A-369 Binder characterization and Evaluation Volume 3: Physical Characterization.* Washington DC: National Academy of Sciences.

Asfalt Impuls. (2018). *Systematiek voor functioneel opleveren.*

ASTM International. (2003). D3497-79. *Standard Test Method for Dynamic Modulus of Asphalt Mixtures*. ASTM International.

Bari, J., & Witczak, M. (2006). Development of a New Revised Version of the Witczak E* Prdeictive Model for Hot Mix Asphalt Mixtures. *Asphalt Paving Technology* (pp. 381-423). Savannah: Association of Asphalt Paving Technologists.

Bonnaure, F., Gest, G., Gravois, A., & Uge, P. (1977). a New Method of Predicting the Stiffness of Asphalt Paving Mixtures. *46*, pp. 64-104. San Antonio: Association of Asphalt Paving Technologists.

Christensen, D., Terhi Pellinen, J., & Bonaquist, R. (2003). Hirsch Model for Estimating the Modulus of Asphalt Concrete. *Asphalt paving technology* (pp. 121-151). Lexington: Association of Asphalt Paving Technologists.

CROW. (2014). *Standaard RAW bepalingen 2015.* Ede: CROW.

Field, A. (2013). *Discovering atatistics using IBM SPSS statistics.* Sage Publications Ltd.

Francken, L. (1982). *Wet van de blijvende vervorming van asfaltbeton - invloed van de samenstelling en rol van de bestanddelen.* Brussel: Opzoekingscentrum voor de Wegenbouw.

Francken, L., & Clauwaert, C. (1987). Characterization and Structural Assessment of Bound Materials for Flexible Road Structures. *Sixth International Conference, Structural design of asphalt pavements. 1*, pp. 130-144. Ann Arbor: University of Michigan.

Francken, L., & Verstraeten, J. (1974). Methods for predicting moduli and fatigue laws of bituminous road mixes under repeated bending. *53rd Annual Meeting of the Highway Research Board* (pp. 114-123). Washington D.C.: Transportation Research Board.

Francken, L., Vanelstraete, A., Leonard, D., & Pilate, O. (2003). New Developments in the Prado Volumetric Mix Design. *Symposium on Performance Testing and Evaluation of Bituminous Materials.* Zurich.

Huang, Y. H. (2004). *Pavement Analysis and Design.* Upper Saddle River: Pearson Education, Inc.

Igwe, E. (2016, May). Comparative Study of Asphalt Institute – Witczak 1-40D Dynamic Moduli for Polythene Bag Modified HMA Concrete Using Predictive Models. *International Journal of Innovative Science, Engineering & Technology, 3*, 47-55.

Jacobs, M., Qiu, J., Frunt, M., & Rering, A. (n.d.). *Analysis of the Relationship between Asphalt Mix Design and Functional Performance.* Utrecht: Bam Infra Asfalt.

Liu, X. (2016). Slides CIE4880 lecture 10 AC Volumetrics and & Physical Props. TU Delft.

Liu, X. (2016). Slides CIE4880 lecture 5 HMA mixture types & Gradations. TU Delft.

Marsac, P. (1999). *Affaire 47_10 Analyse des résultats.*

Mezger, T. G. (2014). *The Rheology Handbook.* Hanover: Vincentz Network GmbH & Co.

Mohan, S. (2010). *Stageverslag.* BAM, TU Delft.

NEN. (1999). NEN-EN 932-2 en. *Beproevingsmethoden voor algemene eigenschappen van toeslagmaterialen - Deel 2: Methoden voor het delen van laboratoriummonsters*.

NEN. (2012). NEN-EN 12697-6:2012 en. *Bituminous mixtures - Test methods for hot mix asphalt - Part 6: Determination of bulk density of bituminous specimens*.

NEN. (2012). NEN-EN 14771:2012 en. *Bitumen and bituminous binders - Determination of the flexural creep stiffness - Bending Beam Rheometer (BBR)*.

NEN. (2014). NEN-EN 12594:2014. *Bitumen and bituminous binders - Preparation of*.

NEN. (2015). NEN-EN 12593:2015 en. *Bitumen and bituminous binders - Determination of the Fraass breaking point*.

NEN. (2015). NEN-EN 12697-2:2015 en. *Bituminous mixtures - Test methods - Part 2: Determination of particle size distribution*.

NEN. (2015). NEN-EN 12697-4. *Bituminous mixtures - Test methods - Part 4: Bitumen recovery: Fractionating column* .

NEN. (2015). NEN-EN 1426:2015 en. *Bitumen and bituminous binders - Determination of needle penetration*.

NEN. (2015). NEN-EN 1427:2015 en. *Bitumen and bituminous binders - Determination of the softening point - Ring and Ball method*.

NEN. (2016). NEN-EN 13108-1:2016 en. *Bituminous mixtures - Material specifications - Part 1: Asphalt Concrete*.

NEN. (2018). NEN-EN 12697-26:2018 en. *Bituminous mixtures - Test methods - Part 26: Stiffness*.

Poel, C. v. (1954). A general system describing the visco-elastic properties of bitumens and its relation to routine test data.

Poeran, N., Sluer, B., & Telman, J. (2018). *Van functioneel verifiëren naar functioneel opleveren.*

Pouget, S., Sauzeat, C., Di Benedetto, H., & Olard, F. (2012). *Prediction of isotropic linear viscoelastic behaviour for bituminous materials - forward and inverse problems.* EIFFAGE Travaux Publics – R&D Department.

QRS Quality research and support. (2017). *Notulen gebruikersoverleg CY-ITT S&F.*

Scarpas, A., Erkens, S., Dollevoet, R., & Houben, L. (2015). *Dictaat CTB3320 Weg- en Railbouwkunde.* Delft: TU Delft.

Shahin, M. Y., & McCullough, B. F. (1972). *Prediction of low-temperature and thermal-fatigue cracking in flexible pavements.* Austin: Center for highway research.

Shen, S., & Carpenter, S. (2007). *Dissipated Energy concepts for HMA performance: Fatique And Healing.* Urbana: Center of excellence For Airport Technology.

Verstraeten, J., Romain, J., & Veverka, V. (1977). The Belgian Road Research Center's Overall Approach to Asphalt Pavement Structural Design. *Fourth International Conference, Structural Design of Asphalt Pavements. 1*, pp. 298-324. Ann Arbor: University of Michigan.

Viswanadham, B. (n.d.). Lecture 7. Bombay, India: Indian Institute of Technology.

Waze. (2017, November 07). *The 2017 Waze Driver Satisfaction Index*. Retrieved from Waze: https://blog.waze.com/2017/11/the-2017-waze-driver-satisfaction-index.html

Appendix A – Van Der Poel Nomograph

The penetration index (PI) has been defined by:

$$\frac{20-PI}{10+PI} = 50 \cdot \frac{\log \text{pen at } T_1 - \log \text{pen at } T_2}{T_1 - T_2}$$

The stiffness modulus, defined as the ratio stress/strain, is a function of time of loading (frequency), temperature difference with $T_{800\,pen}$, and PI. $T_{800\,pen}$ is the temperature at which the penetration would be 800. This is obtained by extrapolating the experimental log penetration versus temperature line to the penetration value 800.

At low temperatures and/or high frequencies the stiffness modulus of all bitumens asymptotes to a limit of approximately 3×10^9 N/m².

Units:

$1 \text{ N/m}^2 = 10 \text{ dyn/cm}^2 =$
$1.02 \times 10^{-5} \text{ kgf/cm}^2 = 1.45 \times 10^{-4} \text{ lbf/in.}^2$
$1 \text{ N s/m}^2 = 10 \text{ P}$

KSLA, August 1953, 3rd edition 1972

Example

Operating conditions

Temperature   10°C
Loading time   0.02 seconds

Characteristics of the bitumen in the mix

$T_{800\,pen}$ (temperature at which the penetration is 800
0.1 mm) is 64°C

PI (penetration index) is 0

Connect .02 seconds on time scale with temperature difference 64 − 10°C on temperature scale.

Record stiffness on network at PI=0

The stiffness of the bitumen determined with this Nomograph is $S_b = 2.0 \times 10^8$ N/m².

Appendix B – Overview Boskalis database

Number of mixes: 7

Number of asphalt concrete specimens per mix: 8 - 12

Parameter group	Parameter	Symbol	Unit	Min value	Max value
Asphalt properties	Asphalt concrete stiffness	S_{mix}	MPa	6234	10787
Volumetric properties	Volume air voids	V_a	%	3.47	6.31
	Volume aggregates	V_g	%	81.76	86.61
	Volume bitumen	V_b	%	9.63	13.39
	Voids in the mineral aggregate	VMA	%	13.39	18.24
	Voids filled with bitumen	VFB	%	60.60	78.05
	Ratio V_g/V_b	V_g/V_b	-	6.19	8.74
	Density	$\rho_{specimen}$	kg/m^3	2324.65	2393.82
	Target density	ρ_{target}	kg/m^3	2350.00	2390.00
Virgin bitumen properties	Stiffness virgin bitumen	$S_{bit,virgin}$	MPa	7.94	24.37
	Glassy modulus virgin bitumen	$S_{bit,inf,virgin}$	MPa	1170.56	2943.44
	Shear glassy modulus virgin bitumen	$G^*_{bit,inf,virgin}$	MPa	450.22	1132.09
	Shear stiffness virgin bitumen	$G^*_{bit,virgin}$	MPa	3.05	9.37
	Penetration virgin bitumen	Pen_{virgin}	dmm	60.83	89.67
	Ring & Ball softening point virgin bitumen	$T_{R\&K,virgin}$	°C	50.45	105.43
	Penetration index virgin bitumen	PI_{virgin}	-	0.05	8.60
	Phase angle virgin bitumen	δ_{virgin}	°	46.49	53.70
	Viscosity at 135°C virgin bitumen	$\eta_{virgin,135°C}$	mPa*s	401	1758
	Viscosity at 150°C virgin bitumen	$\eta_{virgin,150°C}$	mPa*s	242	980
Blended bitumen properties	Stiffness blended bitumen	$S_{bit,blend}$	MPa	12.55	31.86
	Glassy modulus blended bitumen	$S_{bit,inf,blend}$	MPa	1170.56	3440.39
	Shear glassy modulus blended bitumen	$G^*_{bit,inf,blend}$	MPa	450.22	1323.23
	Shear stiffness blended bitumen	$G^*_{bit\_blend}$	MPa	4.83	12.25
	Penetration blended bitumen	Pen_{blend}	dmm	30.67	60.83
	Ring & Ball softening point blended bitumen	$T_{R\&K,blend}$	°C	53.23	63.80
	Penetration index blended bitumen	PI_{blend}	-	0.05	0.96
	Phase angle blended bitumen	δ_{blend}	°	35.88	46.49
	Viscosity at 135°C blended bitumen	$\eta_{blend,135°C}$	mPa*s	493	1229
	Viscosity at 150°C blended bitumen	$\eta_{blend,150°C}$	mPa*s	242	658
Sieve sizes	Percentage passing sieve C22.4	C22.4	%	98.83	100.00
	Percentage passing sieve C16	C16	%	88.44	100.00
	Percentage passing sieve C11.2	C11.2	%	77.50	98.22
	Percentage passing sieve C8	C8	%	65.43	85.00
	Percentage passing sieve C5.6	C5.6	%	51.80	66.70
	Percentage passing sieve 2 mm	2 mm	%	43.00	45.00
	Percentage passing sieve 0.500 mm	0.500 mm	%	23.62	31.47
	Percentage passing sieve 0.180 mm	0.180 mm	%	9.00	14.69
	Percentage passing sieve 0.063 mm	0.063 mm	%	6.00	6.50

US sieve standards	Percentage passing sieve #200	$P200$	%	6.60	7.27
	Percentage retained at sieve #4	$P4$	%	38.67	50.25
	Percentage retained at sieve 3/8 inch	$P38$	%	8.76	28.87
	Percentage retained at sieve 3/4 inch	$P34$	%	0.00	6.69
Sieve curve characteristics	Coefficient of uniformity	C_u	-	27.70	55.54
	Coefficient of curvature	C_c	-	0.18	2.79
Other	Max grain size	D_{max}	mm	11.00	22.00
	Specimen age	age	days	44.50	53.00
	RAP percentage	RAP%	%	0	65

Appendix C – Protocol database expansion

For extending the Boskalis database with other mixes, a protocol is written to obtain values for all predictive parameters.

Perform the following tests for each mix:

1   Asphalt

   a. Perform CIT-CY stiffness measurements according to NEN-EN 12697-26:2018 on a minimum number of 8 specimens with dimensions of 40 mm in height and a diameter of 100 mm. The age of the specimens at testing should be 6 +/- 1 weeks. Start and end with a frequency of 30 Hz. Turn the specimen 90° and repeat the test.
   b. Determine the density of each specimen according to NEN-EN 12697-6:2012 en.

2   Bitumen

Perform tests c-g on the following binders:

In the case of a mix without RAP:

   - The virgin bitumen from the same can / batch as used for producing the asphalt.

In the case of a mix with RAP:

   - The virgin bitumen from the same can / batch as used for producing the asphalt.
   - The blended virgin and RAP bitumen according to paragraph 3.5.

   c. Determine the softening point **twice** according to NEN-EN 1427:2015 en.
   d. Determine the penetration **twice** according to NEN-EN 1426:2015 en.
   e. Perform amplitude sweeps using a DSR at a frequency of 10 rad/s and at temperatures of -10 °C, 20 °C and 40 °C. Determine the LVE range and obtain safe strain levels for the frequency sweep.
   f. Perform frequency sweeps **in duplicate** using a DSR at 0,1 to 100 rad/s using safe strain levels as obtained in the amplitude sweeps. Perform tests at the following temperatures:
      - For pen bitumen / blended bitumen with pen bitumen:
         - -10 °C, 0 °C, 10 °C, 20 °C (PP8) and 20 °C, 30 °C, 40 °C, 50 °C (PP25).
      - For polymer modified bitumen / blended bitumen with polymer modified bitumen:
         - -10 °C, 0 °C, 10 °C, 20 °C (PP8) and 20 °C, 30 °C, 40 °C, 50 °C, 60 °C, 70 °C (PP25).
   g. Perform viscosity tests **in duplicate** at 135 °C and 150 °C at a shear rate of 500 1/s.

Make sure the densities of the bitumen and aggregates (representative density) are known.

In the following table short descriptions are given for the determination of each predictive parameter.

| Parameter	Remarks
S_{mix}	Use the average 8 Hz CIT-CY value. Exclude the value from the database if the 30 Hz stiffness values differ more than 15% or the 8 Hz values before and after turning differ more than 15%.
V_a	Use equations 28, 29, and 30.
V_g	Use equations 28, 29.
V_b	Use equations 28, 29.
VMA	Use equations 28, 29, 30 and 31.
VFB	Use equations 28, 29, 30 and 32.
V_g/V_b	Use equations 28, 29.
$\rho_{specimen}$	Obtain the denisty according to NEN-EN 12697-6:2012 en.
ρ_{target}	Obtain from the mix design.
$S_{bit,virgin}$	Obtain a master curve at 20°C and interpolate at 8 Hz. Use the average of the two independent values. Use equation 18 to convert the shear stiffness values assuming a Poisson ratio of 0.3.
$S_{bit,inf,virgin}$	Obtain glassy modulus values using the asymptote method (section 4.3.7). Use the average of the two independent values. Use equation 18 to convert the shear stiffness values assuming a Poisson ratio of 0.3.
$G^*_{bit,inf,virgin}$	Obtain glassy modulus values using the asymptote method (section 4.3.7). Use the average of the two independent values.
$G^*_{bit,virgin}$	Obtain a master curve at 20°C and interpolate at 8 Hz. Use the average of the two independent values.
Pen_{virgin}	Use the average value.
$T_{R\&K,virgin}$	Use the average value.
PI_{virgin}	Use the average value.
δ_{virgin}	Obtain a master curve at 20°C and interpolate at 8 Hz. Use the average of the two independent values.
$\eta_{virgin,135°C}$	Use the average value of the measurements at varying frequency.
$\eta_{virgin,150°C}$	Use the average value of the measurements at varying frequency.
$S_{bit,blend}$	Obtain a master curve at 20°C and interpolate at 8 Hz. Use the average of the two independent values. Use equation 18 to convert the shear stiffness values assuming a Poisson ratio of 0.3.
$S_{bit,inf,blend}$	Obtain glassy modulus values using the asymptote method (section 4.3.7). Use the average of the two independent values. Use equation 18 to convert the shear stiffness values assuming a Poisson ratio of 0.3.
$G^*_{bit,inf,blend}$	Obtain glassy modulus values using the asymptote method (section 4.3.7). Use the average of the two independent values.
$G^*_{bit\_blend}$	Obtain a master curve at 20°C and interpolate at 8 Hz. Use the average of the two independent values.
Pen_{blend}	Use the average value.
$T_{R\&K,blend}$	Use the average value.
PI_{blend}	Use the average value.
δ_{blend}	Obtain a master curve at 20°C and interpolate at 8 Hz. Use the average of the two independent values.
$\eta_{blend,135°C}$	Use the average value of the measurements at varying frequency.
$\eta_{blend,150°C}$	Use the average value of the measurements at varying frequency.
C22.4	Obtain from the mix design.
C16	Obtain from the mix design.
C11.2	Obtain from the mix design.
C8	Obtain from the mix design.
C5.6	Obtain from the mix design.
2 mm	Obtain from the mix design.
0.500 mm	Obtain from the mix design.

0.180 mm	Obtain from the mix design.
0.063 mm	Obtain from the mix design.
P200	Interpolate from mix design data.
P4	Interpolate from mix design data.
P38	Interpolate from mix design data.
P34	Interpolate from mix design data.
C_u	Use equation 42 and interpolate from mix design data.
C_c	Use equation 43 and interpolate from mix design data.
D_{max}	Obtain from the mix design.
age	The number of days between the production day of the asphalt and the day of the CIT-CY testing.
RAP%	Obtain from the mix design.

Appendix D – Residue plots binder characterization parameters
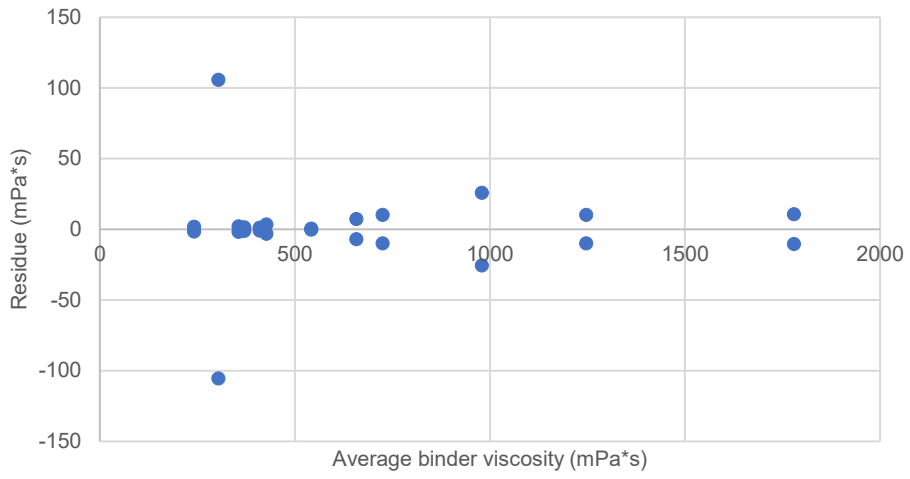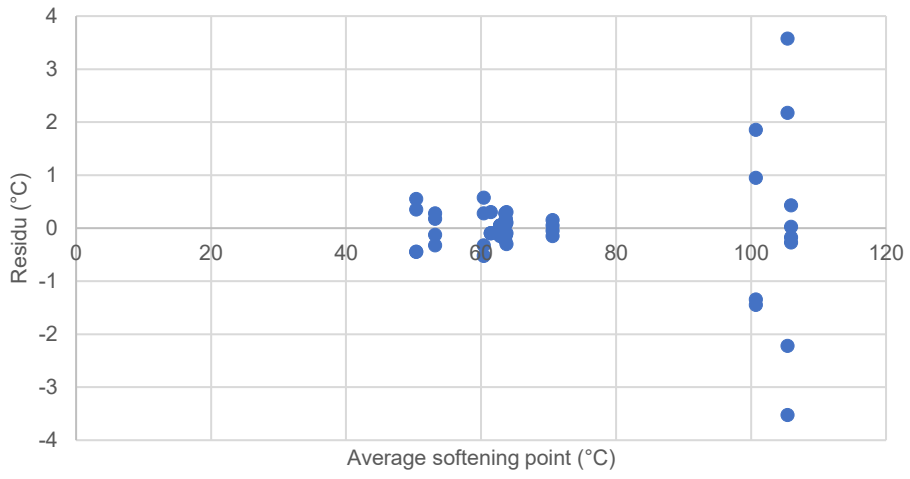
Residue plot binder stiffness
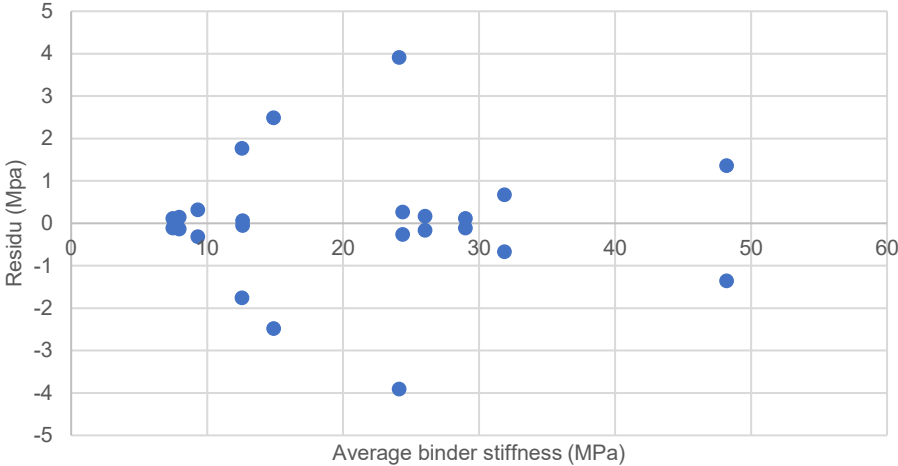
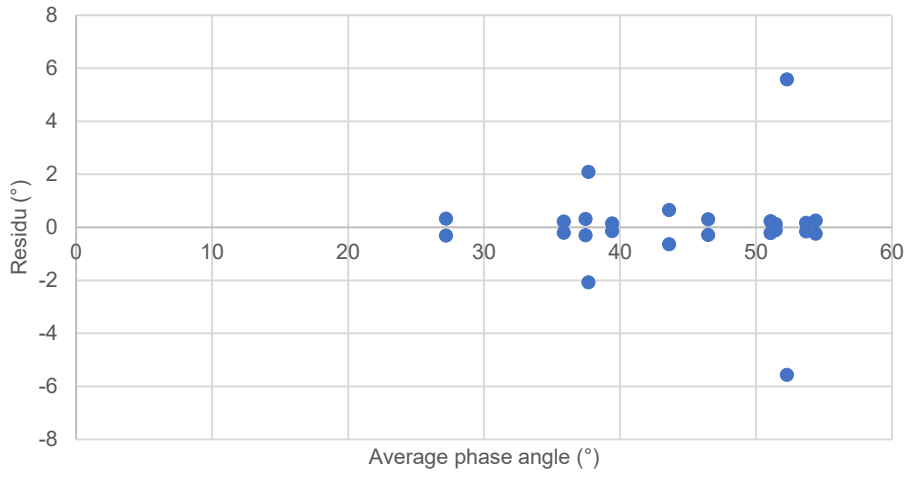### Residue plot binder viscosity 135°C
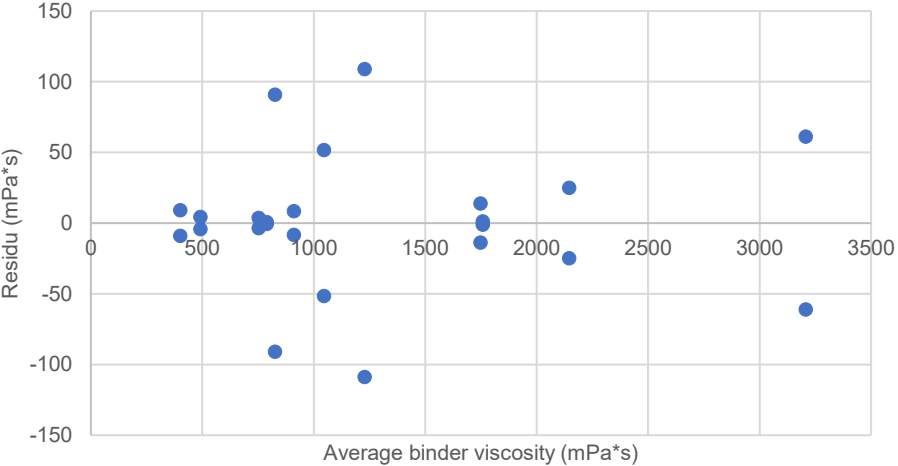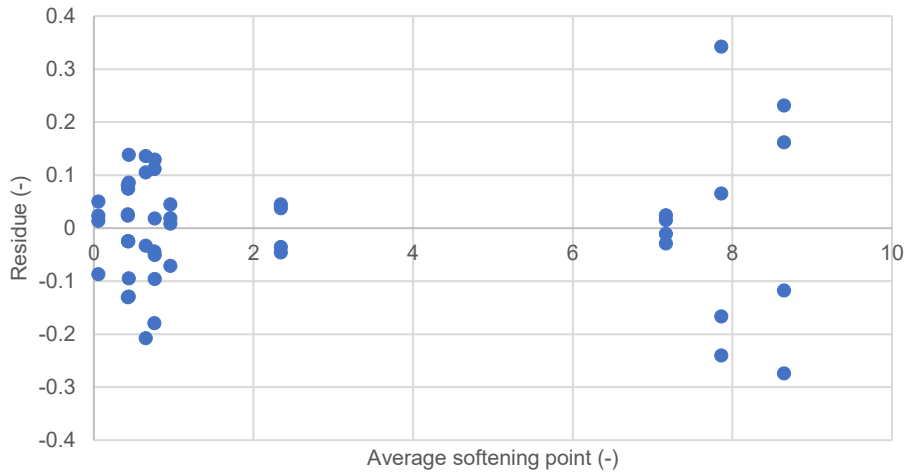
Residue plot binder viscosity 150°C
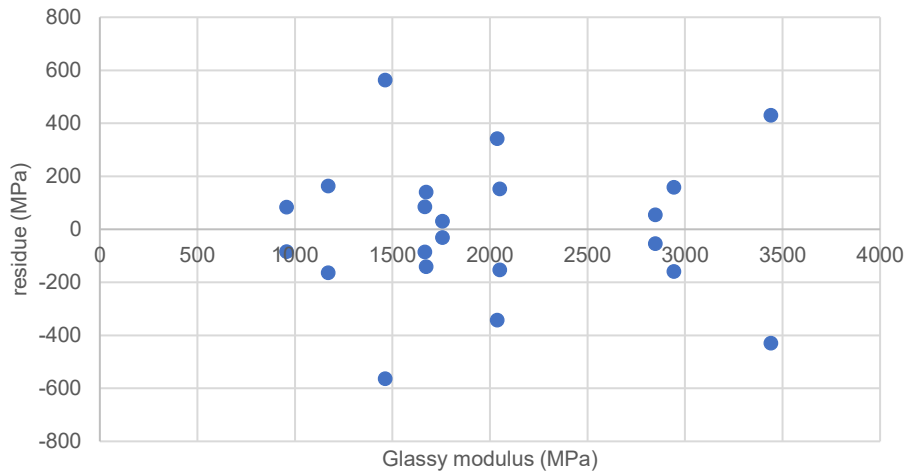

Residue plot softening point

Residue plot phase angle

Residue PI Index

Residue plot glassy modulus

Appendix E – Mutual relations predictive parameters

E-1   Pearson correlation matrix binder characterization parameters

	Shear modulus 8 Hz 20˚C	Stiffness modulus 8 Hz 20˚C	Viscosity 135˚C	Viscosity 150˚C	Penetration	Ring & Ball softening point	Penetration index (PI)	Glassy modulus (asymptote method)
Shear modulus 8 Hz 20˚C	1.00	1.00	-0.17	-0.33	-0.81	-0.37	-0.57	-0.36
Stiffness modulus 8 Hz 20˚C	1.00	1.00	-0.17	-0.33	-0.81	-0.37	-0.57	-0.36
Viscosity 135˚C	-0.17	-0.17	1.00	0.98	0.02	0.89	0.79	0.73
Viscosity 150˚C	-0.33	-0.33	0.98	1.00	0.16	0.91	0.85	0.78
Penetration	-0.81	-0.81	0.02	0.16	1.00	0.28	0.51	0.10
Ring & Ball softening point	-0.37	-0.37	0.89	0.91	0.28	1.00	0.96	0.57
Penetration index (PI)	-0.57	-0.57	0.79	0.85	0.51	0.96	1.00	0.51
Glassy modulus (asymptote method)	-0.36	-0.36	0.73	0.78	0.10	0.57	0.51	1.00

E-2   Pearson correlation matrix volumetric parameters

	Volume air voids	Volume aggregates	Volume bitumen	Voids in the mineral aggregate	Voids filled with bitumen	V_g/V_b	Density	Target density
Volume air voids	1.00	-0.24	-0.26	0.24	-0.85	0.21	-0.97	-0.63
Volume aggregates	-0.24	1.00	-0.88	-1.00	-0.30	0.90	0.43	0.22
Volume bitumen	-0.26	-0.88	1.00	0.88	0.73	-1.00	0.06	0.09
Voids in the mineral aggregate	0.24	-1.00	0.88	1.00	0.30	-0.90	-0.43	-0.22
Voids filled with bitumen	-0.85	-0.30	0.73	0.30	1.00	-0.69	0.72	0.49
V_g/V_b	0.21	0.90	-1.00	-0.90	-0.69	1.00	0.00	-0.06
Density	-0.97	0.43	0.06	-0.43	0.72	0.00	1.00	0.63
Target density	-0.63	0.22	0.09	-0.22	0.49	-0.06	0.63	1.00

E-3   Pearson correlation matrix gradation characterization parameters

	C22,4	C16	C11,2	C8	C5,6	2 mm	0.5 mm	0.180 mm	0.063 mm	#200	3/8 inch	3/4 inch	34	D_{max}
C22,4	1.00	0.99	0.70	0.55	0.29	0.34	-0.34	-0.38	0.72	0.26	-0.30	-0.64	-0.99	-0.89
C16	0.99	1.00	0.80	0.66	0.42	0.47	-0.46	-0.38	0.73	0.27	-0.42	-0.74	-1.00	-0.94
C11,2	0.70	0.80	1.00	0.96	0.79	0.86	-0.89	-0.38	0.67	0.22	-0.81	-0.99	-0.79	-0.94
C8	0.55	0.66	0.96	1.00	0.82	0.96	-0.95	-0.47	0.50	0.02	-0.83	-0.99	-0.65	-0.86
C5.6	0.29	0.42	0.79	0.82	1.00	0.86	-0.86	0.07	0.29	0.27	-1.00	-0.82	-0.41	-0.61
2 mm	0.34	0.47	0.86	0.96	0.86	1.00	-0.98	-0.43	0.29	-0.11	-0.87	-0.92	-0.46	-0.71
0.5 mm	-0.34	-0.46	-0.89	-0.95	-0.86	-0.98	1.00	0.38	-0.39	-0.01	0.88	0.93	0.45	0.71
0.180 mm	-0.38	-0.38	-0.38	-0.47	0.07	-0.43	0.38	1.00	-0.14	0.66	-0.04	0.43	0.38	0.46
0.063 mm	0.72	0.73	0.67	0.50	0.29	0.29	-0.39	-0.14	1.00	0.66	-0.31	-0.59	-0.73	-0.75
#200	0.26	0.27	0.22	0.02	0.27	-0.11	-0.01	0.66	0.66	1.00	-0.27	-0.12	-0.27	-0.23
#4	-0.30	-0.42	-0.81	-0.83	-1.00	-0.87	0.88	-0.04	-0.31	-0.27	1.00	0.83	0.41	0.62
3/8 inch	-0.64	-0.74	-0.99	-0.99	-0.82	-0.92	0.93	0.43	-0.59	-0.12	0.83	1.00	0.73	0.91
3/4 inch	-0.99	-1.00	-0.79	-0.65	-0.41	-0.46	0.45	0.38	-0.73	-0.27	0.41	0.73	1.00	0.94
D_{max}	-0.89	-0.94	-0.94	-0.86	-0.61	-0.71	0.71	0.46	-0.75	-0.23	0.62	0.91	0.94	1.00

Appendix F – Verifications results currently existing models

F-1   Shell

Generalized model:

$$\beta_1 = C1 + \frac{C2 * (C3 - V_g)}{V_g + V_b} \tag{F-1.1}$$

$$\beta_2 = C4 + C5 * V_g + C6 * V_g^2 \tag{F-1.2}$$

$$\beta_3 = C7 * \log(\frac{C8 * V_b^2 + C9}{C10 * V_b + C11}) \tag{F-1.3}$$

$$\beta_4 = C12 * (\beta_1 - \beta_2) \tag{F-1.4}$$

For $5*10^6$ N/m^2 < S_b < 10^9 N/m^2:

$$\log S_m = \frac{\beta_4 + \beta_3}{C13}(\log(S_b) + C14) + \frac{\beta_4 - \beta_3}{C15}|\log S_b + C16| + \beta_2 \tag{F-1.5}$$

For 10^9 N/m^2 < S_b < $3 * 10^9$ N/m^2:

$$\log S_m = \beta_2 + \beta_4 + C17(\beta_1 - \beta_2 - \beta_4)(\log S_b + C18) \tag{F-1.6}$$

Coefficients:

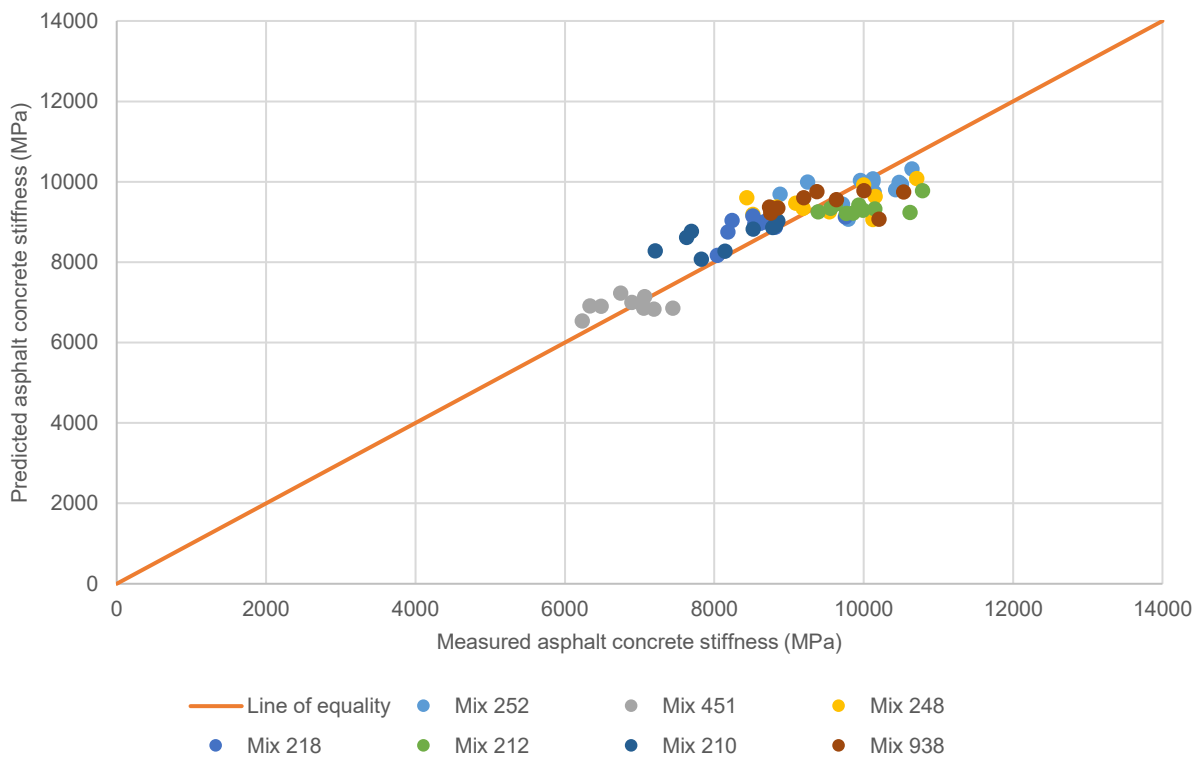|	Original model	Fitted model
C1	10.82	10.73498685
C2	-1.342	0
C3	100	100
C4	8	7.971436965
C5	0.00568	0.005662747
C6	0.0002135	0.000209336
C7	0.6	0.598784145
C8	1.37	1.368832016
C9	-1	-1
C10	1.33	1.331133751
C11	-1	-1
C12	0.7582	0
C13	2	3.023212762
C14	-8	0.042365662
C15	2	2.973600883
C16	-8	0
C17	2.0959	2.107724256
C18	-9	0

Prediction plot:

Shell model prediction (original constants)
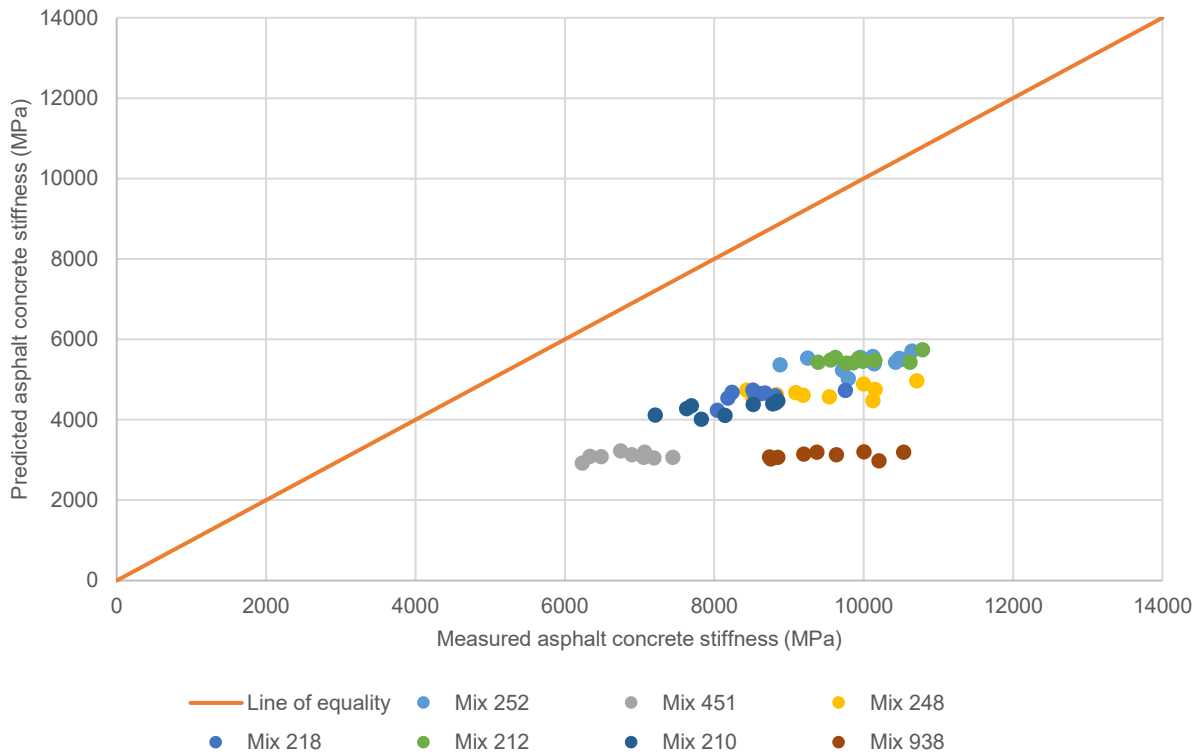
Shell model prediction (fitted constants)

F-2 Asphalt institute

Generalized model:

$$E^* = C1 * C2^{\beta_1} \tag{F-2.1}$$

$$\beta_1 = \beta_3 + C3 * \beta_2 + C4 * \beta_2 f^{C5} \tag{F-2.2}$$

$$\beta_2 = \beta_4{}^{C6} T^{\beta_5} \tag{F-2.3}$$

$$\beta_3 = C7 + C8 * (P_{200} f^{C9}) + C10 * V_A + C11 * \lambda + C12 * f^{C13} \tag{F-2.4}$$

$$\beta_4 = C14 * V_b \tag{F-2.5}$$

$$\beta_5 = C15 + C16 * \log f \tag{F-2.6}$$

Coefficients:

	Original model	Fitted model
C1	100000	552225.3783
C2	10	1.523044514
C3	0.000005	5.39535E-07
C4	-0.00189	0
C5	-1.1	-1.1
C6	0.5	0.483901967
C7	0.553833	0.58585485
C8	0.028829	0.029077409
C9	-0.1703	-0.1703
C10	-0.03476	-0.03476
C11	0.07037	0.048525718
C12	0.931757	1.017300517
C13	-0.02774	-0.02774
C14	0.483	0.486414743
C15	1.3	1.405833659
C16	0.49825	0.512299698

Prediction plot:

Asphalt institute model prediction (original constants)
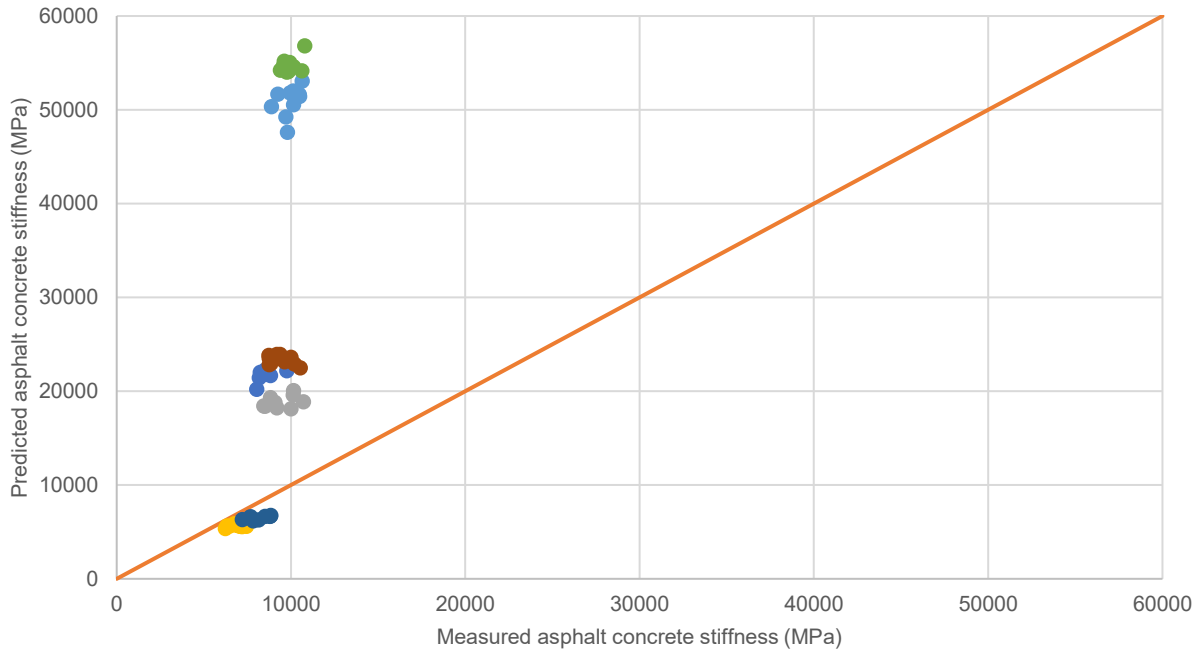
Asphalt institute model prediction (fitted constants)
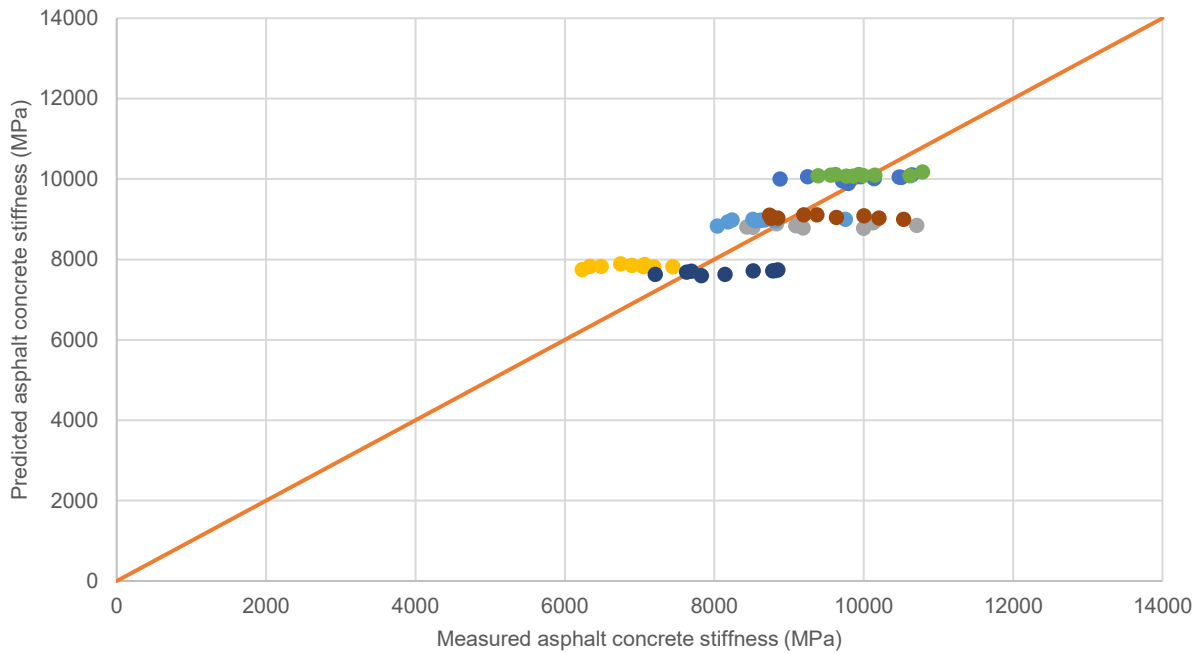
F-3   Francken

Generalized model:

$$|E *|(T, Fr) = E_\propto * R^*(T, Fr) \ (MPa) \tag{F-3.1}$$

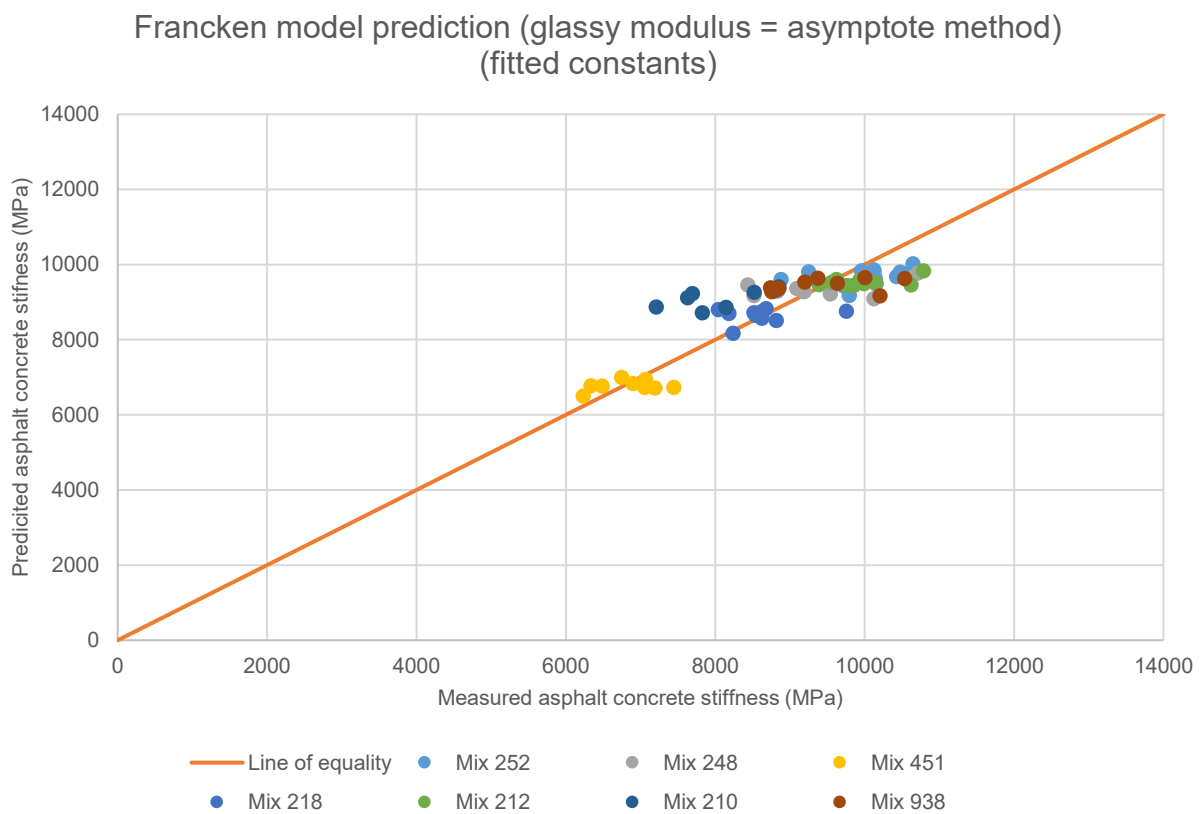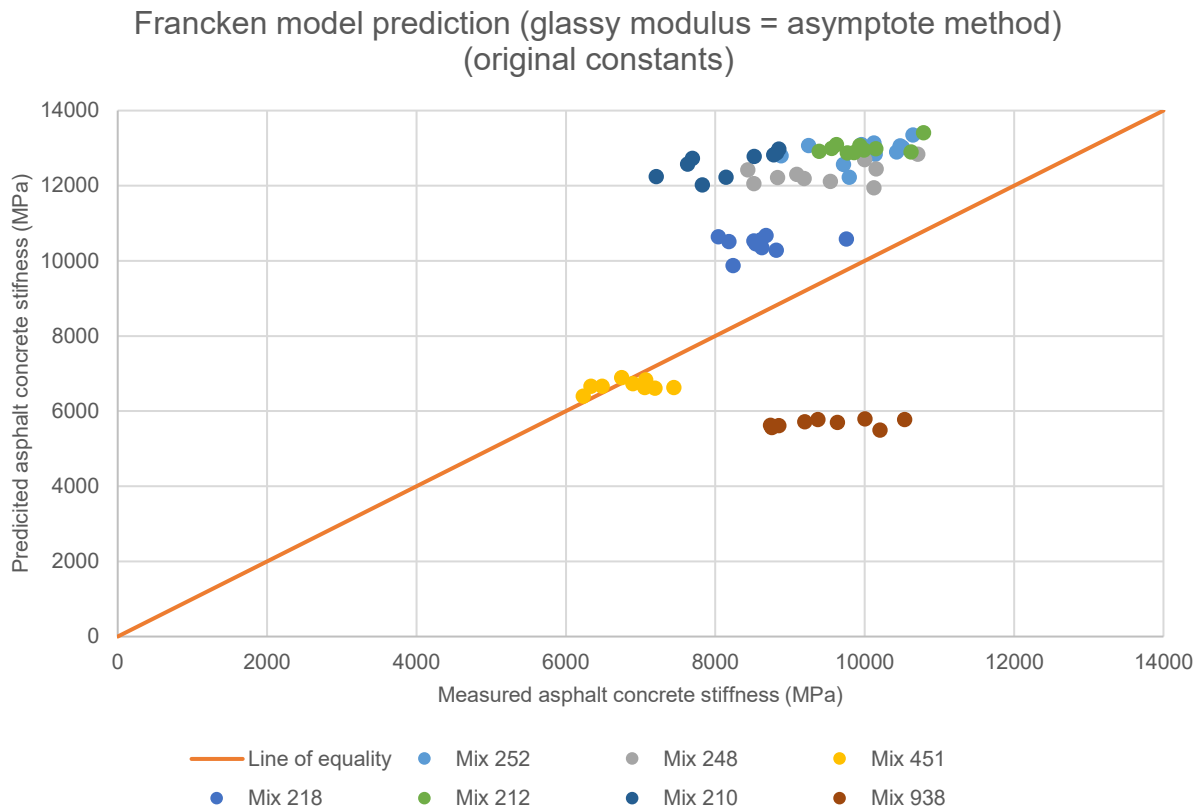$$E_\propto = C1 * \left(\frac{V_g}{V_b}\right)^{C2} \exp(C3 * V_a) \tag{F-3.2}$$

$$\log(R^*) = \log(B *)(C4 + C5(C6 - \exp(C7 * \left(\frac{V_g}{V_b}\right))(C8 + C9 * \log(B *)) \tag{F-3.3}$$

$$B *= \frac{S_{bit}(T, F_R)}{S_{bit,inf}} \tag{F-3.4}$$

Coefficients:

|	Original model	Fitted model (Glassy modulus = asymptote method)	Fitted model (Glassy modulus = 3000 MPa)
C1	14360	173041.8578	103874.8428
C2	0.55	0	0.214323612
C3	-0.0584	-0.0584	-0.110593616
C4	1	1	1
C5	-1.35	-1.35	-0.108054692
C6	1	1	1
C7	-0.13	0.010314936	-0.252546704
C8	1	1	1
C9	0.11	2.121476148	-2.056712658

Prediction plot:

Francken model prediction (glassy modulus = asymptote method)
(original constants)

Francken model prediction (glassy modulus = asymptote method)
(fitted constants)
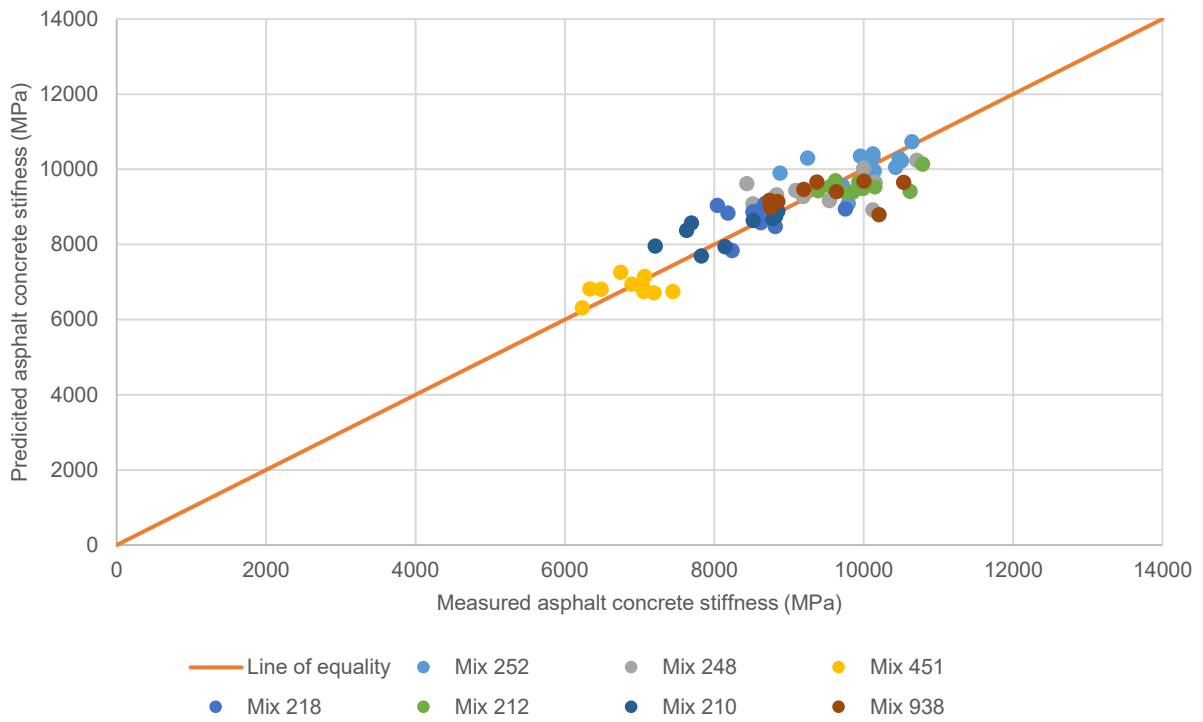
Francken model prediction (glassy modulus = 3000 MPa) (original constants)
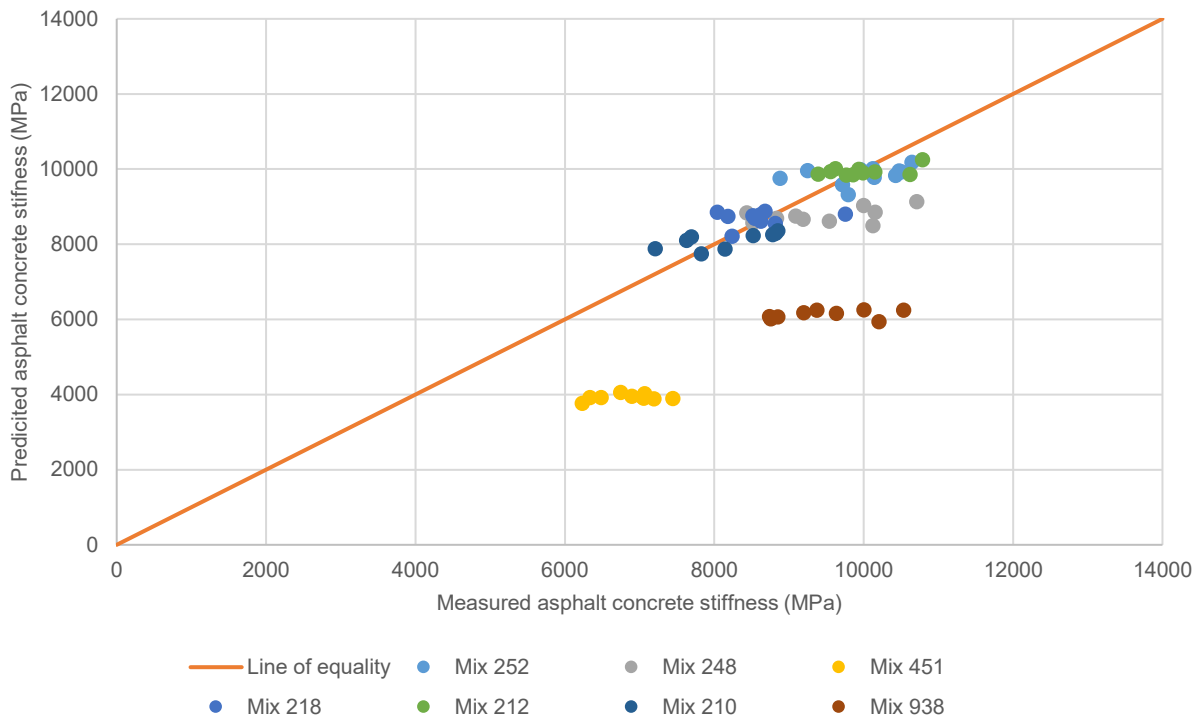
Francken model prediction (glasmodulus = 3000 MPa) (fitted constants)
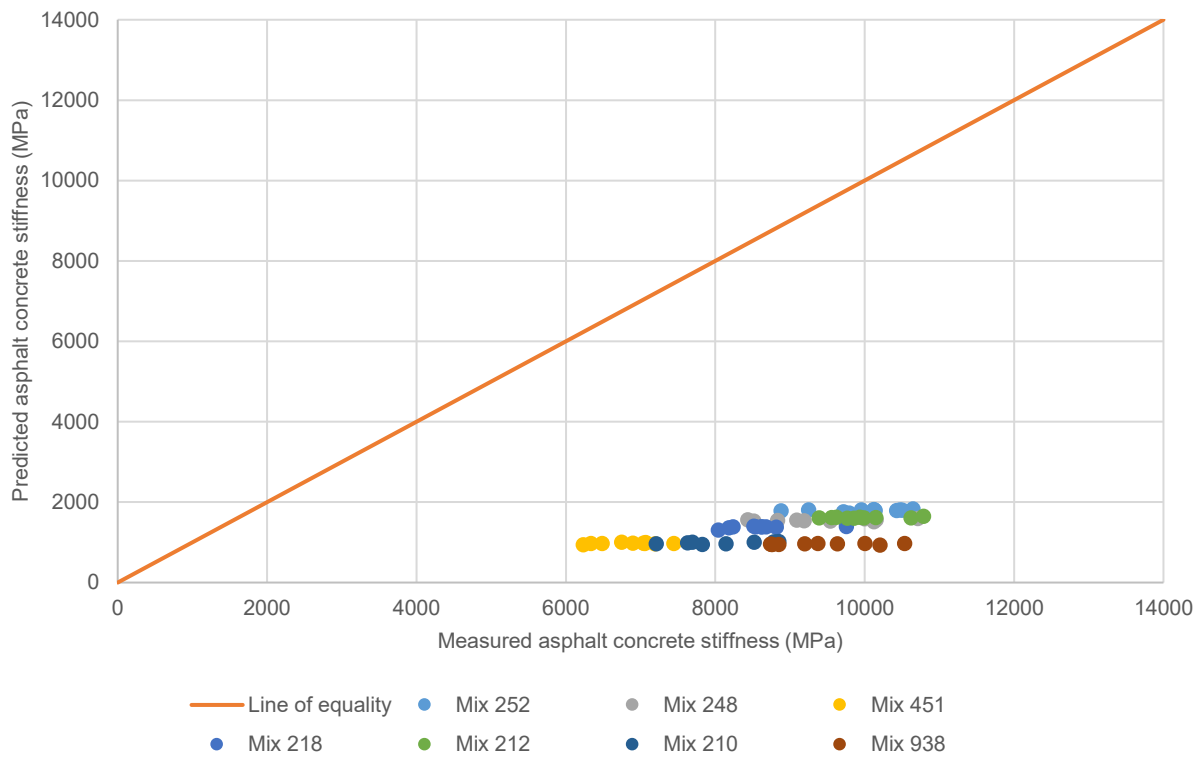
F-4   Witczak 1999

Generalized model:

$$Log|E^*| = C1 + C2 * P_{200} + C3 * (P_{200})^2 + C4 * P_4 + C5 * V_A + C6 * \frac{V_{beff}}{(V_{beff} + V_A)}$$

$$+ \frac{(C7 + C8 * P_4 + C9 * P_{38} + C10 * (P_{38})^2 + C11 * P_{34})}{C12 + e^{(C13 + C14 * log f + C15 * log \eta)}} \qquad \text{(F-4.1)}$$
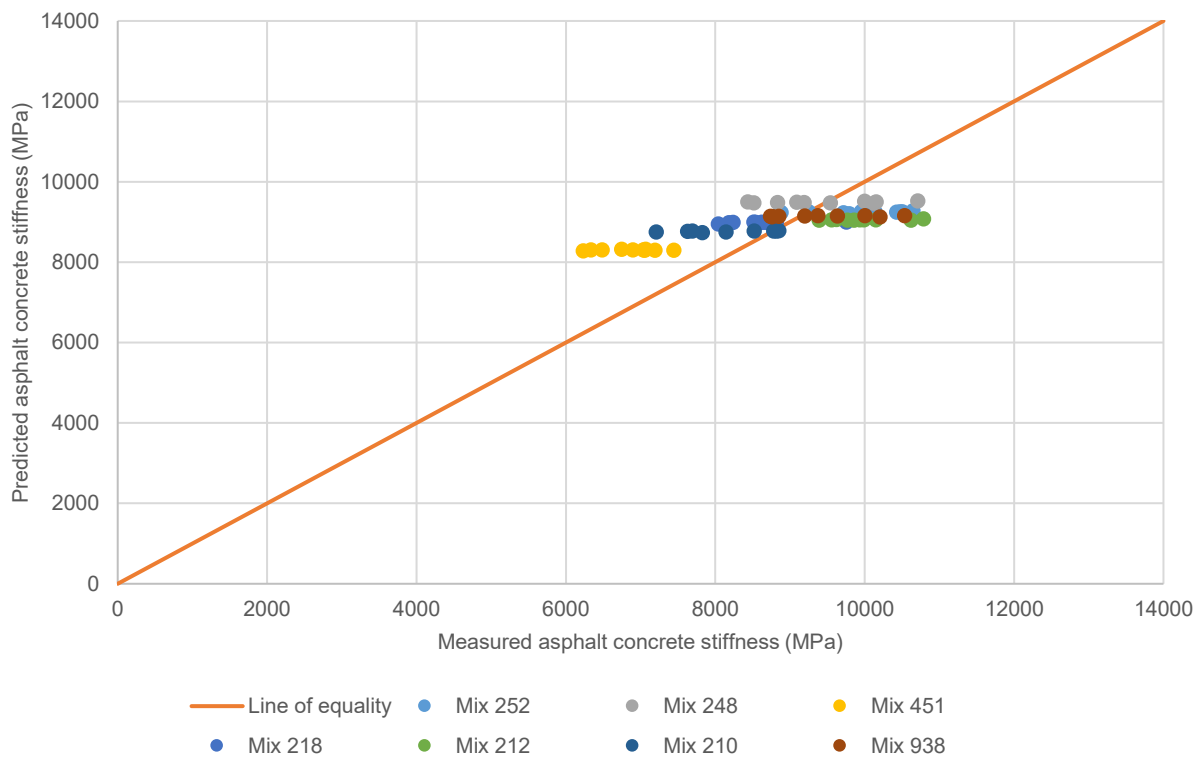
Coefficients:

	Original model	Fitted model
C1	-1.249937	0.195109004
C2	0.029232	0.027560473
C3	-0.001767	0
C4	-0.002841	0.00010907
C5	-0.058097	0
C6	-0.802208	0.039257662
C7	3.871977	1.375842654
C8	-0.0021	6.61425E-07
C9	0.003958	0.004075797
C10	-0.000017	0
C11	0.00547	0.005543838
C12	1	1
C13	-0.603313	0.124264127
C14	-0.313351	0
C15	-0.393532	0

Prediction plot:

Witczak 1999 model prediction (original constants)

Witczak 1999 model prediction (fitted constants)
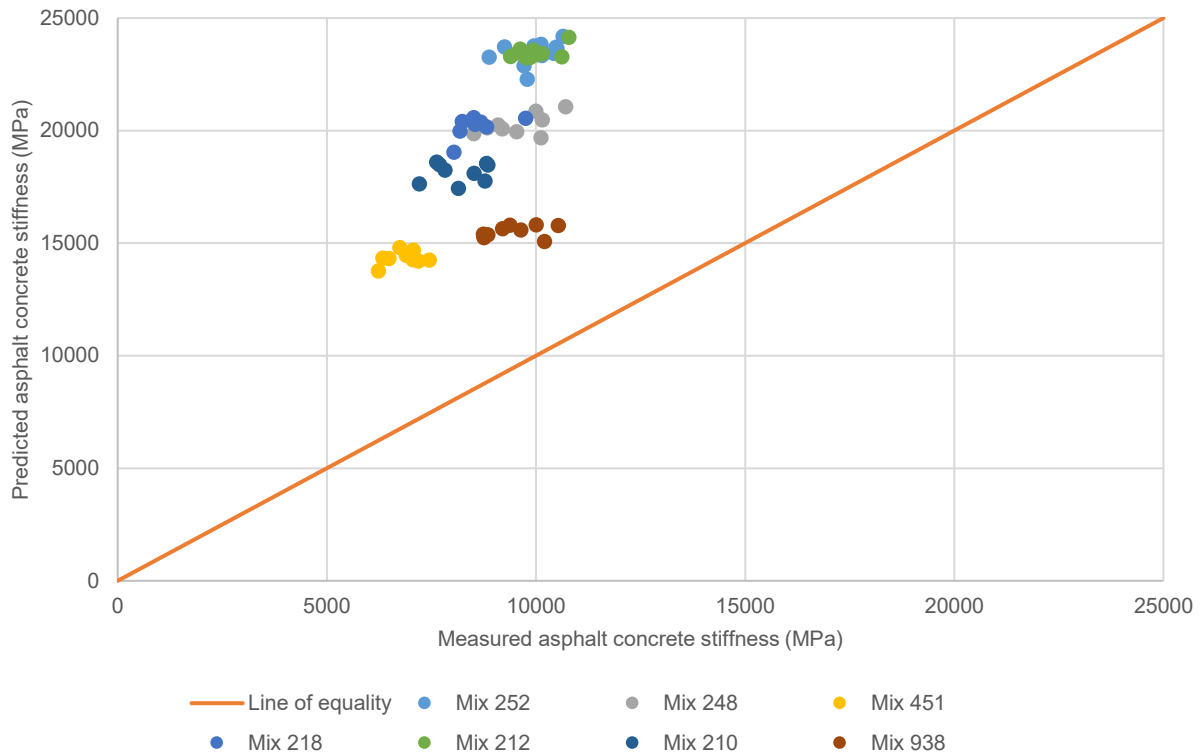
F-5   Witczak 2006

Generalized model:

$$\log_{C1}|E^*|$$
$$= C2 + C3 * \left(|G_b^*|^{C4}\right)$$
$$* \left(C5 + C6 * p_{200} + C7 * p_{200}^2 + C8 * p_4 + C9 * p_4^2 + C10 * p_{38} + C11 * p_{38}^2 + C12 \right.$$
$$\left. * V_A + C13 * \left(\frac{V_{beff}}{V_A + V_{beff}}\right) \right) \qquad \text{(F-5.1)}$$
$$+ \frac{C14 + C15 * V_a + C16 * \left(\frac{V_{beff}}{V_a + V_{beff}}\right) + C17 * P_{38} + C18 * p_{38}^2 + C19 * p_{34}}{C20 + e^{(C21 + C22 * log|G_b^*| + C23 * log\delta_b)}}$$
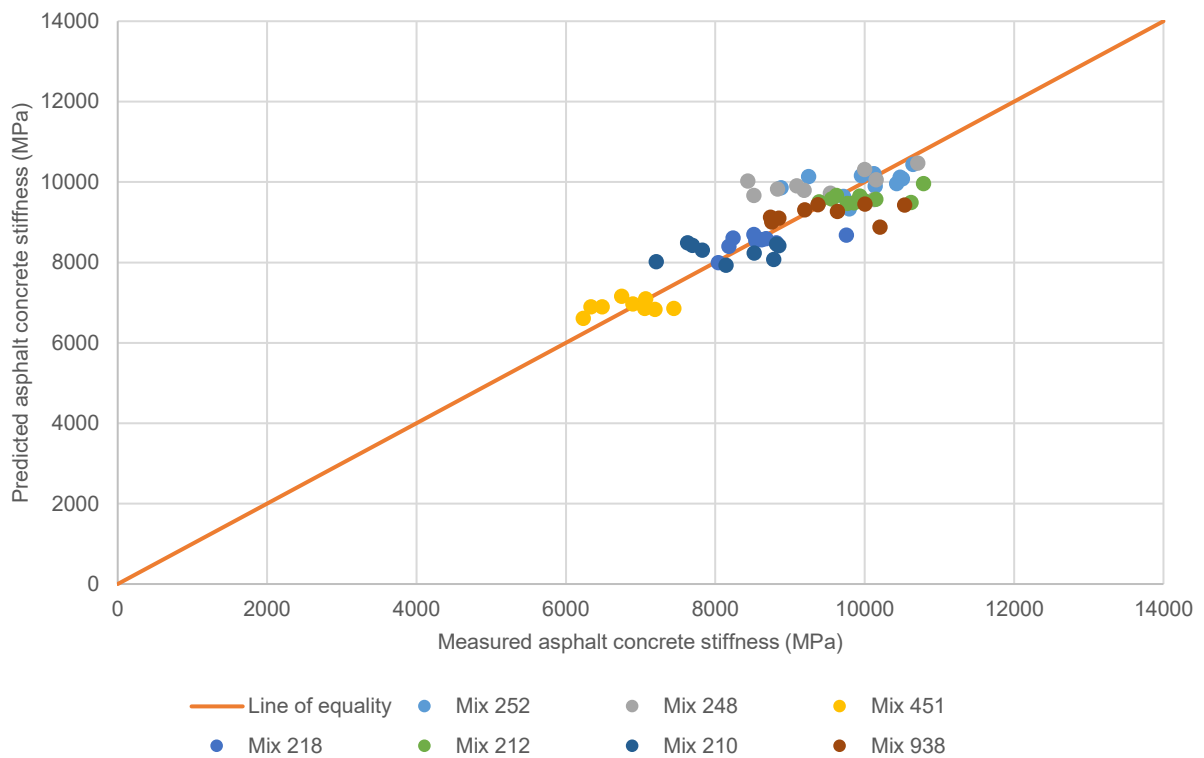
Coefficients:

	Original model	Fitted model
C1	10	12.34461133
C2	-0.349	0
C3	0.754	0.661821405
C4	-0.0052	0
C5	6.65	5.324626695
C6	-0.032	0.00868937
C7	0.0027	0.005331557
C8	0.011	0.015871314
C9	-0.0001	0
C10	0.006	0
C11	-0.00014	0
C12	-0.08	0
C13	-1.06	0.707340798
C14	2.56	4.740970197
C15	0.03	0
C16	0.71	0.510393666
C17	0.012	0.00912732
C18	-0.0001	0
C19	-0.01	0
C20	1	1
C21	-0.7814	0
C22	-0.5785	0.08313625
C23	0.8834	0.699710443

Prediction plot:

Witczak 2006 model prediction (original constants)

Witczak 2006 model prediction (fitted constants)

F-6   Hirsch

Generalized model:

$$|E^*|_{mix} = P_C * \left(C7 \left(C8 - \frac{VMA}{C9} \right) + C10 * |G^*|_{binder} \left(\frac{VFB * VMA}{C11} \right) \right)$$
$$+ \frac{(C12 - P_C)}{\left(\frac{C13 - \frac{VMA}{C14}}{C15} + \frac{VMA}{C16 * VFB|G^*|_{binder}} \right)} \tag{F-6.1}$$

$$P_C = \frac{\left(C1 + \frac{VFB * C2 * |G^*|_{binder}}{VMA} \right)^{C3}}{C4 + \left(\frac{VFB * C5 * |G^*|_{binder}}{VMA} \right)^{C6}} \tag{F-6.2}$$

Coefficients:

	Original model	Fitted model
C1	20	20.13688987
C2	3	3
C3	0.58	0.466599313
C4	650	179.0467333
C5	3	3
C6	0.58	0.58
C7	4200000	7393860.042
C8	1	1
C9	100	100
C10	3	3
C11	10000	10000
C12	1	1
C13	1	1
C14	100	100
C15	4200000	4200850.48
C16	3	3

Prediction plot:

Hirsch model prediction (original constants)

Hirsch model prediction (fitted constants)
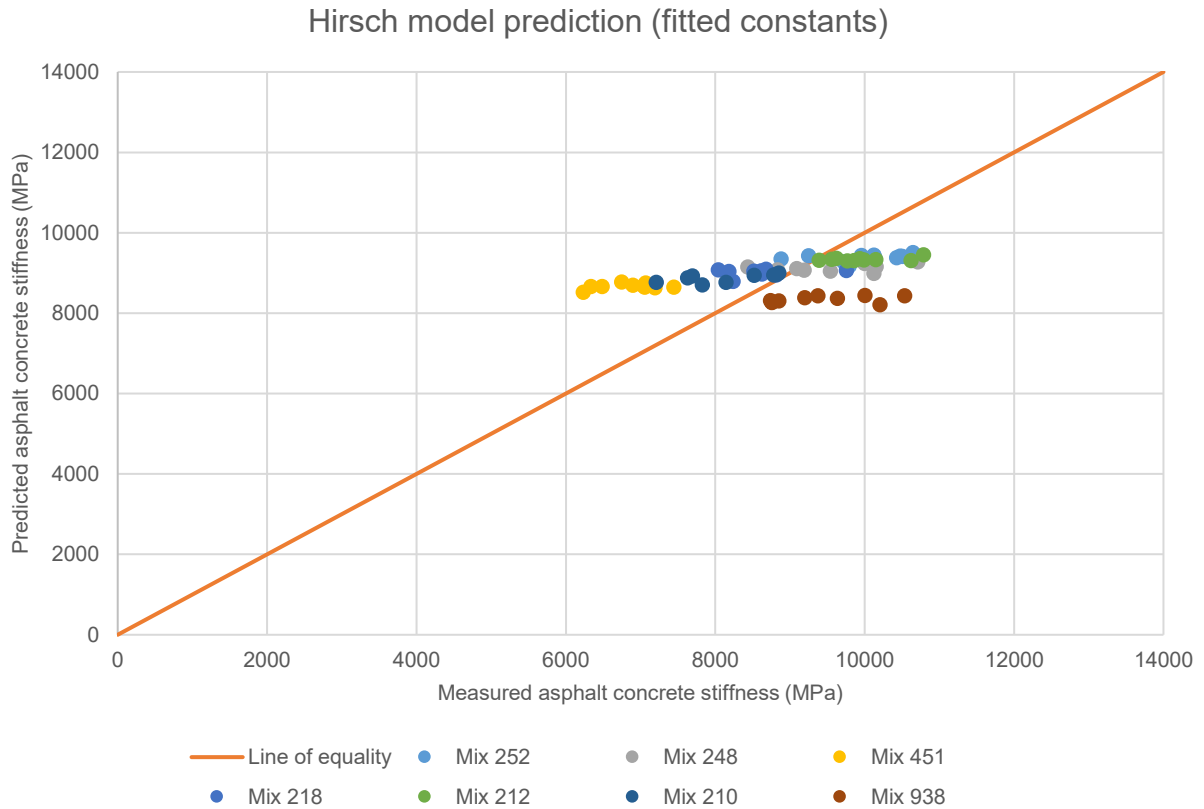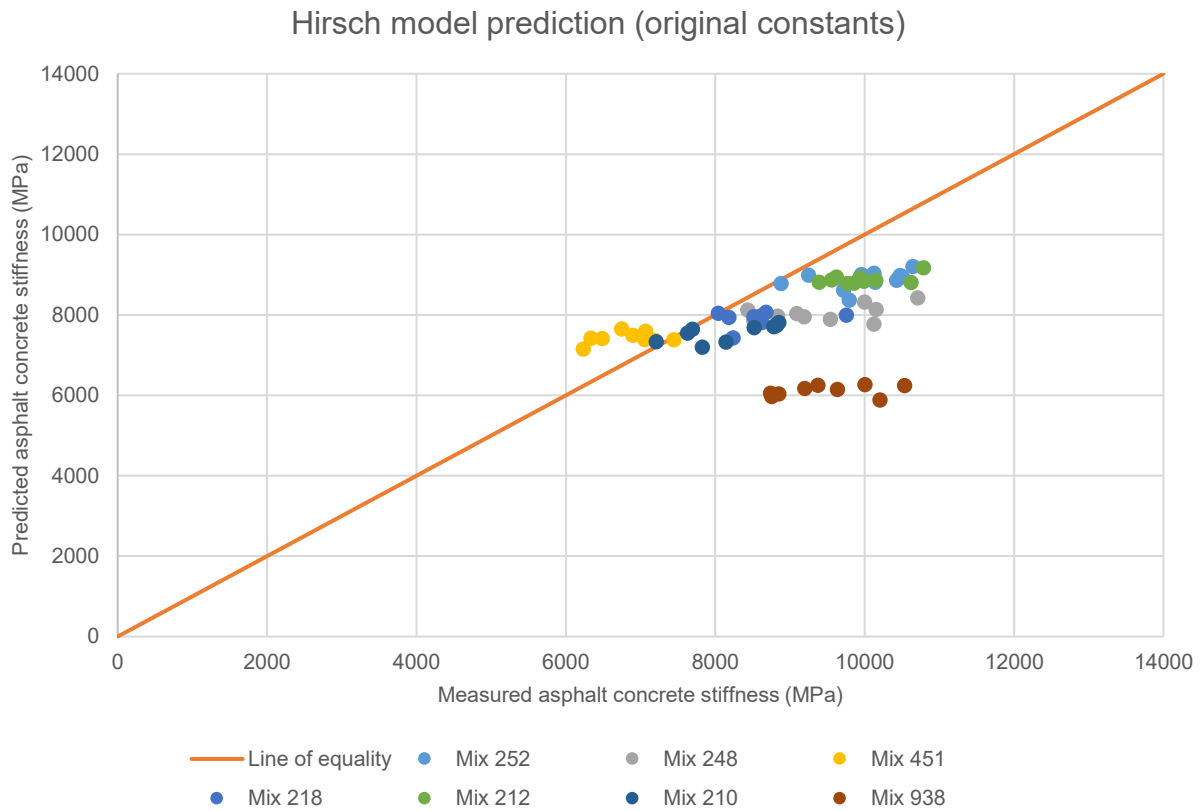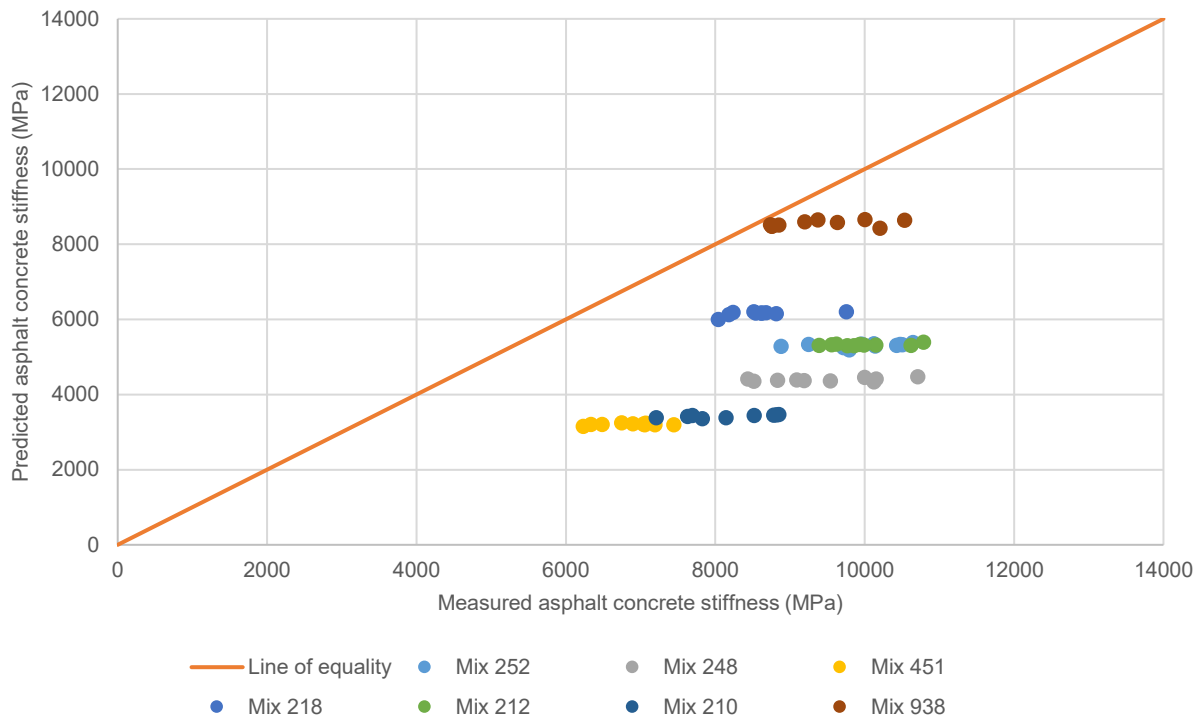
F-7   Al-Khateeb

Generalized model:

$$|E^*| = C1 * \left(\frac{C2 - VMA}{C3}\right) \left(\frac{\left(C4 + C5 * \frac{|G^*|_b}{VMA}\right)^{C6}}{C7 + \left(C8\frac{|G^*|_b}{VMA}\right)^{C9}}\right) |G^*|_g \qquad (F\text{-}7.1)$$
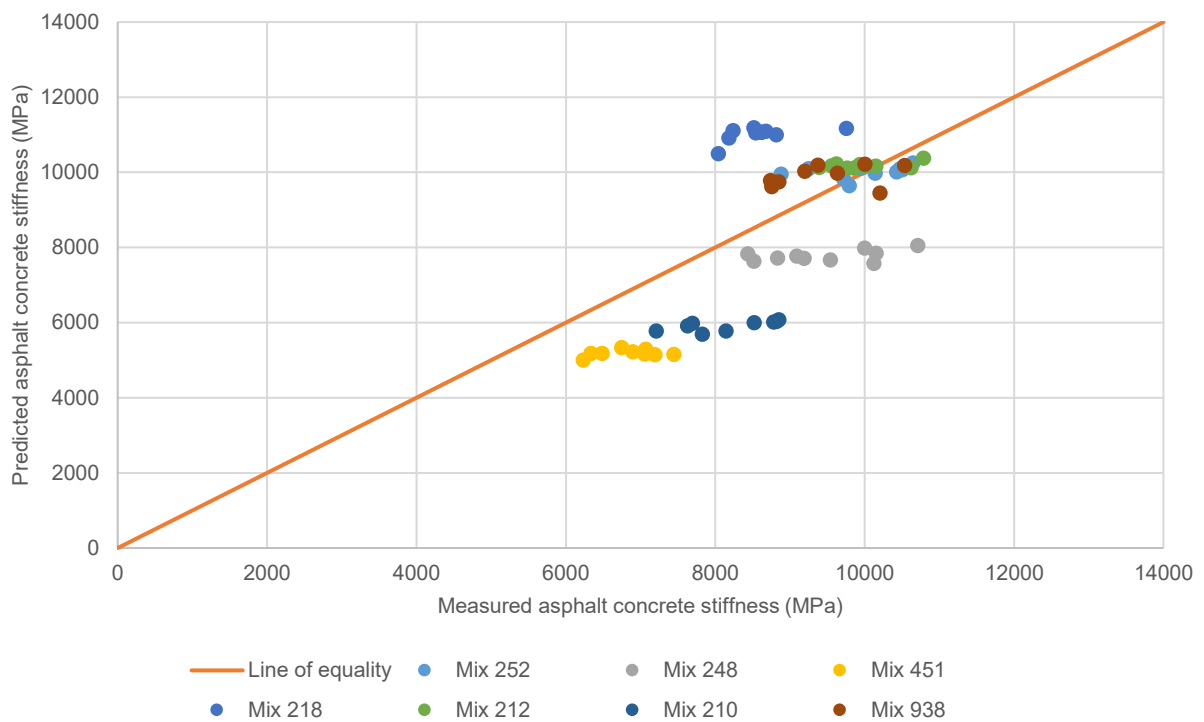
Coefficients:

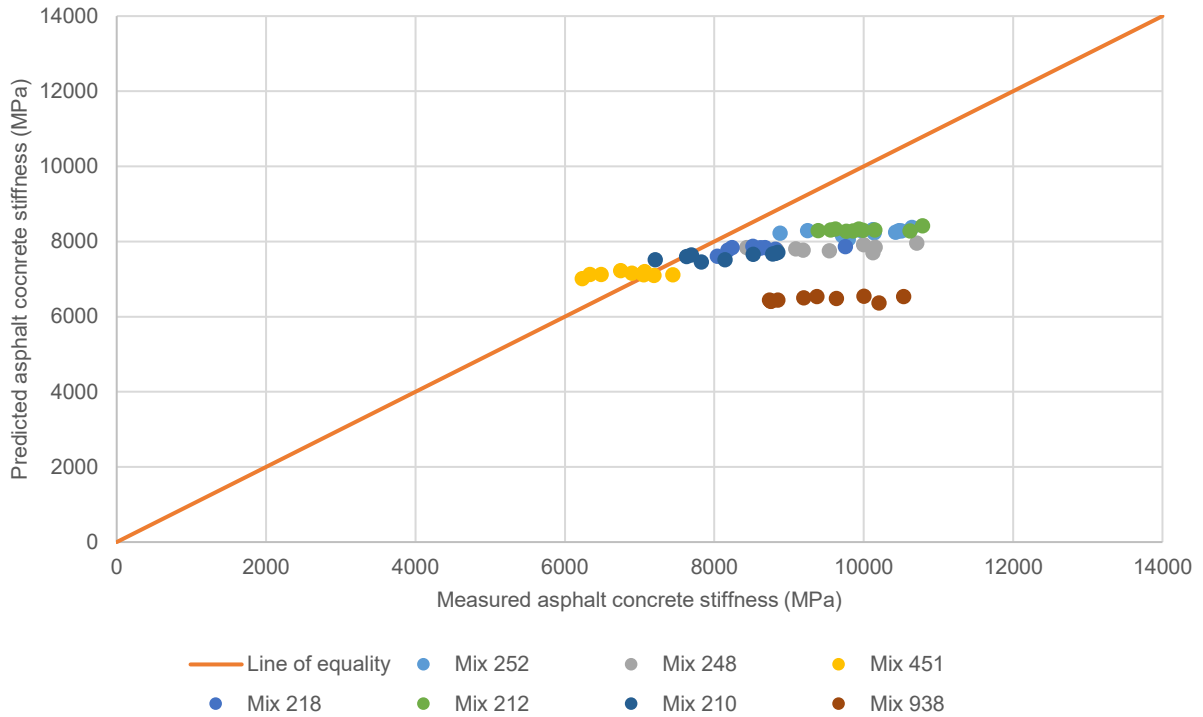|	Original model	Fitted model (glassy modulus = asymptote method)	Fitted model (glassy shear modulus = 1000 MPa)
C1	3	3	3
C2	100	100	100
C3	100	100	100
C4	90	2.66758E-08	91.46158365
C5	1.45	0.002195776	0.287639042
C6	0.66	1.975420506	0.800130678
C7	1100	100562.149	0
C8	0.13	0.000771461	0.557676948
C9	0.66	1.975420506	0.66

Prediction plot:

Al-Khateeb model prediction (glassy shear modulus = asymptote method) (original constants)
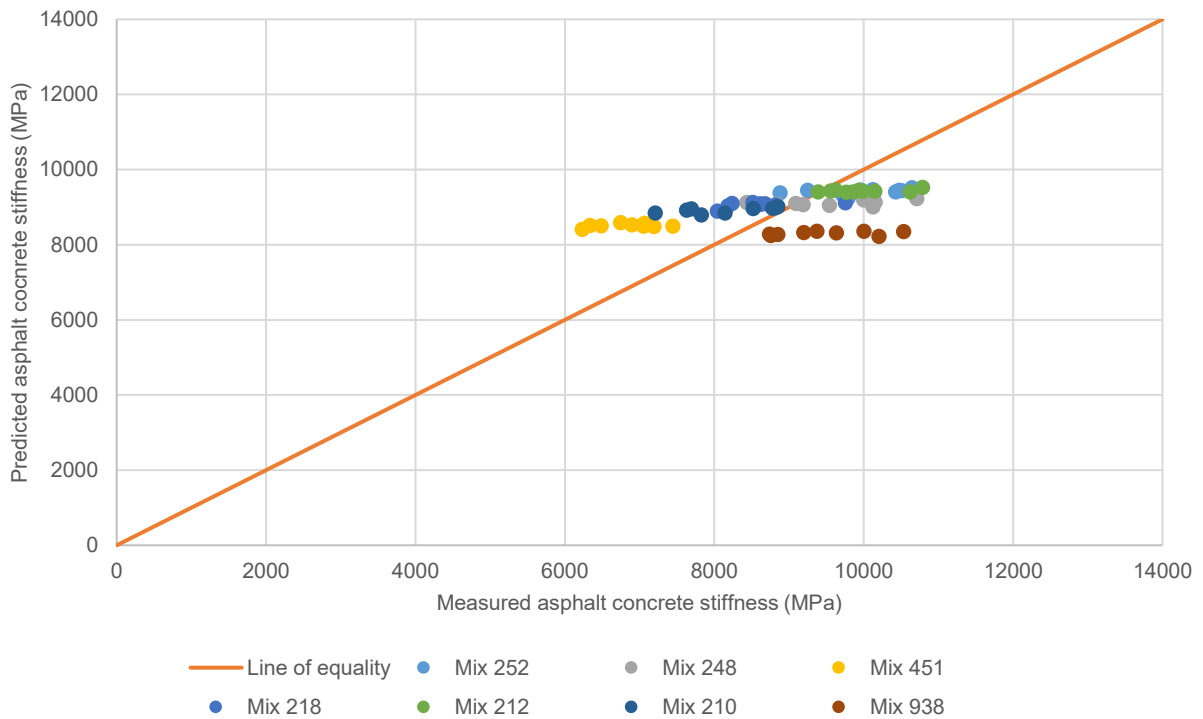

Al-Khateeb model prediction (glassy modulus = asymptote method) (fitted constants)

Al-Khateeb model prediction (glassy shear modulus = 1000 MPa)
(original constants)

Al-Khateeb model prediction (glassy shear modulus = 1000 MPa)
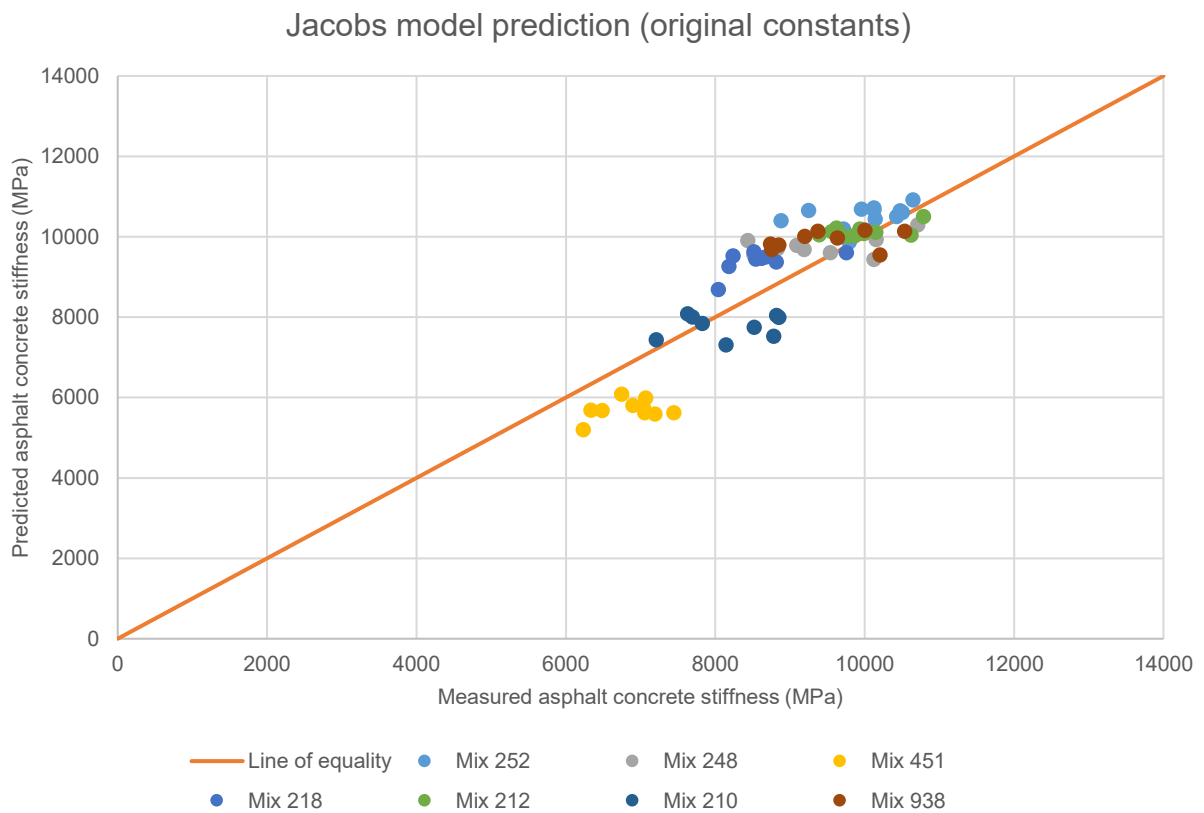(fitted constants)

F-8 Jacobs

Generalized model:

$$S_{mix\_4PB} = -C1 * Pen + C2 * \frac{V_g}{V_b} + C3 * V_a + C4 \ (MPa) \qquad \text{(F-8.1)}$$

Coefficients:
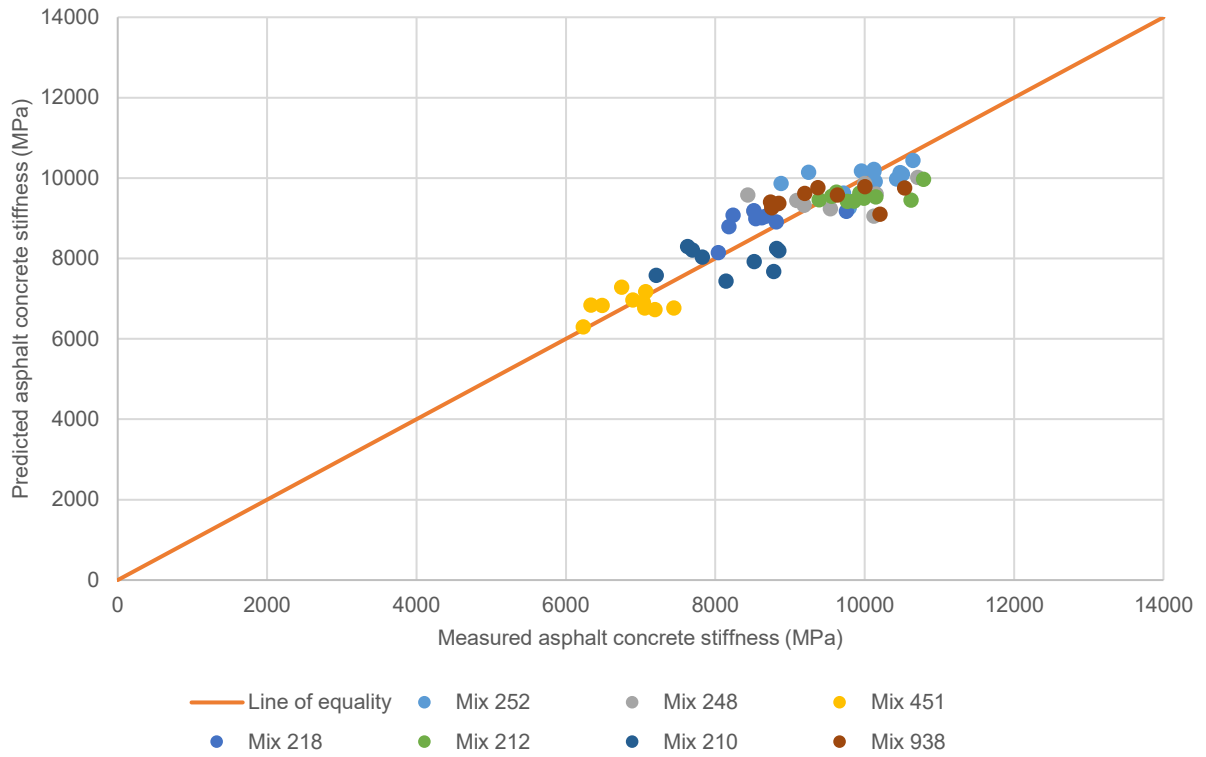
	Original model	Fitted model
C1	-52.3	-25.428
C2	1219.9	866.928
C3	-698.1	-778.725
C4	4344.3	6395.898

Prediction plot:

Jacobs model prediction (fitted constants)

Appendix G – Verification linear regression models

G-1   Multiple linear regression model 1: Engineering judgement

$$S_{mix} = 23.72 * S_{bit,blend} - 1019.74 * V_a + 1130.91 * \frac{V_g}{V_b} + 3670.02 \qquad \text{(G-1)}$$

Where:

$S_{bit,blend}$ = blended bitumen stiffness (MPa)

V_a = volume air voids (%)

V_g = volume aggregates (%)

V_b = volume bitumen (%)

S_{mix} = asphalt concrete stiffness (MPa)

Multiple linear regression model 1: Engineering judgement

G-2 Multiple linear regression model 2: Theory

$$S_{mix} = 19.81 * C_u - 23.93 * D_{max} + 14.31 * S_{bit,blend} - 1066.11 * V_a - 756.49 * V_b \\ + 20885.08 \qquad \text{(G-2)}$$
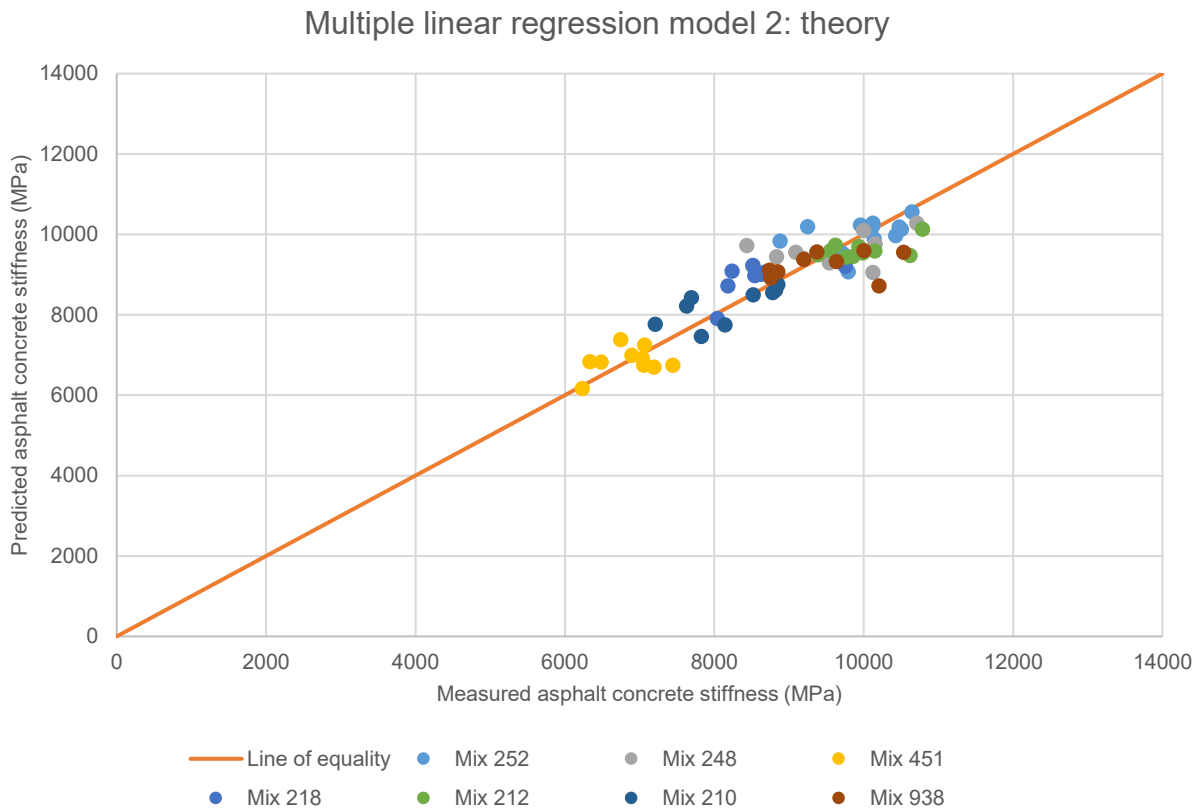
Where:

C_u = coefficient of uniformity (-)

D_{max} = max grain size (mm)

$S_{bit,blend}$ = blended bitumen stiffness (MPa)

V_a = volume air voids (%)

V_b = volume bitumen (%)

S_{mix} = asphalt concrete stiffness (MPa)

G-3   Multiple linear regression model 3: Simplicity

$$S_{mix} = -25.64 * Pen_{blend} - 860.15 * V_a - 634.79 * V_b + 20572.90 \qquad \text{(G-3)}$$

Where:

Pen_{blend} = penetration blended bitumen (dmm)

V_a = volume air voids (%)

V_b = volume bitumen (%)

S_{mix} = asphalt concrete stiffness (MPa)
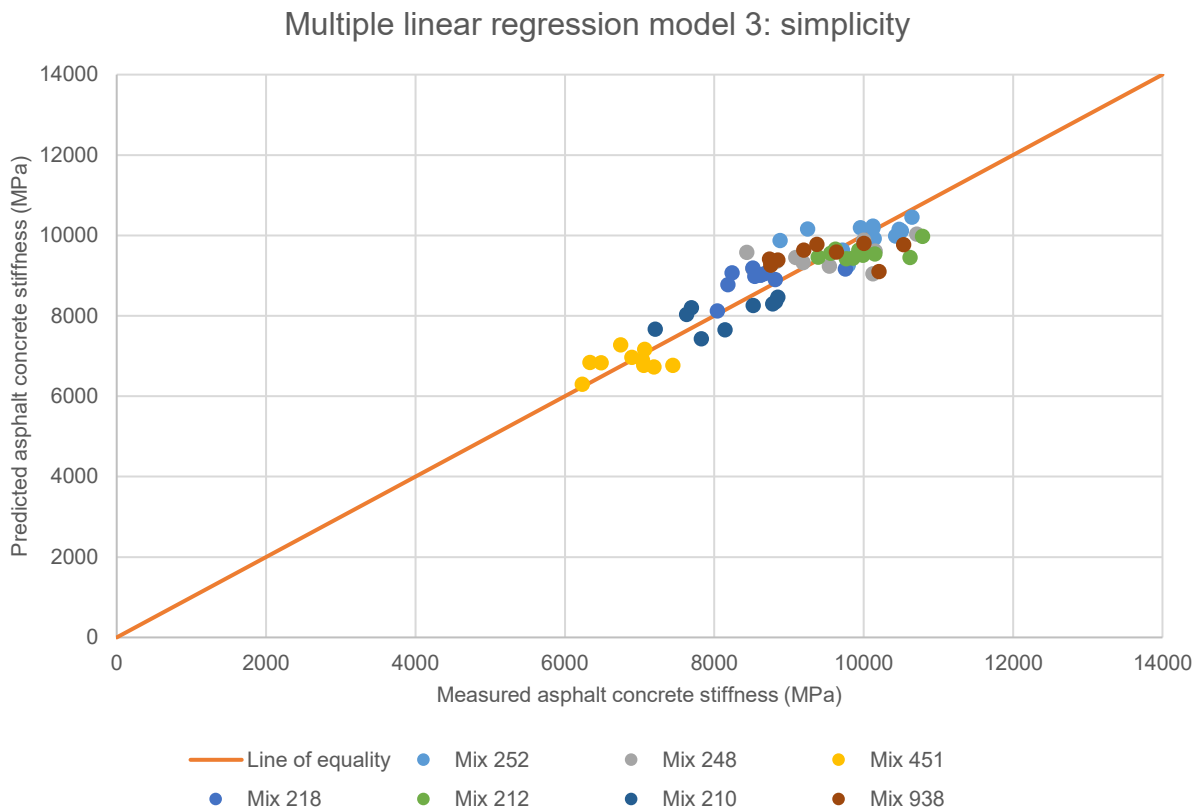
G-4   Multiple linear regression model 4: Maximum correlation

$$S_{mix} = -3.87 * C_u + 72.27 * T_{R+B,blend} + 193.19 * V_b + 851.12 * V_g - 69571.47 \qquad (G-4)$$

Where:

C_u = coefficient of uniformity (-)

$T_{R+B,blend}$ = ring & ball softening point (°C)

V_b = volume bitumen (%)

V_g = volume aggregates (%)

S_{mix} = asphalt concrete stiffness (MPa)

Multiple linear regression model 4: Maximum correlation
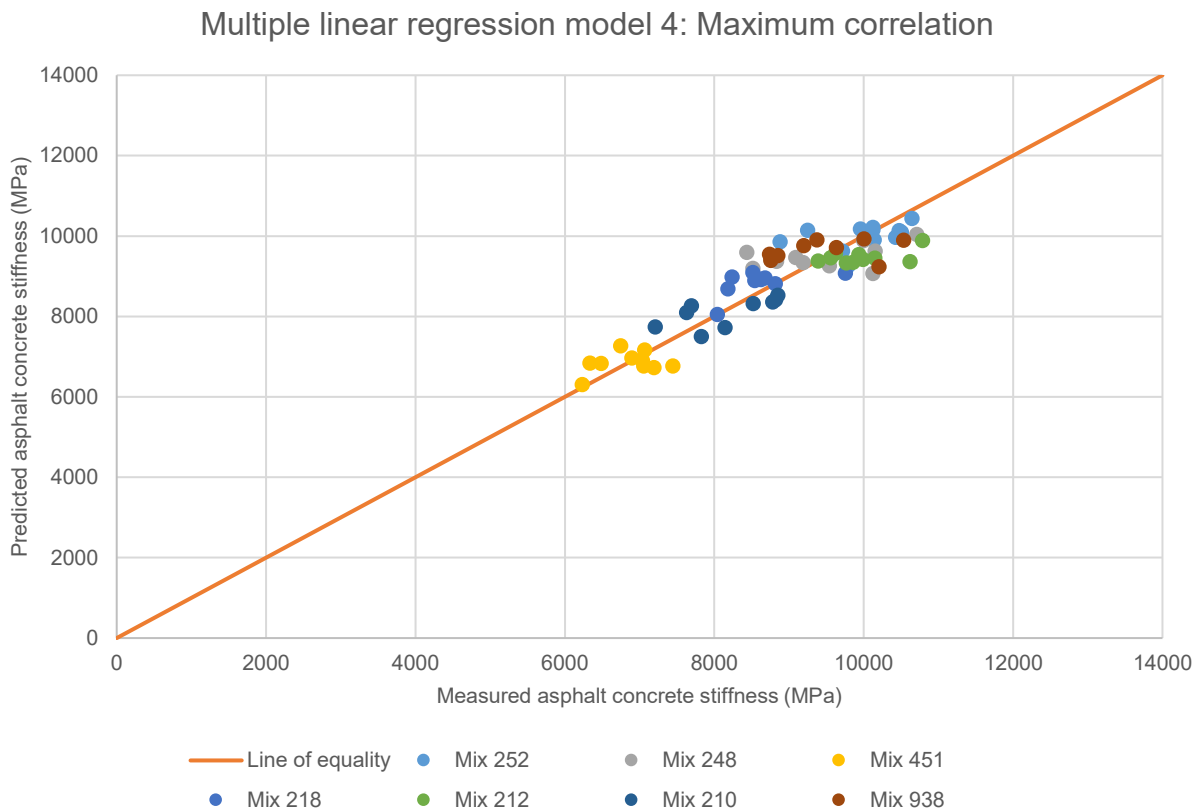
G-5   Multiple linear regression model 5: SPSS forward

$$S_{mix} = -83.21 * Pen_{blend} - 0.93 * S_{bit,inf,new} + 661.07 * V_g - 41557.64 \qquad \text{(G-5)}$$

Where:

Pen_{blend} = penetration blended bitumen (dmm)

$S_{bit,inf,virgin}$ = glassy modulus virgin bitumen (MPa)

V_g = volume aggregates (%)

S_{mix} = asphalt concrete stiffness (MPa)
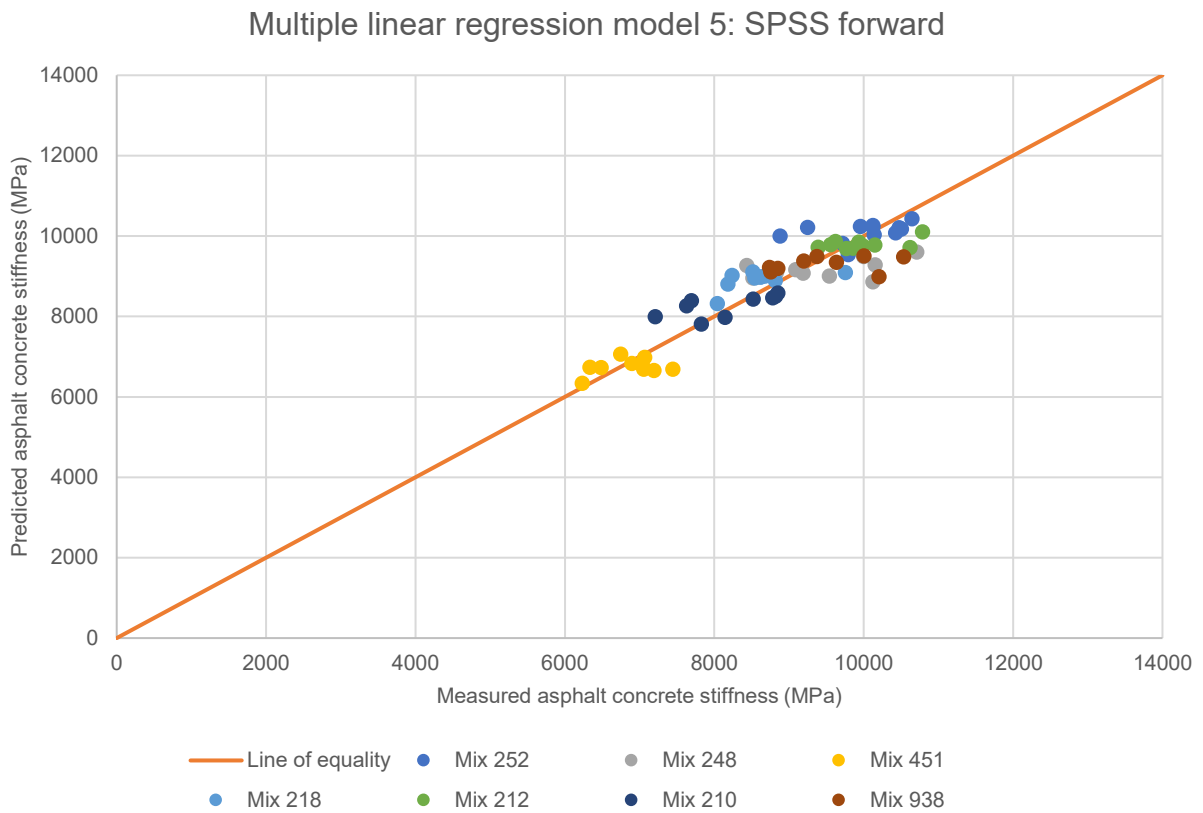
G-6 Multiple linear regression model 6: SPSS backward

$$S_{mix} = 1028.88 * C22.4 - 167.90 * age + 17.90 * RAP\% + 593.72 * V_g + 48.42 \\ * VFB + 0.44 * \eta_{new,135°C} - 140253.95$$

(G-6)

Where:

C22.4 = percentage passing sieve C22,4 (%)

age = specimen age (days)

RAP% = RAP percentage (%)

V_g = volume aggregates (%)

VFB = voids filled with bitumen (%)

$\eta_{virgin,135°C}$ = viscosity at 135°C virgin bitumen (mPa*s)

Multiple linear regression model 6: SPSS backward

Appendix H – Telman, J., & Van den Berg, M. (2018). Voorspelling van E_mix met het model van Hirsch (2003)

Voorspelling van E_mix met het model van Hirsch (2003)

Jan Telman, Melinda van den Berg, Q-Consult Progress Partners, 4 september 2018

1 Het originele Hirsch model

Input van Joost:

$$|E^*|_{mix} = P_C * \left(4200000 \left(1 - \frac{VMA}{100} \right) + 3|G^*|_{binder} \left(\frac{VFB * VMA}{10000} \right) \right) + \frac{(1 - P_C)}{\left(\frac{1 - \frac{VMA}{100}}{4200000} + \frac{VMA}{3VFB|G^*|_{binder}} \right)} \tag{1}$$

$$P_C = \frac{\left(20 + \frac{VFB * 3|G^*|_{binder}}{VMA} \right)^{0.58}}{650 + \left(\frac{VFB * 3|G^*|_{binder}}{VMA} \right)^{0.58}} \tag{2}$$

Waarin:
G_b^*= binder shear modulus (psi)
VMA = voids in the mineral aggregate (%)
VFB = voids filled with bitumen (%)
E^*_{mix} = Asphalt concrete stiffness (psi) (LET OP: GEEN MPa)
P = Proportion of the parallel phase [-]

Verder geldt:
VMA = V_a + V_b   en VFB = (V_b/VMA)x100   met V_a de holle ruimte (%) en V_b het bitumengehalte (%).

2 De data

Er zijn in totaal 84 proefstukken onderzocht, verdeeld over 7 mengsels. De te voorspellen grootheid E_mix en de mogelijk verklarende variabelen Gb, VMA, VFB, V_a en V_b en hun onderlinge samenhang zijn weergegeven in onderstaande figuren.

In Figuur 1 valt mengsel 451 op door een hoger bitumengehalte en mengsel 938 door een lagere Gb.

In Figuur 2 lijkt E_mix een dalende curve te vertonen met VMA. En een stijgend verband met VFB, met nog een niveauverschil voor mix 451 (met het hogere bitumengehalte).

Ook vertonen de voorspellende variabelen VMA en VMF een sterke onderlinge correlatie, met een niveauverschil bij het hogere bitumen %. Dit is een logisch gevolg van de relatie VFB = (V_b/VMA)x100, waarbij V_b eigenlijk alleen maar varieert rond 2 niveaus (9,5 en 13,5%).
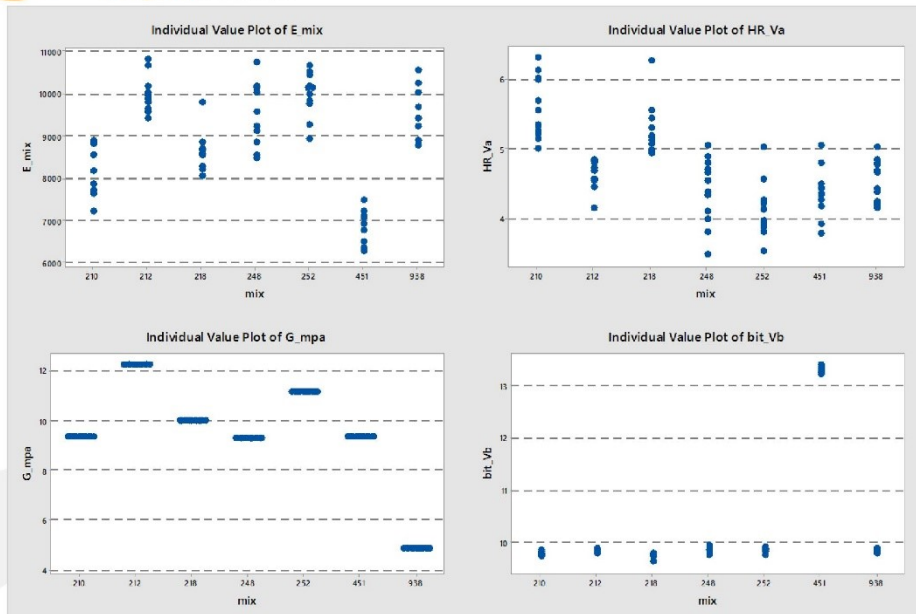
Figuur 1. Gemeten waarden per mengsel (mix).
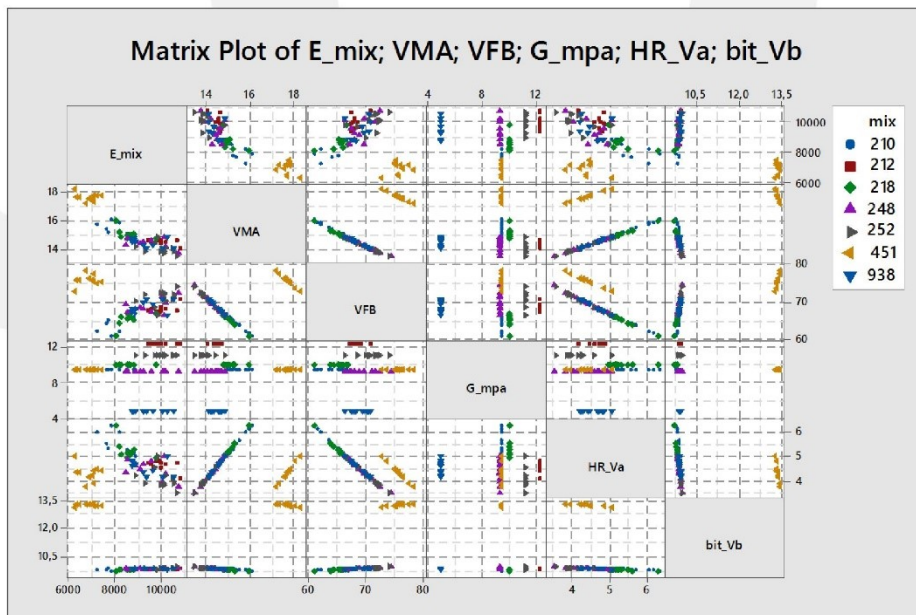
Figuur 2. Samenhang tussen de gemeten waarden, met onderscheid naar mengsel (mix).

2

3 Het Hirsch model herschreven

Het model gebruikt de eenheden psi voor de te voorspellen waarde E_{mix} en de voorspellende variabele G_b. In de dataset zijn de eenheden MPa gebruikt.
Dit betekent dat een omrekeningsfactor moet worden gebruikt: convfac = 145,03773773

dus eerst uit de metingen: G_b (psi) = G_b (MPa) x convfac
en uiteindelijk bij de voorspelling: E_{mix} (MPa) = E_{mix} (psi) / convfac

De binder shear modulus G_b is altijd positief, dus het berekenen van een absolute waarde |...| is niet nodig.

VMA en VFB worden in het model consequent gedeeld door 100 en het product VMA*VFB door 100*100 = 10000. Dus het model kan worden vereenvoudigd door in te vullen: vma=VMA/100 en vfb=VFB/100.

Verder geldt dat P_C een proportie is (Proportion of the parallel phase [-]). We zien in de formule een deel met P_C en een deel met $(1 - P_C)$. Dit doet vermoeden dat relevante warden van P_C liggen tussen 0 en 1.

Het model kan op grond van bovenstaande worden herschreven als:

$$E_{mix} = P_C \times A + (1 - P_C) \times B \quad \text{(in psi)}$$

met

$$P_C = \frac{\left(20 + 3 \times G_b \times \frac{vfb}{vma}\right)^{0.58}}{650 + \left(3 \times G_b \times \frac{vfb}{vma}\right)^{0.58}}$$

$$A = 4.200.000 \times (1 - vma) + 3 \times G_b \times vfb \times vma$$

$$B = \frac{1}{\frac{1 - vma}{4.200.000} + \frac{vma}{3 \times G_b \times vfb}}$$

Opvallend is dat een aantal "constanten" herhaald voorkomen:
- de waarde 3, de Poisson ratio
- de waarde 4.200.000
- de waarde 0,58 in de macht.

Bij het fitten van het Hirschmodel op de nieuwe data kunnen deze constanten worden geoptimaliseerd om de voorspelde waarden E_{mix} zo goed mogelijk te laten aansluiten op de gemeten waarden.
In algemene zin is het model als volgt te schrijven:

3

$$P_C = \frac{\left(C1 + C2 \times G_b \times \frac{vfb}{vma}\right)^{C3}}{C4 + \left(C5 \times G_b \times \frac{vfb}{vma}\right)^{C6}}$$

$$A = C7 \times (C8 - C9 \times vma) + C10 \times G_b \times C11 \times vfb \times vma$$

$$B = \frac{1}{\frac{C13 - C14 \times vma}{C15} + \frac{vma}{C16 \times G_b \times vfb}}$$

en

$$E_{mix} = P_C \times A + (C12 - P_C) \times B$$

Op voorhand is dit model al overbepaald. D.w.z. niet alle parameters zijn niet onafhankelijk te schatten. Dit geldt voor de drietallen C7, C8 en C9 en C13, C14 en C15, en voor het duo C10 en C11.

4 Resultaten oorspronkelijk Hirsch model

Tabel 1 toont de startwaarden voor de parameters volgens het oorspronkelijke Hirsch model. De gele velden tonen de parameters die niet variabel zijn volgens het model op de voorgaande pagina, omdat ze te maken hebben met proportions.

Met gelijke kleuren zijn de parameters aangegeven die gelijke waarden hebben in het oorspronkelijke model. Bij een optimalisatie kunnen ze afzonderlijk of gecombineerd worden gevarieerd.

In de onderste cellen van de tabel staan de resultaten van de voorspelling van Emix met het oorspronkelijke Hirschmodel. De som van de kwadratische afwijkingen is vrij groot, maar op zichzelf moeilijker te interpreteren. Belangrijker is de R^2-waarde, die erg laag is. De voorspelde waarden correleren dus niet goed met de gemeten waarden.

Dit is ook te zien in Figuur 3. Het verloop van de gemeten Emix is steiler dan op grond van het Hirsch model wordt voorspeld. Dit geldt voor de totale puntenwolk, maar ook binnen de wolkjes van dezelfde mix. Verder wijkt mix 938 nog sterk af van het beeld. Dit is een mix met PMB.

De waarden van Pc liggen voor alle monsters keurig binnen de range tussen 0 en 1, namelijk tussen 0,237 en 0,363.

coef	start
C1	20
C2	3
C3	0,58
C4	650
C5	3
C6	0,58
C7	4.200.000
C8	1
C9	1
C10	3
C11	1
C12	1
C13	1
C14	1
C15	4.200.000
C16	3
somerror2	1,85E+08
min_pc	0,237
max_pc	0,363
R2	0,156

Tabel 1. Oorspronkelijk Hirsch model
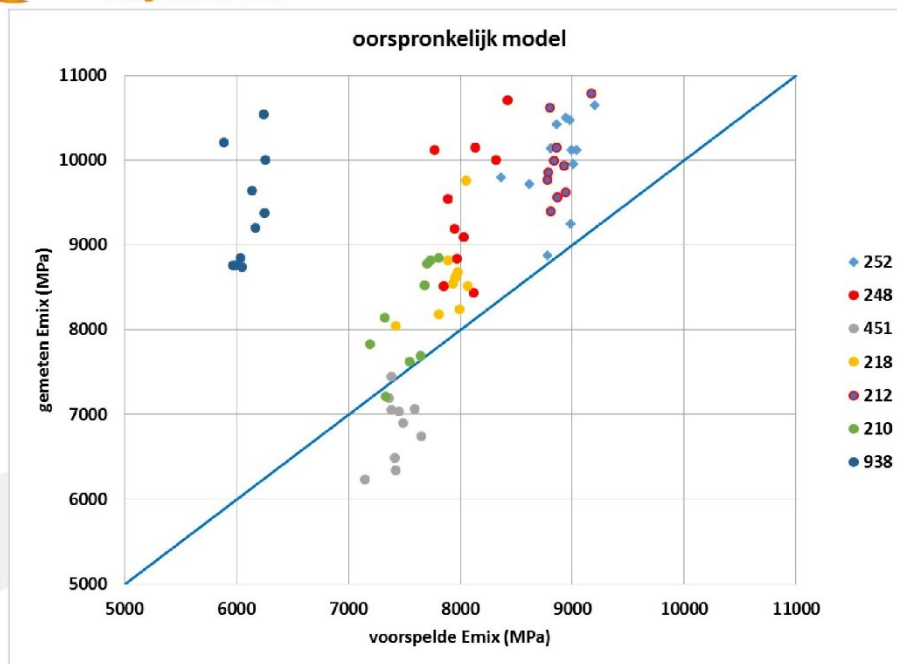
Figuur 3. Oorspronkelijk Hirsch model.

5 Opnieuw fitten van de parameters van het Hirsch model

Nagegaan is of het Hirsch model beter past wanneer de parameters worden geoptimaliseerd. Hierbij zijn de geel gemarkeerde waarden (1) in Tabel 1 niet aangepast. En ook de Poisson ratio is op 3 vastgezet (parameters in de oranje velden).

Optimalisatie is uitgevoerd met de Oplosser (Solver.xlam) in Excel 2013.

De resultaten staan in Tabel 2. Een optimalisatie zonder restricties op Pc levert een betere (maar nog steeds lage) R2 op. En waarden voor Pc die niet tussen 0 en 1 liggen.
Vervolgens is de optimalisatie herhaald (vanuit de oorspronkelijke startwaarden) met steeds strengere restricties op Pc.
Restr01 betekent: Pc tussen 0,01 en 0,99. Restr20: tussen 0,20 en 0,80. Restr25: tussen 0,25 en 0,75. Te zien is dat steeds grenswaarden worden bereikt in de optimalisatie.

Opvallend is dat de waarden voor de macht (C3 en C6) naar 0 toe kruipen.

5

coef	start	optimum	optim_restr01	optim_restr20	optim_restr25
C1	20	32,90	27,42	26,23	24,14
C2	3	3	3	3	3
C3	0,58	0,319	0,135	0,120	0,117
C4	650	2,38	2,47	3,26	10,58
C5	3	3	3	3	3
C6	0,58	0,219	0,042	0,000	0,011
C7	4.200.000	739.904	1.614.084	1.994.105	5.597.227
C8	1	1	1	1	1
C9	1	1	1	1	1
C10	3	3	3	3	3
C11	1	1	1	1	1
C12	1	1	1	1	1
C13	1	1	1	1	1
C14	1	1	1	1	1
C15	4.200.000	4.830.097	4.547.127	4.493.991	4.346.900
C16	3	3	3	3	3
somerror2	1,85E+08	7,61E+07	7,54E+07	7,53E+07	7,51E+07
min_pc	0,237	1,899	0,873	0,705	0,250
max_pc	0,363	2,221	0,990	0,800	0,283
R2	0,156	0,277	0,314	0,309	0,309

Tabel 2. Resultaten van enkele optimalisatieslagen met het Hirsch model.

Voor model restr20 zijn de resultaten weergegeven in Figuur 4. Het model past niet goed, maar wel beter dan het originele model (Figuur 3). Er lijkt namelijk sprake van een lineaire transformatie tussen de voorspelling en de meting van Emix. Met mix 938 (met PMB) als afwijkend mengsel.
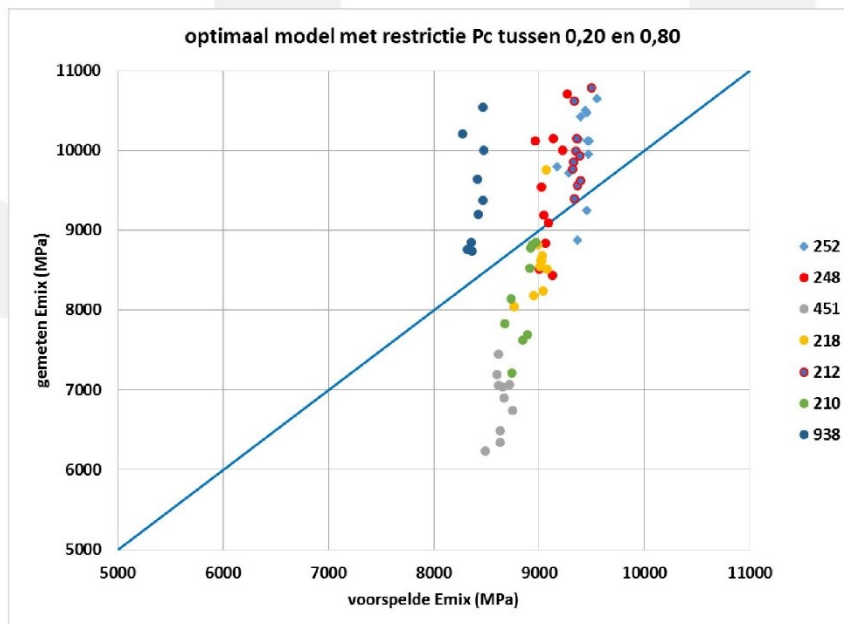
Figuur 4. Geoptimaliseerd Hirsch model.

Twee zaken vallen op:

- In Figuur 2 blijkt dat mix 938 niet afwijkend ligt qua combinatie van Emix, VMA, VFB en Gb. Dat betekent dat het niet waarschijnlijk is dat het gaat lukken het Hirsch model ook op mix 938 te fitten.
- Voor de overige mengsels bestaat wel een lineaire relatie tussen Emix gemeten en Emix voorspeld. Daarom is de verwachting dat na uitsluiting van mix 938 wel een fit kan worden gevonden.
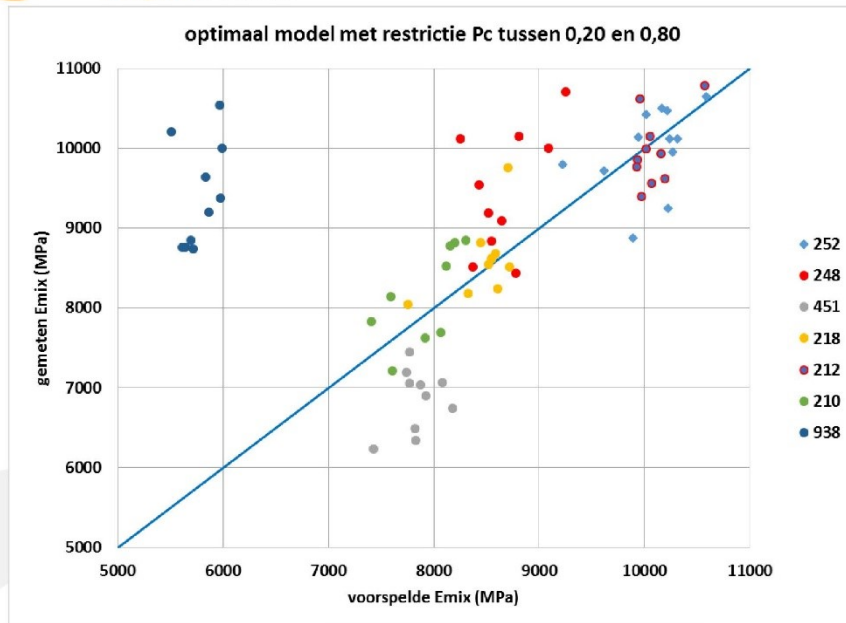
6   Hirsch model, excl mix 938

Voor de data exclusief mix 938 is het resultaat samengevat in onderstaande tabel. De fit is uitgevoerd met de oorspronkelijke parameterwaarden (start), met optimale parameterwaarden (optimum) en met parameterwaarden met een restrictie op Pc.

coef	start	optimum	optim_restr01	optim_restr20	optim_restr25
C1	20	0,00	18,98	19,66	19,78
C2	3	3	3	3	3
C3	0,58	1,255	0,735	0,695	0,683
C4	650	5988,15	1378,22	1213,90	1173,99
C5	3	3	3	3	3
C6	0,58	0,000	0,598	0,552	0,538
C7	4.200.000	58.596	1.798.868	2.219.946	2.365.737
C8	1	1	1	1	1
C9	1	1	1	1	1
C10	3	3	3	3	3
C11	1	1	1	1	1
C12	1	1	1	1	1
C13	1	1	1	1	1
C14	1	1	1	1	1
C15	4.200.000	10.282.886	4.207.955	4.202.640	4.201.816
C16	3	3	3	3	3
somerror2	7,17E+07	2,62E+07	2,95E+07	2,95E+07	2,95E+07
min_pc	0,293	30,279	0,708	0,573	0,537
max_pc	0,363	60,753	0,990	0,800	0,750
R2	0,848	0,852	0,829	0,829	0,828

Tabel 3. Resultaten Hirsch model, excl mix 938

Zonder restrictie wordt een optimum gevonden met extreme waarden voor de proportion Pc (oranje velden bij min_Pc en max_Pc). Bovendien zijn de parameterwaarden C1 en C6 dan 0. Als restricties worden opgelegd aan Pc, worden oplossingen gevonden die dicht bij de grenswaarden voor Pc liggen.

Het model past dan vrij aardig, zoals blijkt in onderstaande figuur.

optimaal model met restrictie Pc tussen 0,20 en 0,80

Tabel 4. Resultaten Hirsch model, excl mix 938.

De punten (behalve natuurlijk die van mix 938) liggen vrij goed op de diagonaal. Wel blijken de punten voor mix 451 net wat onder de diagonaal te liggen, en die van mix 248 liggen voornamelijk boven de diagonaal.

7   Hirschmodel met variabele Poisson ratio, excl mix 938

Vervolgens is nog het effect van de "vaste" parameters voor de Poisson ratio onderzocht. Hierbij zijn de volgende restricties gehanteerd:

- De Pc-waarden moeten tussen 0,01 en 0,99 liggen
- Gelijke parameters (met dezelfde kleur in de kolom coef) mogen wel varieren, maar dan op dezelfde manier.

Met start wordt het originele Hirsch model aangegeven. Bij een volledig vrije optimalisatie wordt de som van kwadratische afwijkingen gehalveerd. Opvallend is:
- De Poisson ratio komt heel laag uit: 0,934
- De waarde voor C7 en C14 wordt heel groot

Vervolgens is een aanvullende restrictie aangebracht: de Poisson ratio moet minimaal respectievelijk 1, 2, 3, 4, 5, 10, 30 zijn. Het effect van deze restricties is:

- De Poisson ratio komt altijd op het toegelaten minimum uit.
- De som van kwadratische afwijkingen verandert nauwelijks

8

- De waarden voor C7 en C15 worden extreem groot
- Ook de waarde voor C4 wordt groot
- De waarden voor Pc kruipen naar 0 (naar de vereiste ondergrens 0,01).

coef	start	optimum	optim_restr1	optim_restr2	optim_restr3	optim_restr4	optim_restr5	optim_restr10	optim_restr30
C1	20	19,28	18,81	14,19	13,36	14,33	14,95	15,54	15,38
C2	3	0,934	1,000	2,000	3,000	4,000	5,000	10,000	30,000
C3	0,58	0,673	0,677	0,618	0,582	0,571	0,561	0,538	0,546
C4	650	3056,32	2981,60	8193,60	27033,84	28774,19	29413,05	33880,89	27073,06
C5	3	0,934	1,000	2,000	3,000	4,000	5,000	10,000	30,000
C6	0,58	0,673	0,677	0,618	0,582	0,571	0,561	0,538	0,546
C7	4.200.000	14.199.073	12.864.011	35.625.018	126.967.842	126.688.007	126.378.738	123.740.810	45.178.420
C8	1	1	1	1	1	1	1	1	1
C9	1	1	1	1	1	1	1	1	1
C10	3	0,934	1,000	2,000	3,000	4,000	5,000	10,000	30,000
C11	1	1	1	1	1	1	1	1	1
C12	1	1	1	1	1	1	1	1	1
C13	1	1	1	1	1	1	1	1	1
C14	1	1	1	1	1	1	1	1	1
C15	4.200.000	14.199.073	12.864.011	35.625.018	126.967.842	126.688.007	126.378.738	123.740.810	45.178.420
C16	3	0,934	1,000	2,000	3,000	4,000	5,000	10,000	30,000
somerror2	7,17E+07	2,95E+07	2,95E+07	2,96E+07	2,97E+07	2,98E+07	2,99E+07	3,02E+07	3,04E+07
min_pc	0,293	0,090	0,099	0,036	0,010	0,010	0,010	0,010	0,024
max_pc	0,363	0,125	0,138	0,049	0,014	0,014	0,014	0,013	0,033
R2	0,848	0,828	0,829	0,828	0,829	0,829	0,830	0,829	0,823

Tabel 5. Hirsch model met variabele Poisson ratios.

Het resultaat voor Poisson ratio 3 is weergegeven in Figuur 5. Het resultaat is vergelijkbaar met het voorgaande resultaat in Figuur 4. Het gecombineerd variëren van gelijke parameters én een flexibele Poisson ratio heeft dus geen effect.
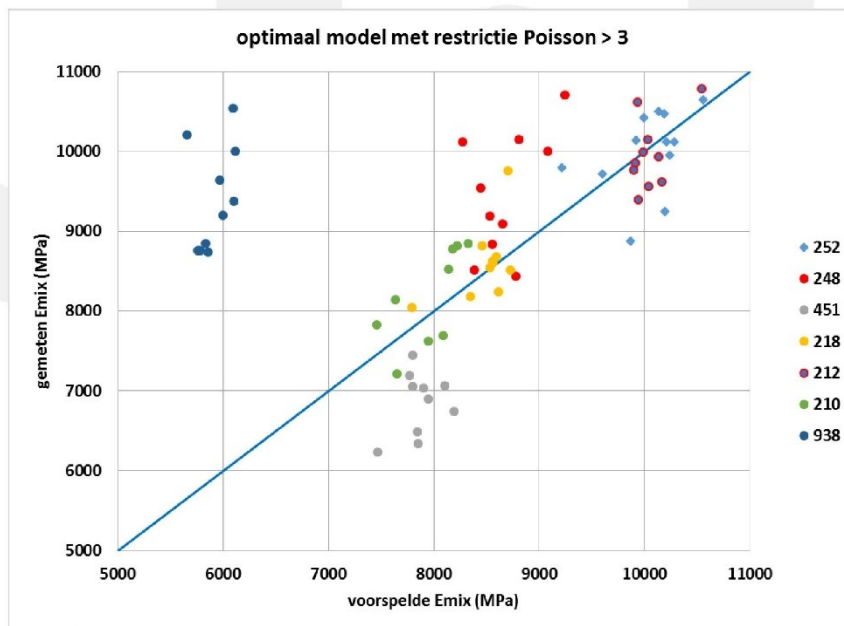
Figuur 5. Resultaat voor model met Poisson ratio 3.